STUDY ON UTILIZATION OF FORMALDEHYDE AS A CARBONYL SOURCE IN CATALYTIC ARYLATIVE CARBONYLATION

(触媒的アリール化カルボニル化反応における
ホルムアルデヒドの利用に関する研究)

CHUANG WANG
NARA INSTITUTE OF SCIENCE AND TECHNOLOGY
(NAIST)

September, 2014

Abbreviation

Ac	acetyl
Ar	aryl
BINAP	2,2'-bis(diphenylphosphino)-1,1'-binaphthyl
BIPHEP	2,2'-bis(diphenylphosphino)-1,1'-biphenyl
Bu or *n*-Bu	(primary) butyl
cod	1,5-cyclooctadiene
dppb	1,4-bis(diphenylphosphino)butane
dppe	1,2-bis(diphenylphosphino)ethane
dppp	1,3-bis(diphenylphosphino)propane
dppf	1,1'-bis(diphenylphosphino)ferrocene
eq.	equivalent
h	hour
HRMS	high-resolution mass spectrometry
J	coupling constant (in Hertz)
Me	methyl
min	minute
MS	mass spectrometry
m/z	mass-to-charge ratio (in mass spectrometry)
NMR	nuclear magnetic resonance
nOe	nuclear overhauser effect
Nu	nucleophile
Ph	phenyl
PKR	Pauson-Khand (-type) reaction
Pr or *n*-Pr	(primary) propyl
Pd	Palladium
RT	room temperature
Rh	rhodium
Ru	ruthenium
TFA	trifluoroacetic acid
xantphos	9,9-dimethyl-4,5-bis(diphenylphosphino)xanthene

Contents

CHAPTER 1 General Introduction

The development of environmentally benign and efficient synthetic methods continues to be a central goal of current research in chemistry. In this regard, catalysis and organometallic chemistry are key techniques for achieving these objectives and for contributing to a "greener" chemistry in the future. Among various catalytic reactions, the refinement of readily available feedstocks to more-functionalized products is of particular importance. Prime examples for such transformations are carbonylation processes, where carbon monoxide (CO) is currently often-used as the most important C_1 building block.[1] Carbonylation refers to reactions that introduce carbon monoxide into organic and inorganic substrates. Carbon monoxide is abundantly available and conveniently reactive, so it is widely used as a reagent in industrial chemistry.[2] Transition-metal-catalyzed carbonylation represents an essential type of reaction leading to the efficient preparation of a wide class of carbonyl-containing compounds that lie in nature product, pharmaceuticals, and organic materials.[3]

1.1 Transition-Metal-Catalyzed Carbonylation Protocol Using CO

Main contributions about transition-metal-catalyzed carbonylation in the presence of CO have been described as follows.

1.1.1 General Palladium-Catalyzed Carbonylation of Aromatic (Pseudo) Halides

The palladium-catalyzed carbonylation of aryl-halides or their related compounds **1** to give carboxylic acid derivatives **2** has become a valuable tool in organic synthesis.[4] The carbonylation covers a large number of closely related reactions, where all the reactions in common involve carbon monoxide incorporation into aryl-, benzyl- or vinylpalladium complexes in the presence of various nucleophiles (Scheme 1-1).

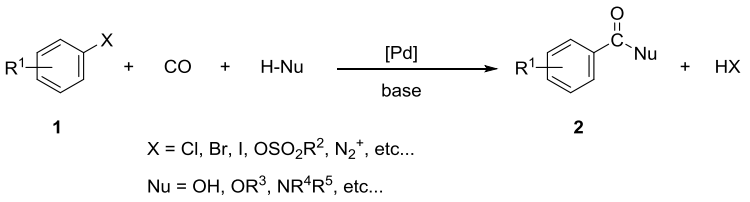

Scheme 1-1 General scheme for the carbonylation of aryl-X compounds

In general, aromatic halides are treated with an appropriate electrophile under carbon monoxide atmospheres in the presence of a catalytic amount of a palladium complex, whereby, the leaving group X is formally replaced by a nucleophile during the incorporation of one or two molecules of carbon monoxide. Typically, the reactions take place at 60–140 °C and 5–60 atm of carbon monoxide, and require a stoichiometric amount of base to regenerate the catalyst. In line with the C–X bond energy, the rate of oxidative addition of organic halide to an electronically unsaturated metal complex decreases in the order: C–I > C–OTf > C–Br>> C–Cl >> C–F. In addition to (hetero) aryl halides, alkenyl-X compounds as well as steroidal derivatives have been successfully employed as reagents.

Not only carboxylic acids, esters, and amides are accessible by carbonylation, but anhydrides, acid fluorides, aldehydes, and ketones can also be easily synthesized. The structure of product depends on a nucleophile: water (hydroxycarbonylation), alcohols (alkoxycarbonylation), amines (aminocarbonylation), carboxylate salts, fluorides, hydrides, or organometallic reagents can be used.

1.1.1.1 Palladium-Catalyzed Reductive Carbonylation

One of the most synthetically useful carbonylation reactions is the reductive carbonylation (formylation) of aryl-X or vinyl-X derivatives **3** to aromatic or *α,β*-unsaturated aldehydes **4** (Scheme 1-2).

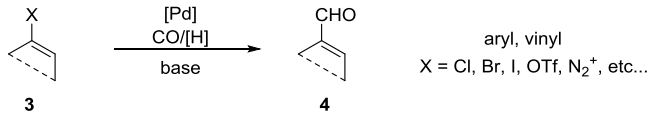

Scheme 1-2 General scheme for palladium-catalyzed reductive carbonylation reaction

It is well-known that the formyl group readily undergoes a wide range of transformations, for example, C-C and C-N coupling reactions, or reductions. The palladium-catalyzed reductive carbonylation was discovered by Schönberg and Heck in 1974.[5] However, high pressure (80–100 atm) and temperatures of 80–150 °C were essential to convert aryl and vinylbromides or iodides in the presence of synthesis gas into the corresponding aldehydes. Furthermore, a comparably large amount of $[PdX_2(PPh_3)_2]$ was required to achieve good yields. One decade later, this formylation method was improved upon by Baillargeon and Stille,[6] who employed metal hydrides as the reducing agents. Aryl iodides, benzylic halides, vinyl iodides and triflates, and allylic halides were successfully carbonylated in 2.5–3.5 h under mild conditions (50 °C, 1–3 atm CO) by using tributyltin hydride (Bu_3SnH). Despite their general application in the past, tin hydrides should not be used today because of their toxicity and waste generation. An alternative approach is based on the use of organosilanes[7] in conjunction with carbon monoxide.

1.1.1.2 Palladium-Catalyzed Carbonylative Cross-Coupling Reactions

While reductive carbonylations make use of hydrogen or hydride as a nucleophile, related carbonylative cross-coupling reactions (Carbonylative Cross-Coupling Reactions) proceed in the presence of organometallic reagents, with organoboranes or -borates, organoaluminum, organotin, organosilane, organoantimony, and organozinc compounds being the most popular. From a synthetic viewpoint, the palladium-catalyzed multicomponent cross-coupling reactions of organic electrophiles **5**, carbon monoxide, and organometallic reagents **6** are a useful method for the preparation

of (un)symmetrical ketone derivatives 7 (Scheme 1-3).

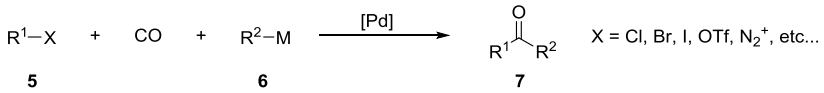

Scheme 1-3 General scheme for the three-component cross-coupling reaction

In 2011, Feng and co-workers reported the carbonylative Stille coupling reactions of 2-bromobenzyl bromides **8** with tributylallylstannane to produce 2-bromobenzyl *β,γ*-unsaturated ketones **9** in satisfactory to excellent yields (Scheme 1-4).[8] The isomerization of 2-bromobenzyl *β,γ*-unsaturated ketones **9** can readily occur under basic conditions to generate 2-bromobenzyl *α,β*-unsaturated ketones **10.** The 2-bromobenzyl *α,β*-unsaturated ketones **10** can be transformed into 2-naphthols **11** via intramolecular Heck reaction in satisfactory good yields.

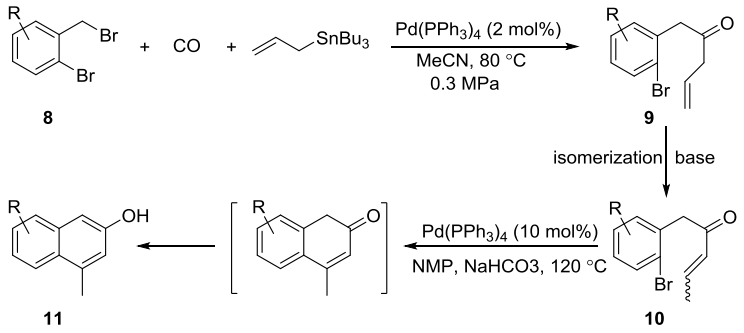

Scheme 1-4 Carbonylative Stille coupling reactions for synthesis of 2-bromobenzyl *β,γ*-unsaturated ketones

The carbonylative Suzuki coupling reaction between aryl iodides **12**, carbon monoxide (1 atm), and arylboronic acids **13** in the presence of palladium catalyst and base has been first reported by Suzuki in 1993, where unsymmetrical biaryl ketones **14** were synthesized in high yields (Scheme 1-5).[9] Boronic acids increase importance over tin compounds because they are generally nontoxic, thermally stable, inert to oxygen, and moisture. The choice of a suitable base and solvent was essential to achieve selective formation of the unsymmetrical biaryl ketones without biaryl by-products.

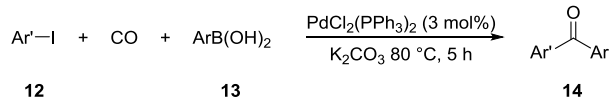

Scheme 1-5 Carbonylative Suzuki coupling reaction

Several improvements and applications of the original synthetic protocol have been described,[10] but limitations (the formation of biaryl side products, employment of additives, or restriction to special substrates) still remain.

The carbonylative three-component cross-coupling of aryl halides **15** with terminal alkynes **16** and carbon monoxide in the presence of amines as a base to give alkynyl ketones **17** is known as the carbonylative Sonogashira reaction. Typically, this reaction requires anhydrous/anaerobic conditions, relatively high CO pressures, and a copper(I) co-catalyst (Scheme 1-6).

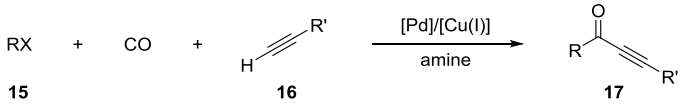

Scheme 1-6 General scheme for carbonylative Sonogashira coupling reaction

A notable modification was developed by Mohamed Ahmed and Mori in 2003 that the direct carbonylative coupling of phenylacetylene **18** with aryl iodides **19** by using 1 mol% [$PdCl_2(PPh_3)_2$] and 0.5 M aqueous ammonia in THF gave the corresponding α,β-alkynyl ketone **20** (Scheme 1-7).[11] In this case noncarbonylative coupling product was not obtained.

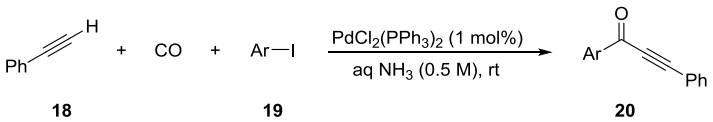

Scheme 1-7 Carbonylative Sonogashira coupling of phenylethyne with aqueous ammonia without copper(I).

1.1.2 Ruthenium-Catalyzed Carbonylation

1.1.2.1 Ruthenium-Catalyzed Carbonylative C-H Activation

The first ruthenium-catalyzed carbonylative C-H activation reaction was discovered in 1992, by Moore and co-workers.[12] Ortho-acylation of pyridine **21** and other nitrogen-containing aromatic compounds can be performed with olefins **22** and CO, using $Ru_3(CO)_{12}$ as catalyst (Scheme 1-8). The suggested mechanism for this reaction is that the coordinatively unsaturated metal center of the trinuclear cluster is attacked and coordinated by pyridine and subsequent ortho-metalation gives the key intermediate **A**. Olefin insertion to a linear and branched alkyl species followed by CO migration gives the acyl species, leading to the acylated products **23** and **24** by reductive elimination.

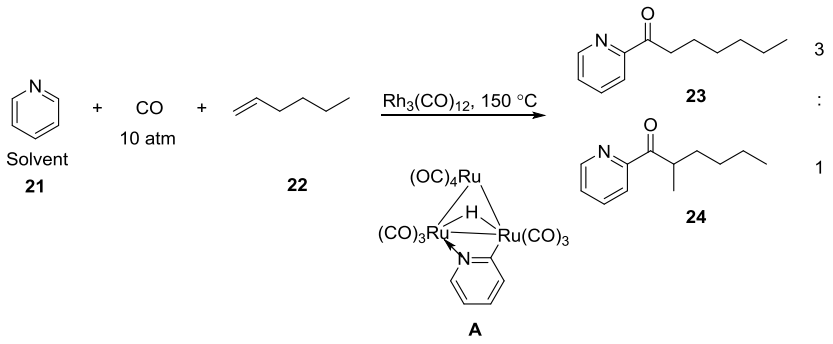

Scheme 1-8 $Ru_3(CO)_{12}$ catalyzed carbonylation of pyridine

One problem in Moore's procedure is that the reaction needs substrate as a solvent. In 1996, Murai and co-workers solved this challenge by carrying out the coupling reaction of imidazoles **25** with alkene **26** under 20 atm of CO in toluene at 160 °C for 20 h (Scheme 1-9).[13]

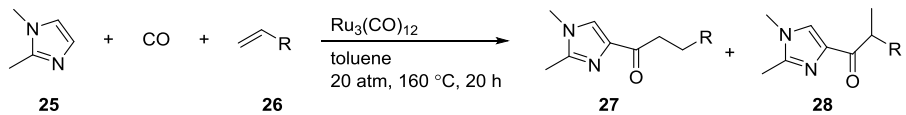

Scheme 1-9 $Ru_3(CO)_{12}$-catalyzed coupling of heteroaromatic C-H/CO/olefins.

The reaction proceeded with excellent linear selectivity (**27** > **28**). Additionally,

imidazoles, 1-methylpyrazoles could also be acylated in good yields and not only aliphatic alkenes, but styrenes could be successfully applied as the coupling partner.

1.1.2.2 Ruthenium-Catalyzed Carbonylative Lactones Synthesis

Lactones are heterocyclic rings with a widespread occurrence in natural compounds, which exhibit potential biological activities. The first ruthenium-catalysed oxidative cyclocarbonylation of 1,1-disubstituted allylic alcohols **29** to 2-furanones **30** was developed by Watanabe and co-workers in 1994 (Scheme 1-10).[14]

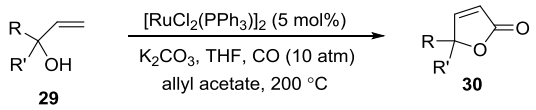

Scheme 1-10 Ruthenium-catalyzed oxidative carbonylation of allylic alcohols

In 1998, Chatani and Murai reported the first ruthenium-catalyzed cyclocarbonylation of yne-aldehydes **31** (Scheme 1-11).[15] Bicyclic α,β-unsaturated γ-butyrolactones **32** were synthesized in good to excellent yields.

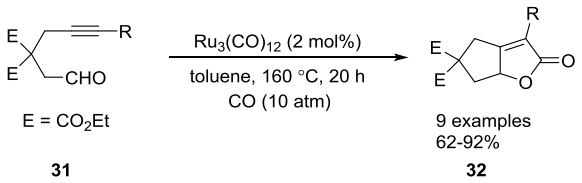

Scheme 1-11 Ruthenium-catalyzed hetero-Pauson–Khand reactions

Two possible reaction mechanisms were proposed for this transformation. One involves a ruthenium acyl intermediate I formed by the oxidative addition of an aldehyde C-H bond to the ruthenium center (Scheme 1-12a). The other involves a five membered metallacycle formed via a [2+2 +1] cycloaddition (Scheme 1-12b).

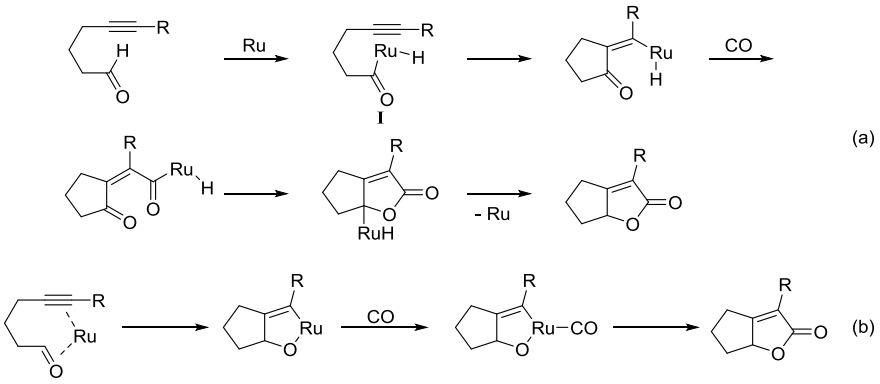

Scheme 1-12 Plausible reaction pathway involves Ru-acyl intermediate

1.1.3 Phosphine-free Rhodium-Catalyzed Carbonylations

In 2006, the group of Artok reported on a rhodium-catalyzed carbonylative arylation of internal alkynes **31** with arylboronic acids **34** yielding 5-aryl-2(5*H*)-furanones **35** in moderate to good yields (Scheme 1-13a).[16] Addition of TFA changed the structure of main product from furanone compounds to *α,β*-unsaturated ketones **36** (Scheme 1-13b).[16b, 17] By variation of catalysis, indanones **38** can be produced as the main product using triarylboroxines **37** (Scheme 1-13c).[16b]

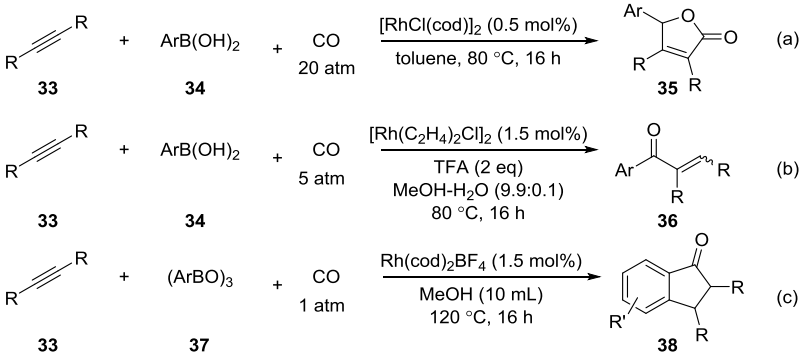

Scheme 1-13 Rhodium catalyzed carbonylation of alkynes with organoborons

In the case of terminal alkynes **39** either *α,β*-unsaturated ketones **40** (Scheme 1-14a)[18] or furans **42**[19] starting from propargylic alcohols **41** are produced (Scheme 1-14b).

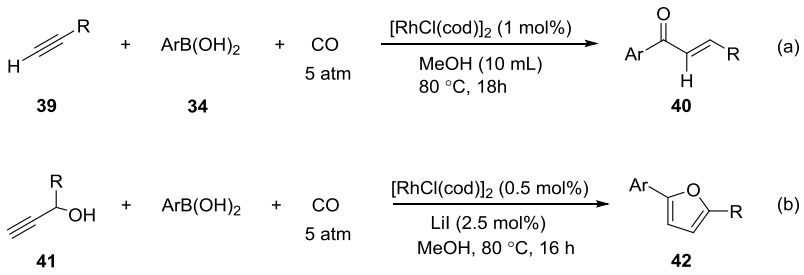

Scheme 1-14 Rhodium catalyzed carbonylation of alkynes with arylboronic acids.

In 2007, Chatani reported the carbonylative cyclization of alkynes **33** with 2-bromophenylboronic acids **43**.[20] Here, indenones **38** were produced by this novel rhodium-catalyzed carbonylation reaction (Scheme 1-15).

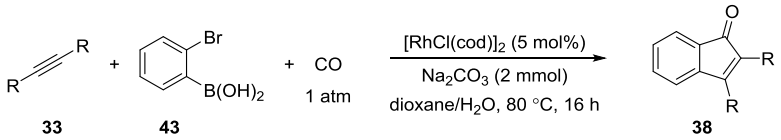

Scheme 1-15 Rh(I)-catalyzed reaction of alkynes with 2-bromophenylboronic acids and CO

The key steps in this reaction are the transmetalation of RhOH **B** with 2-bromophenylboronic acids and the subsequent insertion of an alkyne to give vinylrhodium(I) species D. The oxidative addition of C-Br bonds on the adjacent phenyl ring provides a benzorhodacyclopentene species **E**; CO insertion and reductive elimination give the desired indenone **H** (Scheme 1-16). An alkyne with a bulky and electron-withdrawing group favors the α-position of indenones, which shows that both the electronic and the steric nature of the alkyne influence the regioselectivity.

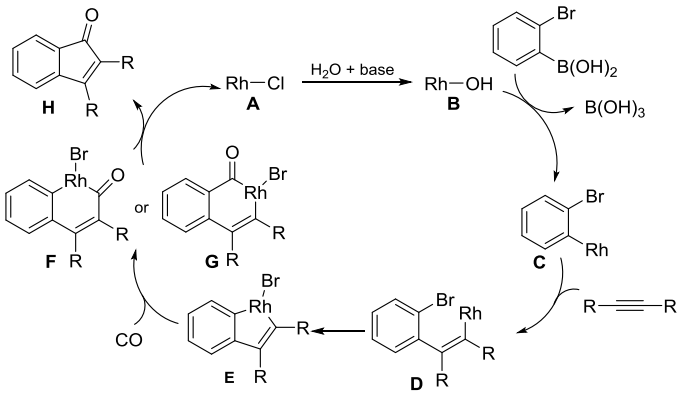

Scheme 1-16 Plausible reaction pathway for Rh(I)-catalyzed reaction of alkyne with 2-bromophenylboronic acid and CO

1.2 Easy-to-handle CO Substitutes

Carbonylation chemistry catalyzed by a variety of transition metal complexes has regained a central position *via* employing a toxic gas carbon monoxide. However, the methods suffer from some major disadvantages; the difficulty in handling toxic and gaseous carbon monoxide, including its storage and transport, represents real problems. Unfortunately, such a disadvantage reduces the overall utility of carbonylation. Recently, considerable attempts have been made to simplify the experimental manipulation and to exploit novel carbonylative transformation, that is, the CO gas-free carbonylation methods using carbonyl donors (Scheme 1-17),[21] such as formic acid,[22] formates,[23] formamides,[24] chloroform,[25] alcohols,[26] acid halides,[27] metal carbonyls,[28] and aldehydes. To our knowledge, aldehyde was used as one of the most common substitutes for carbon monoxide, especially formaldehyde.

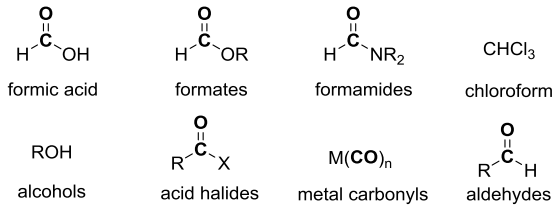

Scheme 1-17 Easy-to handle CO substitutes as carbonyl source

1.3 Formaldehyde–Sustainable Carbon Resource

Formaldehyde can be regarded as a sustainable carbon resource and has a wide source. It can be produced industrially by the catalytic oxidation of methanol (formox process). The most common catalysts are silver metal or a mixture of an iron and molybdenum or vanadium oxides. In the commonly used formox process, methanol and oxygen react at 250–400 °C in presence of iron oxide in combination with molybdenum and/or vanadium to produce formaldehyde according to the chemical equation (eq 1).[29]

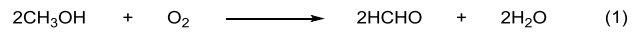

Moreover formaldehyde can be generated by carbon monoxide with hydrogen under some electric discharge conditions and even produced using carbon dioxide under some transition-metal catalysts.[30] Previous works show that formaldehyde can easily generate metal-carbonyl species during the decarbonylation process.

1.4 Synthetic Utilization of Formaldehyde as a Carbonyl Source

The group of Kakiuchi and Morimoto reported on the development of a convenient carbonylation protocol using formaldehyde as a carbonyl source and applied to this procedure to some carbonylation reactions, which results in an easily-handled transformation without the direct use of toxic CO. Some examples are showed as below.

In 2003, they have first reported the development of an aqueous catalytic Pauson–Khand-type reaction of enynes **44** in the presence of formaldehyde **45** as a water-soluble source of carbon monoxide to cyclopentenones **46** (Scheme 1-18).[31] The decarbonylation and the carbonylation processes are thought to take place independently in different phases of the reaction system, namely in the aqueous and micellar phases, respectively, which results in a more efficient catalytic carbonylation reaction. The use of the low-cost feedstock formaldehyde as the source of carbon monoxide gives rise to a

more convenient Pauson–Khand-type reaction of enynes than the conventional reactions currently in use.

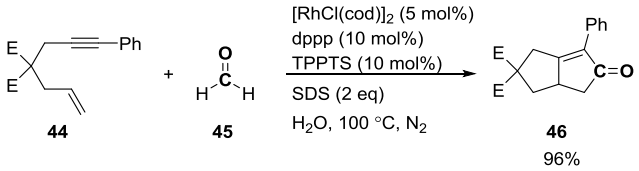

Scheme 1-18 Catalytic Pauson-Khand-type reaction of enyne in the presence of formaldehyde in an aqueous medium

In 2005, they also developed the rhodium(I)-catalyzed reaction of alkyne **47** with formaldehyde proceeds *via* the double incorporation of a carbonyl moiety derived from formaldehyde, resulting in a CO gas-free cyclohydrocarbonylation to *α*,*β*-butenolides **48** under aqueous (Scheme 1-19a) and non-aqueous reaction condition (Scheme 1-19b).[32]

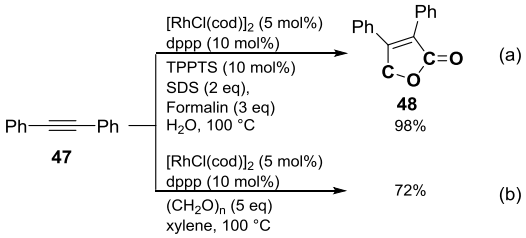

Scheme 1-19 Rh(I)-catalyzed CO gas-free cyclohydrocarbonylation of alkyne with formaldehyde to *α*,*β*-butenolides

They also described a highly linear-selective hydroformylation of 1-alkenes **47** using formaldehyde **45** without the direct use of syngas in 2010 (Scheme 1-20).[33] One rhodium(I) complex catalyzes two processes in the overall hydroformylation of 1-alkenes using formaldehyde as a syngas substitute to give hydroformylated aldehydes (**48** and **49**) with excellent regioselectivities. A high regioselectivity (linear **48** / branched **49** = up to 98/2) and chemical yield (up to 95%) can be achieved by the simultaneous use of two types of phosphanes as ligands.

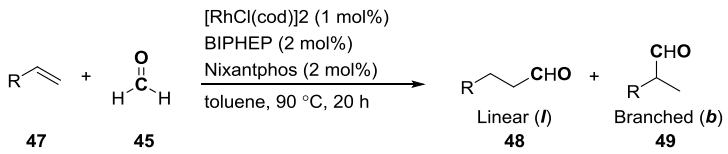

Scheme 1-20 Highly linear-selective hydroformylation of 1-alkenes using formaldehyde as a syngas substitute

In 2009, the Rh(I)-catalyzed reaction of alkynes **33** with 2-bromophenylboronic acids **43** in the presence of formaldehyde **45** resulted in a CO gas-free carbonylative cyclization reaction to give indenone derivatives **38**, which has been reported by them (Scheme 1-21).[34] The key for this efficient reaction is to control the amount of phosphines ligand so that phosphine-ligated and -free rhodium complexes are present, thus permitting both decarbonylation and carbonylation to proceed in a single catalyst system.

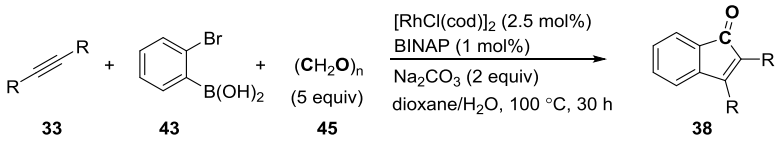

Scheme 1-21 Rh(I)-catalyzed CO gas-free carbonylative cyclization reactions of alkynes with 2-bromophenylboronic acids using formaldehyde

1.5 The Purpose of My Research

During the study of CO gas-free carbonylation synthsis involving phosphine-free and -ligated dual rhodium catalysts, I would like to apply the aforementioned CO gas-free strategy using formaldehyde as a carbonyl source to other carbonylation reactions catalyzed by phosphine-free rhodium catalyst without direct use of toxic carbon monoxide.

By controlling the amount of added phosphine ligands, the *in-situ* generated phosphine-ligated rhodium species and intact phosphine-free rhodium species would be involved in the decarbonylation and carbonylation processes, respectively (Scheme 1-22).

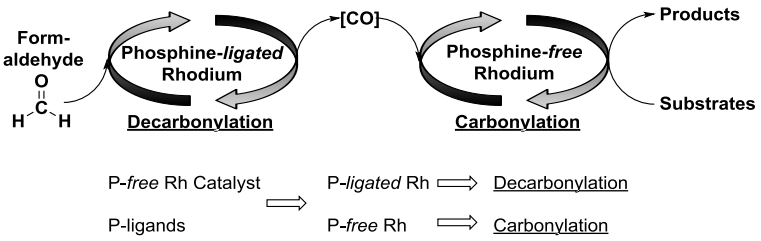

Scheme 1-22 Phosphine-free and -ligated dual rhodium catalysts for carbonylation

I study herein on the formaldehyde-substituted reactions of alkynes with arylboronic acids using such a catalyst system, leading to the arylative carbonylation to give enones and butenolides derivatives. It can substitute for the conventional phosphine-free rhodium(I)-catalyzed reaction and avoids directly employing carbon monoxide.

In this thesis, there are 3 main Chapters:

1st: Rh(I)-catalyzed arylative mono-carbonylation of alkynes with arylboronic acids using formaldehyde to enones (Chapter 2).

2nd: Rh(I)-catalyzed arylative double-carbonylation of alkynes with arylboronic acids using formaldehyde to butenolides (Chapter 3).

3rd: Summary and perspective (Chapter 4).

References

(1) Brennführer, A.; Neumann, H.; Beller, M. *Angew. Chem. Int. Ed.* **2009**, *48*, 4114.

(2) Colquhoun, H. M.; Thompson, D. J.; Twigg, M. V. Carbonylation; Springer: New York, **1991**.

(3) (a) Kollár, L. Modern Carbonylation Methods; Wiley-VCH: Weinheim, **2008**. (b) Beller, M. Catalytic Carbonylation Reaction; Springer: Berlin, **2006**.

(4) Beller, M.; Bolm, C. Transition Metals for Organic Synthesis, 2nd ed.; Wiley-VCH: Weinheim, **2004**.

(5) Schönberg, A.; Heck, R. F. *J. Am. Chem. Soc.* **1974**, *96*, 7761.

(6) (a) Baillargeon, V. P.; Stille, J. K. *J. Am. Chem. Soc.* **1983**, *105*, 7175. (b) Baillargeon, V. P.; Stille, J. K. *J. Am. Chem. Soc.* **1986**, *108*, 452.

(7) (a) Behenna, D. C.; Stockdill, J. L.; Stoltz, B. M. *Angew. Chem. Int. Ed.* **2007**, *46*, 4077. (b) Kotsuki, H.; Datta, P. K.; Suenaga, H. *Synthesis* **1996**, *1996*, 470.

(8) Dai, Y.; Feng, X.; Liu, H.; Jiang, H.; Bao, M. *J. Org. Chem.* **2011**, *76*, 10068.

(9) Ishiyama, T.; Kizaki, H.; Miyaura, N.; Suzuki, A. *Tetrahedron Lett.* **1993**, *34*, 7595.

(10) (a) Gao, S.; Wang, Q.; Chen, C. *J. Am. Chem. Soc.* **2008**, *131*, 1410. (b) Bartali, L.; Guarna, A.; Larini, P.; Occhiato, E. G. *Eur. J. Org. Chem.* **2007**, *2007*, 2152.

(11) Mohamed Ahmed, M. S.; Mori, A. *Org. Lett.* **2003**, *5*, 3057.

(12) Moore, E. J.; Pretzer, W. R.; O'Connell, T. J.; Harris, J.; LaBounty, L.; Chou, L.; Grimmer, S. S. *J. Am. Chem. Soc.* **1992**, *114*, 5888.

(13) Chatani, N.; Fukuyama, T.; Kakiuchi, F.; Murai, S. *J. Am. Chem. Soc.* **1996**, *118*, 493.

(14) Kindo, T.; Kodoi, K.; Mitsudo, T.-A.; Watanabe, Y. *J. Chem. Soc. Chem. Commun.* **1994**, 755.

(15) Chatani, N.; Morimoto, T.; Fukumoto, Y.; Murai, S. *J. Am. Chem. Soc.* **1998**, *120*, 5335.

(16) (a) Aksn, O.; Dege, N.; Artok, L.; Turkmen, H.; Cetinkaya, B. *Chem. Commun.* **2006**, 3187. (b) Artok, L.; Kuş, M.; Aksın-Artok, Ö.; Dege, F. N.; Özkılınç, F. Y. *Tetrahedron* **2009**, *65*, 9125.

(17) Kuş, M.; Artok, Ö. A.; Ziyanak, F.; Artok, L. *Synlett* **2008**, *17*, 2587.

(18) Dheur, J.; Sauthier, M.; Castanet, Y.; Mortreux, A. *Adv. Synth. Catal.* **2007**, *349*, 2499.

(19) Dheur, J.; Sauthier, M.; Castanet, Y.; Mortreux, A. *Adv. Synth. Catal.* **2010**, *352*, 557.

(20) Harada, Y.; Nakanishi, J.; Fujihara, H.; Tobisu, M.; Fukumoto, Y.; Chatani, N. *J. Am. Chem. Soc.* **2007**, *129*, 5766.

(21) Morimoto, T.; Kakiuchi, K. *Angew. Chem. Int. Ed.* **2004**, *43*, 5580.

(22) Brancour, C.; Fukuyama, T.; Mukai, Y.; Skrydstrup, T.; Ryu, I. *Org. Lett.* **2013**, *15*, 2794.

(23) Ueda, T.; Konishi, H.; Manabe, K. *Org. Lett.* **2012**, *14*, 3100.

(24) Ju, J.; Jeong, M.; Moon, J.; Jung, H. M.; Lee, S. *Org. Lett.* **2007**, *9*, 4615.

(25) Grushin, V. V.; Alper, H. *Organometallics* **1993**, *12*, 3846.

(26) Park, J. H.; Cho, Y.; Chung, Y. K. *Angew. Chem. Int. Ed.* **2010**, *49*, 5138.

(27) Bjerglund, K.; Lindhardt, A. T.; Skrydstrup, T. *J. Org. Chem.* **2012**, *77*, 3793.

(28) Nordeman, P.; Odell, L. R.; Larhed, M. *J. Org. Chem.* **2012**, *77*, 11393.

(29) Reuss, G.; Disteldorf, W.; Gamer, A. O.; Hilt, A., Formaldehyde. In *Ullmann's Encyclopedia of Industrial Chemistry*, ed.; Wiley-VCH Verlag GmbH & Co. KGaA: **2000**.

(30) Jessop, P. G.; Ikariya, T.; Noyori, R. *Chem. Rev.* **1995**, *95*, 259.

(31) Fuji, K.; Morimoto, T.; Tsutsumi, K.; Kakiuchi, K. *Angew. Chem. Int. Ed.* **2003**, *42*, 2409.

(32) Fuji, K.; Morimoto, T.; Tsutsumi, K.; Kakiuchi, K. *Chem. Commun.* **2005**, 3295.

(33) Makado, G.; Morimoto, T.; Sugimoto, Y.; Tsutsumi, K.; Kagawa, N.; Kakiuchi, K. *Adv. Synth. Catal.* **2010**, *352*, 299.

(34) Morimoto, T.; Yamasaki, K.; Hirano, A.; Tsutsumi, K.; Kagawa, N.; Kakiuchi, K.; Harada, Y.; Fukumoto, Y.; Chatani, N.; Nishioka, T. *Org. Lett.* **2009**, *11*, 1777.

CHAPTER 2 Rh(I)-Catalyzed Arylative Mono-Carbonylative of Alkynes with Arylboronic Acids Using Formaldehyde to Enones

2.1 Introduction

The discovery of convenient and easy-to-handle strategies to acquire estimable compounds derived from readily available starting materials is one of the primary goals of modern synthetic organic chemistry. During the last decades, transition-metal-catalyzed carbonylation are accepted as an interesting and important chemical transformation, both in academic and industrial research where toxic carbon monoxide (CO) is used as one of the cheapest C_1 sources.[1] Recent considerable efforts owing to green chemistry have been made to simplify the experimental procedure and to exploit novel carbonylative transformation, that is, the CO gas-free carbonylation methods using much easier handling carbonyl unit providers,[2] such as formic acid,[3] formates,[4] formamides,[5] chloroform,[6] alcohols,[7] acid halides,[8] and metal carbonyls.[9] To the best of our knowledge, aldehyde was used as a one of the most common substitutes for carbon monoxide. Several research groups have developed convenient carbonylation protocols using aldehydes as a carbonyl source.[10] In the methodology, the essential critical process is the rhodium(I)-catalyzed decarbonylation of an aldehyde as a carbonyl donor. However, effective catalyst toward carbonylation process is inconsistent with a rhodium(I)-phosphine complex with regard to the decarbonylation process normally.

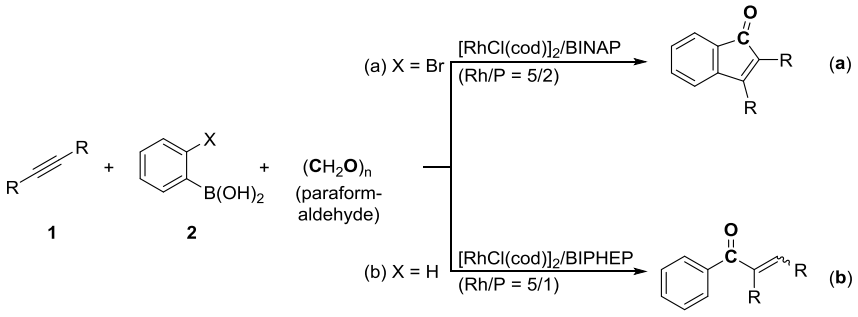

Scheme 2-1 Phosphine-free and ligated dual-Rh-catalyzed carbonylation using formaldehyde

Among the examples some research groups developed, the rhodium(I)-catalyzed CO gas-free carbonylative cyclization of alkynes **1** with 2-bromophenylboronic acid (**2**) corresponds with such a situation (Scheme 2-1a).[10g] The group of Chatani revealed the original reaction in the presence of carbon monoxide catalyzed by a phosphine-free rhodium(I) complex.[11] In this case, the group of Kakiuchi and Morimoto achieved a similar transformation using formaldehyde instead of carbon monoxide by controlling the amount of added phosphine ligand so that rhodium complexes both with and without phosphine ligand are present, thus permitting both decarbonylation of formaldehyde and carbonylative cyclization of alkynes with 2-bromophenylboronic acids and resulting carbonyl moiety to proceed in a single catalyst system. During the study of the CO gas-free carbonylation catalysis involving phosphine-free and ligated dual rhodium catalysts, I considered that the catalyst system can be applicable for another carbonylation catalyzed by a phosphine-free rhodium(I) complex. I report herein on the formaldehyde-substituted reactions of alkynes with arylboronic acids using such a catalyst system, leading to a carbonylative arylation to give enone derivatives (Scheme 2-1b). It can substitute for the conventional phosphine-free rhodium(I)-catalyzed carbonylation and avoids directly employing carbon monoxide.[12]

2.2 Results and Discussion

The group of Artok revealed that a phosphine-free rhodium(I) catalyst such as $[RhCl(C_2H_4)_2]_2$ is effective for the arylative mono-carbonylation of diphenylacetylene **1a** with phenylboronic acid **2a** using carbon monoxide to enone derivatives **3** (scheme 2-2).[12a, b]

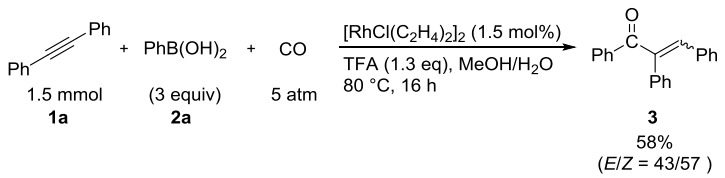

Scheme 2-2 Rh(I)-catalyzed arylative mono-carbonylation of alkynes with arylboronic acids under CO

Next, the reaction of diphenylacetylene (**1a**) with phenylboronic acid (**2a**) in the presence of paraformaldehyde was used as a model reaction.

2.2.1 Effect of BINAP

Initially I examined the reaction of **1a** with **2a** in the presence of paraformaldehyde as a carbonyl source under the catalytic reaction condition consisting of 2.5 mol% $[RhCl(cod)]_2$ and 1 mol% of BINAP in 2 mL dioxane/H_2O (100/1) at 80 °C for 20 h (Table 2-1, entry 1). This reaction conditions are the similar those which have been developed to synthesize indenone derivatives (Scheme 1-21). The reaction resulted in a CO gas-free arylative mono-carbonylation, affording enone **3aa** in 25% yield as a mixture of (*E*)- and (*Z*)-isomers in a ratio of 37 to 63, along with a 16% yield of the hydroarylated product **4aa.** The geometry of (*E*)- and (*Z*)-**3aa** was assigned by X-ray crystallographic analysis and the ORTEP drawings are shown in Figure 2-1. The ratio of the stereoisomers in **3aa** was determined by ^1H NMR analysis.

Table 2-1 Effect of BINAP in Rh(I)-Catalyzed Reaction of **1a** with **2a** Using Paraformaldehyde as a CO Source[a]

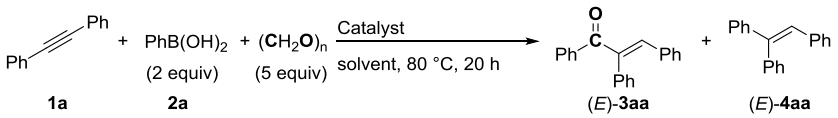

Entry	$PhB(OH)_2$ (**2a**)	Solvent	$[RhCl(cod)]_2$	BINAP	Yield(%)[b]	
		Dioxane/H_2O	(mol%)	(mol%)	**3aa**(*E*/*Z*)[c]	**4aa**
1	3 mmol	2 mL (100/1)	2.5	1	25 (37/63)	16
2				0	17 (39/61)	58
3				0.5	30 (38/62)	19
4				5	trace	trace
5			5	1	50 (34/66)	14
6	2 mmol	1 mL (100/0)	5	1	52 (36/64)	11

[a] Reaction conditions: **1a** (1 mmol), paraformaldehyde (5 mmol) at 80 °C for 20 h.

[b] Isolated yield.

[c] Determined by ^1H NMR.

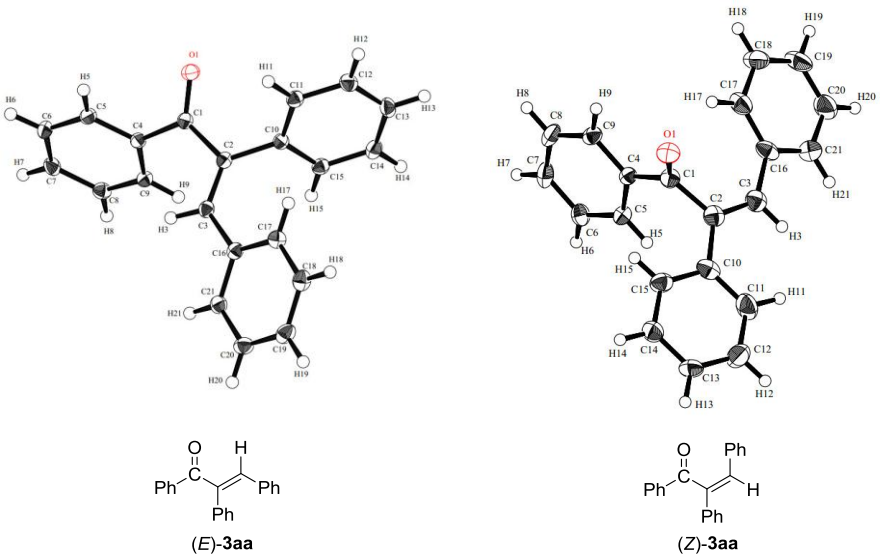

Figure 2-1 ORTEP representation of (*E*) and (*Z*)-**3aa** (50% thermal ellipsolids)

Next, I screened the amount of BINAP on the arylative mono-carbonylation (Table 2-1, entries 2 – 4). The reaction just afforded enone in 30% yield as a mixture of (*E*)- and (*Z*)-isomers in a ratio of 38 to 62 under 2.5 mol% $[RhCl(cod)]_2$ and 0.5 mol% of BINAP (Table 2-1, entry 3). Consequently, I increased the amount of catalyst and BINAP as the ratio of 5 to 1 unchanged. The reaction gave enone **3aa** in 50% yield as a mixture of (*E*)- and (*Z*)-isomers in a ratio of 34 to 66 (Table 2-1, entry 5). Furthermore, the reaction of **1a** with 2 mmol of **2a** in 1 mL dioxane without any added water slightly increased the yield of enone **3aa**, affording it in 52% yield as a mixture of (*E*)- and (*Z*)-isomers in a ratio of 36 to 64 (Table 2-1, entry 6).

2.2.2 Phosphine Ligands Screening

To elucidate the best phosphine ligand based on the established catalytic reaction condition, I examined various phosphines to the rhodium catalyst in the carbonylative arylation of **1a** with **2a**. The results are summarized in Table 2-2. With the addition of a monodentate phosphine, such as PPh_3, **3aa** was obtained in low yield of 26%, along with 54% of the hydroarylated product (*E*)-**4aa** in 54% yield (Table 2-2, entry 1). It is possible that the migratory insertion of CO in PhRhCO to PhCORh intermediate

employing PPh_3 was difficulty to proceed. Among other bidentate ligands tested (Table 2-2, entries 2 – 7), BIPHEP gave the best yield, 62% yield as a mixture of (*E*)- and (*Z*)-isomers in a ratio of 32 to 68.

In the catalytic conditions, I think that the effect of ligand for this arylative mono-carbonylation depends on the bite angle[13] (angle of P-M-P, see Scheme 2-3). Bite angle is the key factor that has a significant variation within a series of issues (the differences in electronic or steric properties are minimal) which have been applied to study the bite angle effect on the coordination mode, selectivity, and activity in the CO-transfer reaction (Figure 2-2).[14] Smaller bite angle of Rh-diphosphine complex can decrease the steric congestion around the metal center and phosphine-free Rh complex can smoothly approach the carbonyl moiety in smaller bite angle of Rh-diphosphine complex, where thus the CO moiety in phosphine-ligated Rh complex can easily be transferred to phosphine-free Rh one which is responsible for the arylative carbonylation. Increased steric hindrance of the large bite angles ligands leads to take place CO transfer step with difficulty to produce the poor yield of enones derivatives.

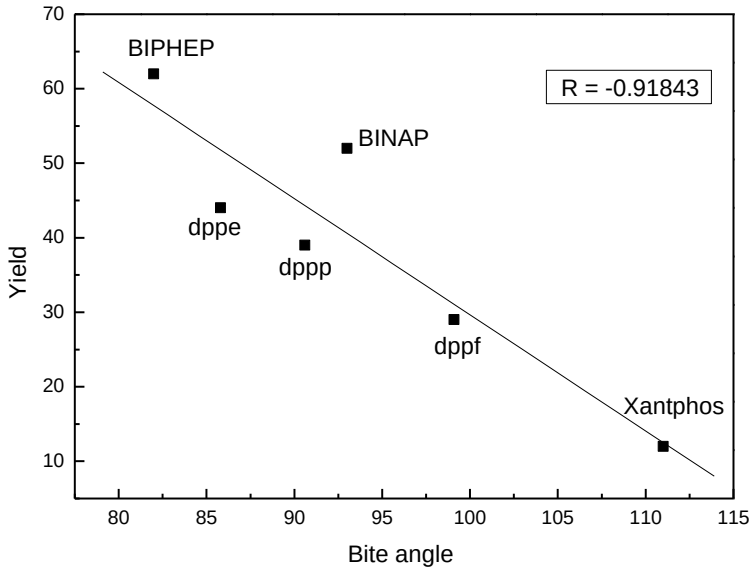

Figure 2-2 Plots of yield versus bite angle of different diphosphine ligands

Table 2-2 Screening of Phosphine Ligands in Synthesis of **3aa**[a]

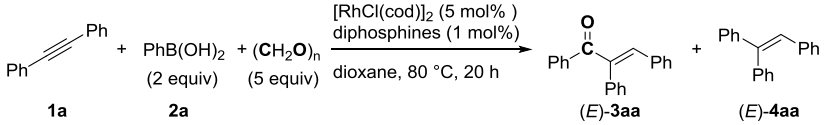

Entry	Phosphine	Yield (%)[b]	
		3aa (*E*/*Z*)[c]	(*E*)-**4aa**
1	2 Ph_3P	26 (37/63)	54
2	BINAP	52 (46/54)	11
3	Xantphos	12 (35/65)	58
4	dppe	44 (37/63)	21
5	dppp	39 (35/65)	18
6	dppf	29 (37/63)	48
7	BIPHEP	62 (32/68)	7

[a] Reaction conditions: **1** (1 mmol), **2** (2 mmol), paraformaldehyde (5 mmol), $[RhCl(cod)]_2$ (5 mol%), phosphine as ligand (1 mol%) except for Ph_3P (2 mol%) in dioxane (1 mL) at 80 °C for 20 h.

[b] Isolated yield.

[c] Determined by ^1H NMR.

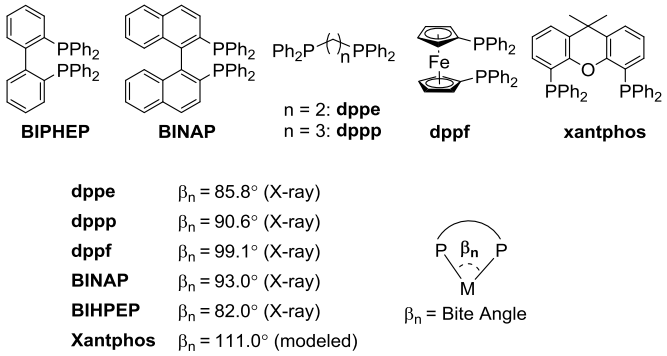

Scheme 2-3 The structure and bite angle of diphosphine ligands

2.2.3 Effect of BIPHEP

I subsequently examined varying amounts of added BIPHEP from 0 mol% to 10 mol% with keeping 5 mol% of $[RhCl(cod)]_2$ (Table 2-3, entries 1 – 5). Employing 1 mol% of BIPHEP produced the best result, 62% yield of **3aa** (Table 2-3, entry 2). The hydroarylation product **4aa** was primarily obtained in the absence of BIPHEP was absent (Table 2-3, entry 1). When 10 mol% of BIPHEP was introduced, **3aa** was

produced in much lower yield (Table 2-3, entry 5). The standard catalytic conditions for the reaction were determined to be 5 mol% of $[RhCl(cod)]_2$ and 1 mol% of BIPHEP. These results imply that $[RhCl(BIPHEP)]_2$ (*vide infra*) and $[RhCl(cod)]_2$ are predominantly involved in the decarbonylation and carbonylative arylation processes, respectively.

Table 2-3 Effect of BIPHEP in Rhodium(I)-Catalyzed Reaction of **1a** with **2a** Using Paraformaldehyde as a CO Source[a]

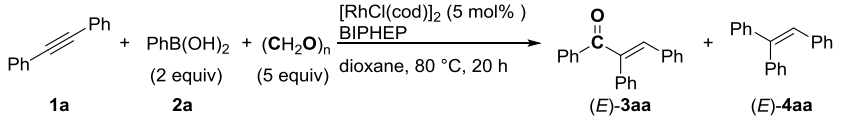

1a **2a** (*E*)-**3aa** (*E*)-**4aa**

Entry	Phosphine	Yield (%)[b]	
		3aa (*E*/*Z*)[c]	(*E*)-4aa
1	0	32 (39/61)	56
2	1	62 (32/68)	7
3	2	46 (37/63)	9
4	5	27 (35/65)	4
5[d]	10	04 (57/43)	1

[a] Reaction conditions: **1a** (1 mmol), **2a** (2 mmol), paraformaldehyde (5 mmol), $[RhCl(cod)]_2$ (5 mol%) in dioxane (1 mL) at 80 °C for 20 h.

[b] Isolated yield.

[c] Determined by ^1H NMR.

[d] A small amount of arylative double-carbonylation products (16%) were obtained, the detail is shown in the Chapter 3.

2.2.4 Diverse Arylboronic Acids on Arylative Mono-Carbonylation

With the above optimized conditions in hand, I next investigated the effect of the electronic nature of the substituent on the aromatic ring of arylboronic acids **2** on the carbonylative arylation of diphenylacetylene (**1a**). Reactions with arylboronic acids having an electron-donating group at the *para*-position of the aromatic ring, such as *p*-methoxyphenylboronic acid (**2b**) and *p*-methylphenylboronic acid (**2c**), yielded the corresponding carbonylated products **3ab** and **3ac** in 77% and 70% yields as a mixture

of *E*/*Z* isomers, along with a trace amount and a 2% yield of the hydroarylated (non-carbonylated) products **4ab** and **4ac**, respectively (Table 2-4, entries 1 and 2). On the other hand, the introduction of an electron-withdrawing group (*p*-Cl: **2d**; *p*-CF_3: **2e**) decreased the yields of the carbonylated products **3ad** (53%) and **3ae** (45%), while the yields of non-carbonylated products **4ad** and **4ae** were increased (Table 2-4, entries 4 and 5).

Table 2-4 Reactions of **1a** with Various **2** Using Paraformaldehyde as a CO Source[a]

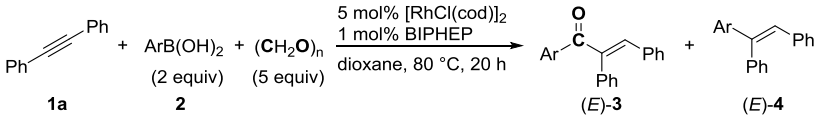

Entry	Ar (2)	Yield (%)[b]	
		3 (*E*/*Z*)[c]	(*E*)-4
1	4-$MeOC_6H_4$ (**2b**)	**3ab** 77 (26/74)	**4ab** trace
2	4-MeC_6H_4 (**2c**)	**3ac** 70 (27/73)	**4ac** 02
3	C_6H_5 (**2a**)	**3aa** 62 (32/68)	**4aa** 07
4	4-ClC_6H_4 (**2d**)	**3ad** 53 (35/65)	**4ad** 09
5	4-$CF_3C_6H_4$ (**2e**)	**3ae** 45 (41/59)	**4ae** 12
6	3-$MeOC_6H_4$ (**2f**)	**3af** 61 (28/72)	**4af** 02
7	2-$MeOC_6H_4$ (**2g**)	**3ag** 23 (30/70)	**4ag** 18

[a] Reaction conditions: **1** (1 mmol), **2** (2 mmol), paraformaldehyde (5 mmol), $[RhCl(cod)]_2$ (5 mol%), BIPHEP (1 mol%) in dioxane (1 mL) at 80 °C for 20 h.

[b] Isolated yield.

[c] Determined by ^1H NMR.

Generally, the more electron-donating R group becomes, the more smoothly the migratory insertion of the R group onto the carbonyl ligand takes place to shift the equilibrium between acyl-metals (RCO-M) and aryl-metal-carbonyls (R-M-CO), which are essential to formations of carbonylated **3** and non-carbonylated products **4**, respectively (Scheme 2-4) to the generation of the RCO-M species, due to the thermodynamic strength of the R-M bond.[15] Aryl transition metal compounds have M-C single bonds. The electron-rich R group can stabilize the aryl-metal-carbonyl (R-M-CO),

where electrons of R is donated to the vacant carbon monoxide π* orbital. Therefore, it is reasonable to say that the yields of the carbonylated product **3** increased in the case of the electron-donating group. In the present cases, the former analogue would be involved in the formation of the carbonylated products **3**, and the latter in that of non-carbonylated products **4**. Thus, as the electron-donating strength of the substituent on the aromatic ring of $ArB(OH)_2$ decreases, the yields of enones **3** decrease and those of **4** increase.

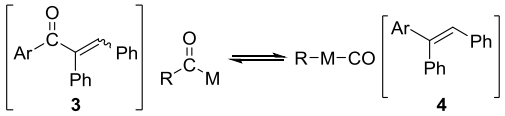

Scheme 2-4 Equilibrium between RCO-M and R-M-CO

As the position of the substituent was changed from *para* to *meta* (**2f**) and *ortho* (**2g**), the yield of the carbonylative arylation products (**3ab**, **3af**, and **3ag**) decreased, and that of the hydroarylated products (**4ab**, **4af**, and **4ag**) increased (Table 2-4, entries 1, 6 and 7). The position of the substituent has almost no impact on the ratio of the (*E*)- and (*Z*)-isomers of **3ab**, **3af**, and **3ag**. Low yield of using **2g** would be probably attributed to the steric hindrance between OMe and Rh, which make CO moiety and alkyne difficult insertion. 20% yield of **1a** was recovered (Scheme 2-5).

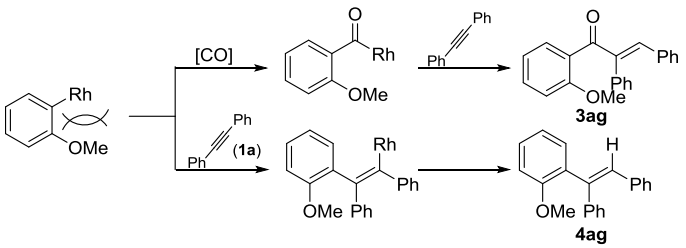

Scheme 2-5 Steric hindrance between Rh and OMe

2.2.5 Various Alkynes with Arylboronic Acids on Arylative Mono-Carbonylation

The applicability of other alkynes under the present carbonylation conditions was examined (Table 2-5). In most cases, the present method leads to the efficient formation of enone products even without trifluoroacetic acid as an additive, which is need for the reaction using carbon monoxide.[12a, b] Reactions of diphenylacetylene derivatives (**1b**) and (**1c**) with *para*-substituted electron-rich arylboronic acids *p*-$MeOC_6H_4B(OH)_2$ (**2b**) gave the corresponding enones **3bb** and **3cb** in 60% (*E*/*Z* = 32/68) and 54% (*E*/*Z* = 25/75) yields, respectively (Table 2-5, entries 1 and 4). The same tendency which is no less than that for the reactions of diphenylacetylene (**1a**) with varying electronic nature of *para*-substituted arylboronic acids **2** (Table 2-5, entries 1 – 5) has been observed. When the electron-donating strength of the substituent at the para position on the aromatic ring of $ArB(OH)_2$ adds, the yields of enone derivatives **3** increase.

Table 2-5 Reactions of Various Alkynes **1** with **2b** Using Paraformaldehyde as a CO Source[a]

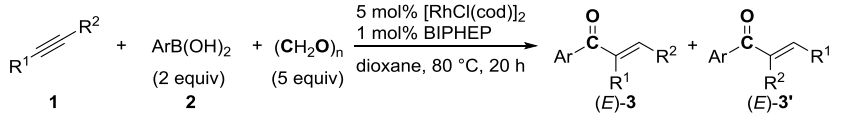

Entry	**1**	**2**	R^1	R^2	Yield (%)[b] **3** (*E*/*Z*)
1	**1b**	4-$MeOC_6H_4$ **(2b)**	4-$MeOC_6H_4$		**3bb** 60 (32/68)[c]
2		C_6H_5 (**2a**)			**3ba** 41 (37/63)[c]
3		4-$CF_3C_6H_4$ (**2e**)			**3be** 15 (40/60)[c]
4	**1c**	4-$MeOC_6H_4$ **(2b)**	4-$CF_3C_6H_4$		**3cb** 54 (25/75)[d]
5		C_6H_5 (**2a**)			**3ca** 45 (35/65)[d]
6		4-$CF_3C_6H_4$ (**2e**)			**3ce** 20 (42/58)[d]
7[e]	**1d**	4-$MeOC_6H_4$ **(2b)**	*n*-Pr		**3db** 41 (93/ 7)[d]
8	**1e**	4-$MeOC_6H_4$ **(2b)**	Me	Ph	**3eb** 42 (80/20)[c]
					3'eb 15 (37/63)[c]
9	**1f**	4-$MeOC_6H_4$ **(2b)**	*n*-Bu	Ph	**3fb** 42 (75/25)[c]
					3'fb 22 (34/66)[c]

[a] Reaction conditions: **1** (1 mmol), **2** (2 mmol), paraformaldehyde (5 mmol), $[RhCl(cod)]_2$ (5 mol%), BIPHEP (1 mol%) in dioxane (1 mL) at 80 °C for 20 h.

[b] Isolated yield.

[c] Determined by ^1H NMR.

[d] Ratios of isolated products .

[e] 2 eq of TFA was added.

An alkyl substituent (*n*-Pr) at the terminus of the alkyne was tolerant in the present reaction, although the addition of 2 equiv of trifluoroacetic acid was required (Table 2-5, entry 7). While at present the role of trifluoroacetic acid is unclear. I postulate the following two possibilities: (i) it promotes the generation of free formaldehyde from paraformaldehyde, and (ii) it accelerates the protonation of the vinylrhodium species **E** to give the product (Scheme 2-6).

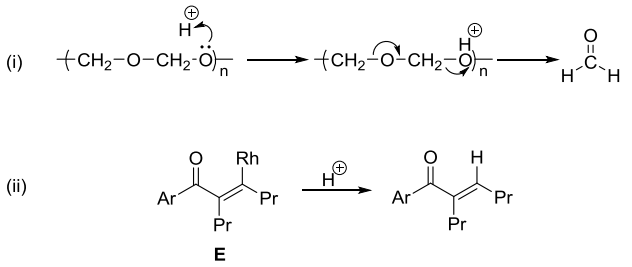

Scheme 2-6 The role of TFA

For unsymmetrical alkynes having phenyl and alkyl groups (**1e** and **1f**), the reactions proceeded with moderate regioselectivity to give predominantly the enones **3eb** and **3fb**, respectively (Table 2-5, entries 8 and 9), in both of which phenyl group is located at the *β*-position of the enones due to the steric hindrance between Ar and R_L groups (Scheme 2-7).

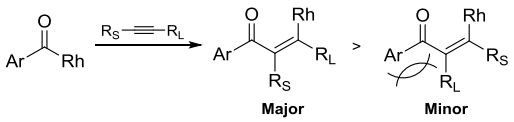

Scheme 2-7 Regioselectivity due to steric hindrance

Unfortunately, trimethylsilylacetylene derivatives with phenyl and methyl at the terminus and phenylpropargyl alcohol were not tolerated in the catalytic system.

2.2.6 Deuterium-Labelling Experiments

In order to ascertain the origin of the hydrogen at the *β*-position of the enones **3aa**, I carried out deuterium-labeling experiments. Initially, the reaction of diphenylacetylene (**1a**) with phenylboronic acid (**2a**) in the presence of paraformaldehyde-d_2 ($(CD_2O)_n$) was exposed to the above reaction conditions to give **3aa** as a mixture of (*E*)- and (*Z*)-isomers in a ratio of 34:66. A ^{1}H NMR analysis revealed that less than 2% of deuterium was incorporated into the *β*-position of the enones **3aa** (Scheme 2-8a). On the other hand, when 2,4,6-triphenylboroxine ($(PhBO)_3$) and D_2O, which should generate

the deuterated phenylboronic acid ($PhB(OD)_2$) *in situ*, was used instead of phenylboronic acid (**2a**), 76% and 87% D were incorporated into *β*-position of (*E*)- and (*Z*)-**3aa** (Scheme 2-8b). The fact that the deuteration of the *β*-position of the enones **3aa** does not reach 99% is due to H-D exchange via 1,3- and 1,4- shift of the rhodium in the intermediate **E** to other Ph rings at *β*-position.[16] Indeed, the H-integration of the aromatic ring is lower than that of **3aa** from the reaction of **1a** with $PhB(OH)_2$ using $(CH_2O)_n$. These results indicate that the origin of the hydrogen is the acidic proton of phenylboronic acid or water derived from trimerization. It is not from the hydrogen derived from the decarbonylation of formaldehyde.

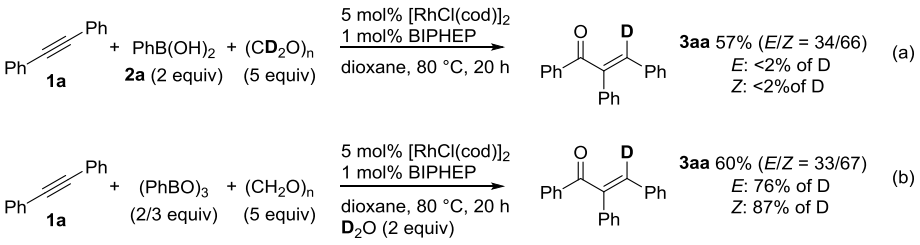

Scheme 2-8 Deuterium-labelling experiments

2.2.7 *E*/*Z*-Isomerization

2.2.7.1 *E*/*Z*-Isomerization Attempts under the Catalytic Conditions

Each of (*E*)- and (*Z*)-**3aa** isolated in pure form was introduced into the reactions of *p*-methoxyphenylboronic acid (**2b**) and alkyne (**1a**) under the standard conditions (Scheme 2-9). Each reaction gave the product **3ab** in almost the same yields and ratios. **3aa** was obtained in the same *E*/*Z*-ratio (*E*/*Z* = 32/68) in each case and that they are also same as that of the reaction in the entry 7 of Table 2-2. I speculate that Rh–H derived from Rh–Cl with H_2 is responsible for the *E*/*Z*-isomerization (*vide infra*).

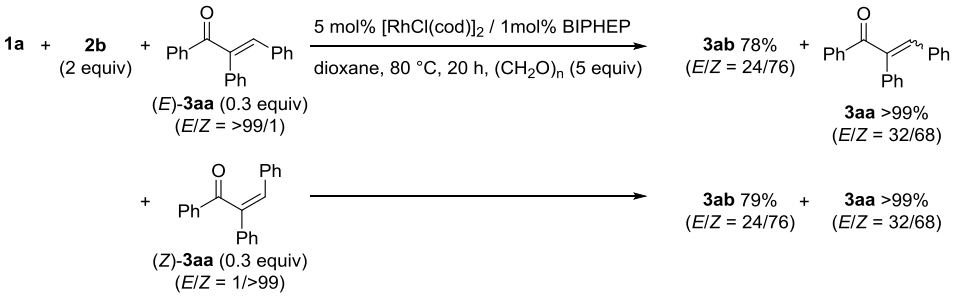

Scheme 2-9 *E*/*Z*-isomerization under reaction conditions

2.2.7.2 *E*/*Z*-Isomerization Attempts Using $RhH(CO)(PPh_3)_3$ as a Catalyst

The reaction of (*E*)- and (*Z*)-**3aa** isolated in pure form in the presence of a catalytic amount of $RhH(CO)(PPh_3)_3$ which contains Rh–H species in dioxane at 80 ℃ for 20 h gave a *E*/*Z*-mixture of **3aa** quantitative yield in a similar ratio, *E*/*Z* = 36/64 and 34/66, respectively (Scheme 2-10).

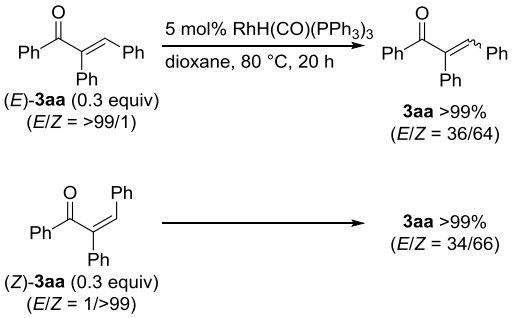

Scheme 2-10 *E*/*Z*-isomerization reactions catalyzed by $RhH(CO)(PPh_3)_3$

In the presence of the Rh–H species, *E*/*Z* isomerization proceeds *via* the hydrorhodation of Rh–H species to the primary (*E*)-enone product and the subsequent rotation of the C–C single bond, followed by the *β*–H elimination to (*Z*)-enone (Scheme 2-11).

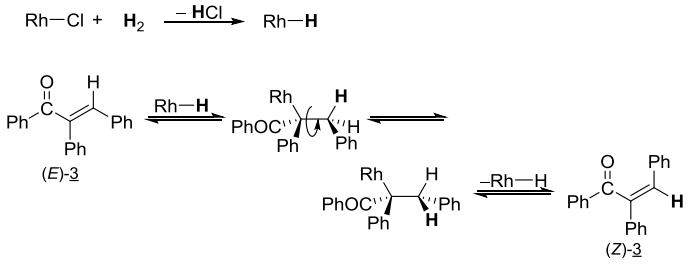

Scheme 2-11 *E*/*Z*-isomerization reactions catalyzed by Rh–H species

2.2.8 ^{31}P and ^{103}Rh NMR Experiments

^{31}P and ^{103}Rh NMR analysis in a similar mixture of $[RhCl(cod)]_2$ and BINAP (Scheme 2-12) revealed that the existence of two kinds of rhodium species, which can be assigned to $[RhCl(cod)]_2$ and $[RhCl(BINAP)]_2$ (Figures 2-2 and 2-3). Thus, as expected, it is estimated that *in situ* generated $[RhCl(BIPHEP)]_2$ and $[RhCl(cod)]_2$ are mainly involved in the decarbonylation and carbonylative arylation processes, respectively.

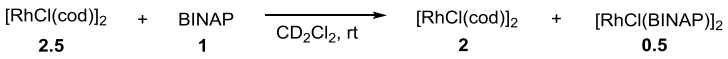

Scheme 2-12 The mixture of 2.5 mol% of $[RhCl(cod)]_2$ with 1 mol% of BINAP

^{31}P NMR Experiments. All the operations were conducted in a glove-box. The ^{31}P NMR analysis revealed that the treatment of 10 μmol of $[RhCl(cod)]_2$ with 4 μmol of BINAP in 0.65 mL of CD_2Cl_2 afforded the a doublet signal at 49.5 ppm (d, $J_{P\text{-}Rh}$ = 199 Hz) (Figures 2-3). The signal was consistent with that of $[RhCl(BINAP)]_2$, which was prepared by using the reported method.[17]

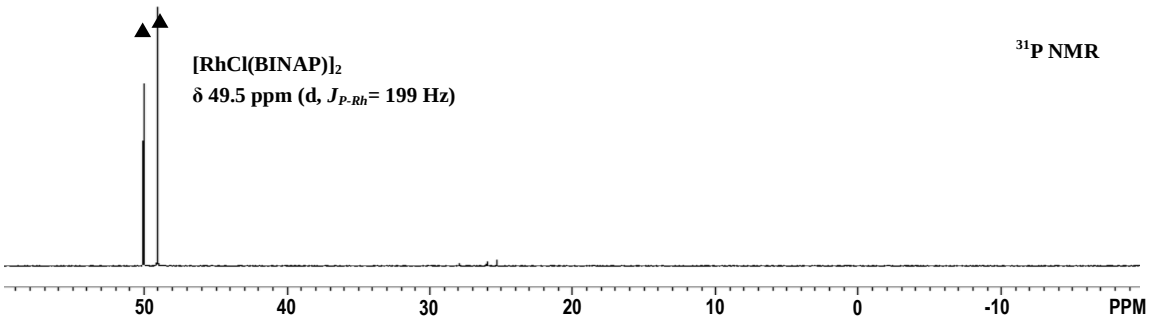

Figure 2-3 ^{31}P NMR for the mixture of 2.5 mol% of $[RhCl(cod)]_2$ with 1 mol% of BINAP

^{103}Rh NMR experiments. All the operations were conducted in a glove-box. It was clarified that, from ^{103}Rh NMR, the combination of 0.406 mmol of $[RhCl(cod)]_2$ with 0.162 mmol of BINAP in 0.65 mL of CD_2Cl_2 and 4 mL of CH_2Cl_2 afforded two signals: one was the singlet at 2438 ppm and the other was the triplet at 1620 ppm ($J_{Rh\text{-}P}$= 199 Hz) (Figures 2-4). Although the ^{103}Rh NMR analysis of $[RhCl(BINAP)]_2$ failed because of extremely low solubility in all the solvents tested ($CHCl_3$, CH_2Cl_2, acetone, benzene, and toluene), the latter one could be assigned to that of $[RhCl(BINAP)]_2$ from its coupling constant. In ^{31}P NMR experiment, a doublet signal at 49.5 ppm (d, $J_{P\text{-}Rh}$ = 199 Hz) was observed. A triplet signal at 1620 ppm ($J_{Rh\text{-}P}$ = 199 Hz) was shown in ^{103}Rh NMR experiment. Based on the same coupling constant between Rh and Phosphine ligand, I can confirm the presence of $[RhCl(BINAP)]_2$ catalyst in ^{103}Rh NMR analysis.

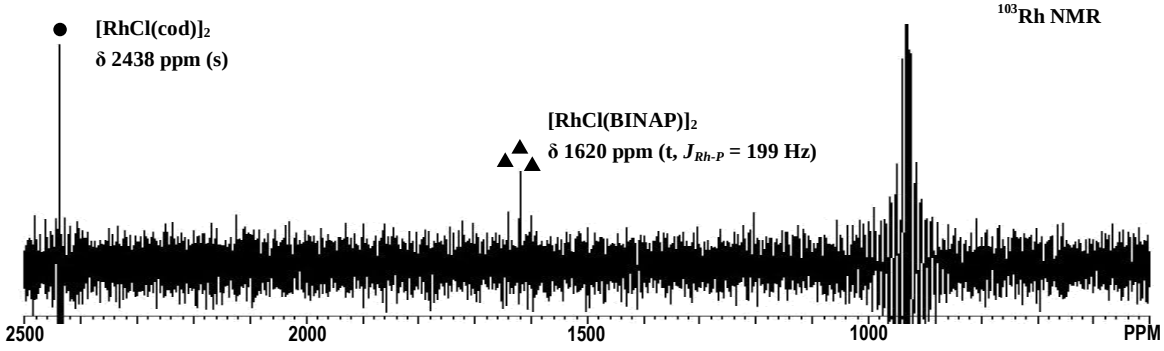

Figure 2-4 ^{103}Rh NMR for the mixture of 2.5 mol% of $[RhCl(cod)]_2$ with 1 mol% of BINAP

2.2.9 Proposed Reaction Pathway

A possible reaction pathway for the present reaction is shown in Scheme 2-13. As in our previous report,[10g] the addition of BIPHEP, the amount of which cannot account for all of the loaded rhodium metal, leads to the partial formation of a Rh-BIPHEP species, probably $[RhCl(BIPHEP)]_2$, along with the intact $[RhCl(cod)]_2$. The former BIPHEP-ligated Rh(I) species mainly decarbonylates formaldehyde to generate the carbonyl unit and hydrogen, while the latter predominantly catalyzes the actual carbonylation process. Thus, Rh–OH (**A**) generated *in situ* from Rh–Cl and H_2O is transmetalated with $PhB(OH)_2$ to generate Rh–Ph (**B**). The carbonyl moiety from the decarbonylation process is transferred to **B**, followed by the insertion of the Rh–C bond in **C** to yield Rh–COPh (**D**). The subsequent aroylrhodation to an alkyne **1** in a *syn*-manner, followed by the protonation of the formed vinylrhodium (**E**), produces the primary product, (*E*)-**3aa**, along with the regeneration of **A**. (*E*)-**3aa** isomerizes to give an equilibrium mixture of (*E*)- and (*Z*)-**3aa**, probably *via* Rh–H species generated from Rh and the decarbonylation counterpart, hydrogen.

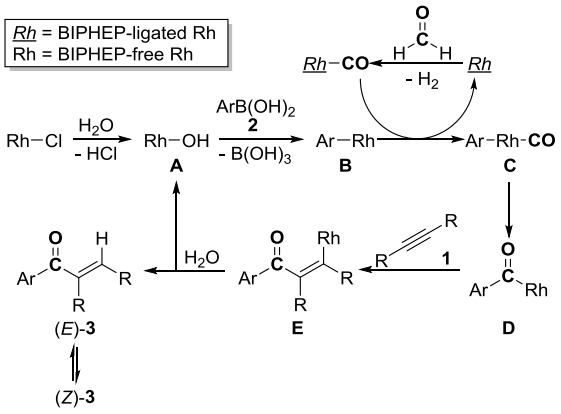

Scheme 2-13 Possible reaction pathway for the Rh-catalyzed arylative mono-carbonylation

The ^{31}P NMR analysis revealed that the combination of 2.5 mol% of $[RhCl(cod)]_2$ with 0.5 mol% of BIPHEP in 0.65 mL of $CDCl_3$ at room temperature afforded the a doublet signal at 47.9 ppm (d, $J_{P\text{-}Rh}$ = 197 Hz) (Scheme 2-14). The signal can be

assigned to $[RhCl(BIPHEP)]_2$ (Figure 2-5).

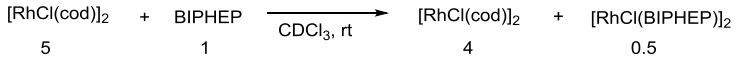

Scheme 2-14 The mixture of 5 mol% of $[RhCl(cod)]_2$ with 1 mol% of BIPHEP

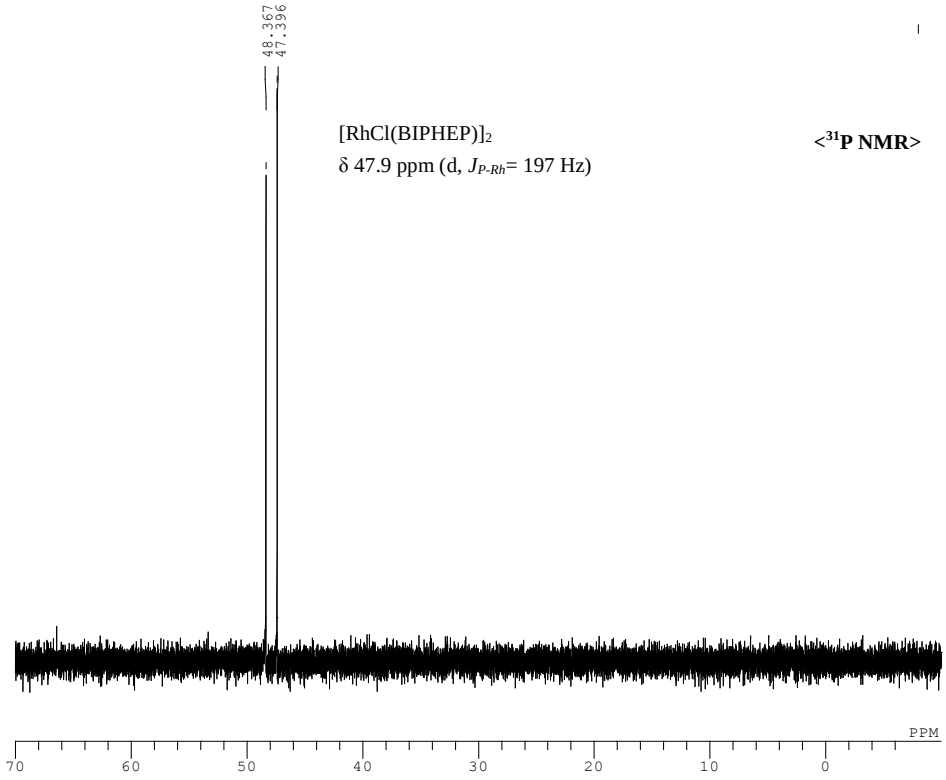

Figure 2-5 ^{31}P NMR for the mixture of 5 mol% of $[RhCl(cod)]_2$ with 1 mol% of BIPHEP

When paraformaldehyde (1 equiv) was added to the above-mentioned mixture of $[RhCl(cod)]_2$ and BIPHEP in $CDCl_3$ at room temperature, the signal at 47.9 ppm (d, $J_{P\text{-}Rh}$ = 197 Hz) weakened (e), and new signals (large proportion) were observed at 23.2 ppm (dd, $J_{P\text{-}Rh}$ = 128 Hz, $J_{P\text{-}P}$ = 47 Hz) (a) and 43.5 ppm (dd, $J_{P\text{-}Rh}$ = 162 Hz, $J_{P\text{-}P}$ = 47 Hz) (b), which are assigned to [RhCl(CO)(BIPHEP)].[10f] Another new signals were observed at 19.4 ppm (dd, $J_{P\text{-}Rh}$ = 110 Hz, $J_{P\text{-}P}$ = 35 Hz) (c) and 29.4 ppm (dd, $J_{P\text{-}Rh}$ = 117 Hz, $J_{P\text{-}P}$ = 35 Hz) (d), which are probably assigned to [RhCl(CO)(H2)(BIPHEP)].[17]

This result indicates that $[RhCl(BIPHEP)]_2$ is an effective catalyst for the decarbonylation of formaldehyde at room temperature (Figure 2-6). On the other hand, the group of Hayashi found that the rate of transmetallation step using phosphine-free Rh complex is much faster than that employing phosphine-ligated one.[16a, 18] Consequently, I can confirm that rhodium complexes both with and without BIPHEP ligand are present, permitting the decarbonylation of formaldehyde and arylative mono-carbonylation processes in this catalytic system.

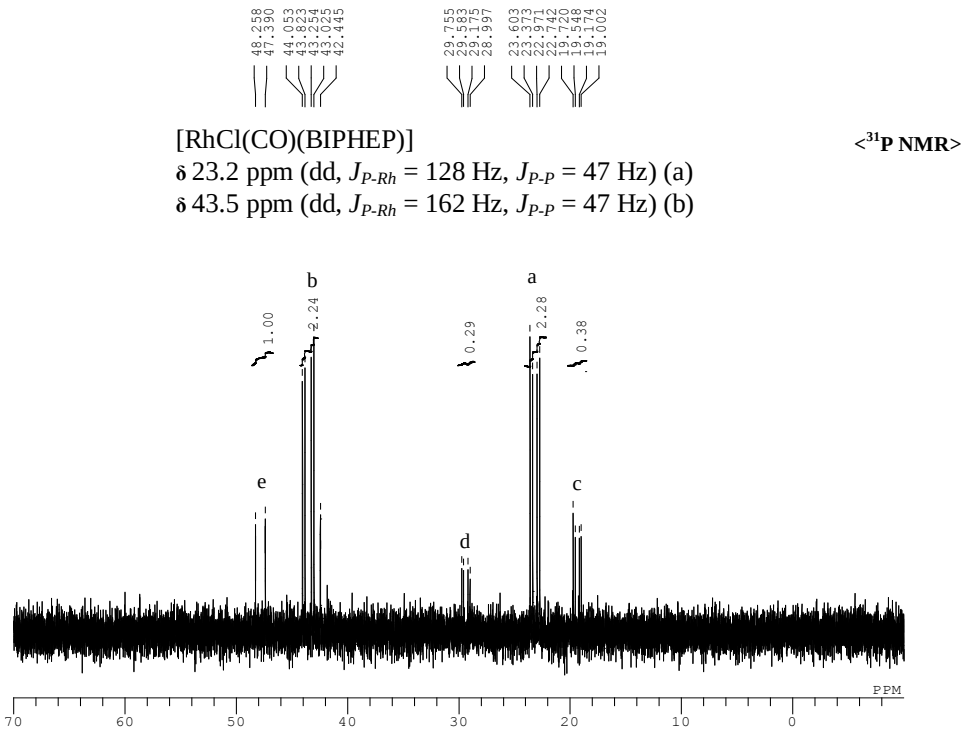

Figure 2-6 ^{31}P NMR for the mixture of 5 mol% of $[RhCl(cod)]_2$ with 1 mol% of BIPHEP in the presence of formaldehyde

Even when C_6F_5CHO, which should not generate a Rh–H species, was used as a carbonyl source, the reaction gave unselectively a mixture of (*E*)- and (*Z*)-**3aa** in 2% yield (*E*/*Z* = 37/63). The reason of the formation of trace amount of **3aa** would be attributed to relative low temperature that is difficult to take place decarbonylation of

C_6F_5CHO. Propably, *E*/*Z* isomerization proceeds *via* rotation of the C–C single bond of intermediate **F** derived from enol–ketone tautomerism (Scheme 2-15), differing from the mechanism as mentioned in Scheme 2-11. The group of Artok have observed the similar result when carbon monoxide was employed as a CO source.[12a, b]

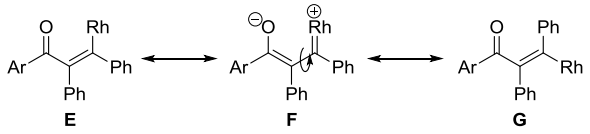

Scheme 2-15 Isomerization of vinylrhodium intermidate **E**

I have excluded the possibility that is the nucleophilic substitution reaction of Rh–Ph with formaldehyde, which obtain $PhCH_2ORh$ (**H**) followed by *β*-H elimination to afford benzaldehyde.[19] Obtained benzaldehyde could not generate PhCORhH intermediate (**I**) *via* oxidative addition of C–H bond, followed by acylrhodation to diphenylacetylene (**1a**), yielding enone **3aa** (Scheme 2-16). It is possible that a competition pathway to the decarbonylation of benzaldehyde operates to give smoothly Rh–CO and benzene.

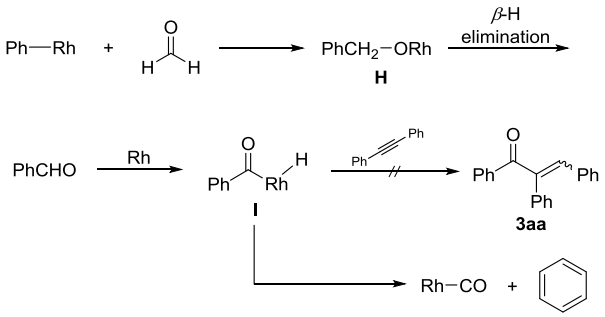

Scheme 2-16 Elimination of plausible reaction pathway for the formation of enone

In order to confirm the above-mentioned reaction pathway that doesn't take place, I introduced *para*-methoxy substituted benzaldehyde into the reaction of **1a** with **2a** in the presence of formaldehyde under optimized reaction condition, I recovered more than 99% yield of *para*-methoxy substituted benzaldehyde and isolated enone **3ab** in trace amount (Scheme 2-17). So with this result in hand, I can exclude the aforementioned

plausible pathway (Scheme 2-16).

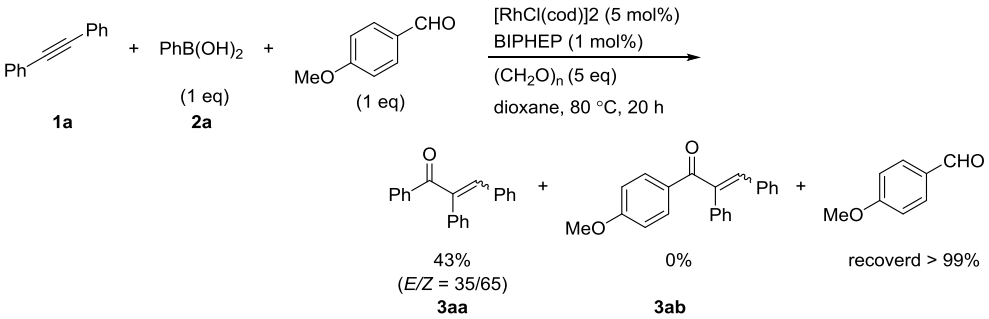

Scheme 2-17 *Para*-methoxy substituted benzaldehyde introduced into general reaction

2.3 Conclusion

In this chapter, I report on the Rh(I)-catalysed carbonylative arylation of alkynes with various arylboronic acids in the presence of formaldehyde as a carbonyl source, resulting in a CO gas-free reaction to afford enones derivatives. The addition of BIPHEP, the amount of which must not account for all the total phosphine-free rhodium complex $[RhCl(cod)]_2$ leads to the partial formation of phosphine-ligated complex $[RhCl(BIPHEP)]_2$ along with intact $[RhCl(cod)]_2$, which are mainly involved in the decarbonylation of formaldehyde to produce a carbonyl moiety and the subsequent carbonylative arylation of alkynes with arylboronic acids using the resulting carbonyl moiety, respectively, leading to an efficient carbonylative arylation to produce α,β-enones (Scheme 2-18).

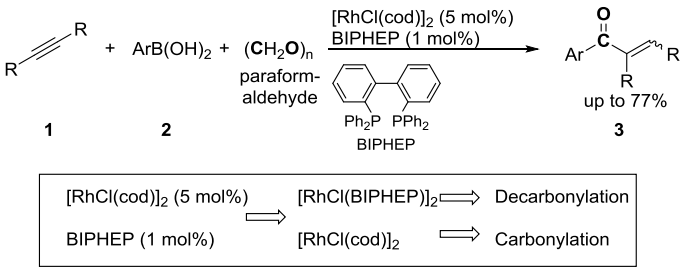

Scheme 2-18 Rh(I)-catalyzed arylative mono-carbonylation of alkynes with arylboronic acids in the presence of formaldehyde

2.4 Experiment Section

2.4.1 General measurement

^{1}H NMR and ^{13}C NMR were recorded on a JEOL JNM-ECP500 spectrometer in $CDCl_3$ using tetramethylsilane (0 ppm) as an internal standard and ^{31}P NMR was also recorded on a JEOL JNM-ECP500 spectrometer in CD_2Cl_2 with phosphoric acid (0 ppm) as an external standard. ^{103}Rh NMR was recorded on a JEOL Lambda300WB spectrometer using CD_2Cl_2 with $[C_5M_5RhCl_2]_2$ (3678 ppm) as an external standard. Data are reported as follows: chemical shift in ppm (δ), multiplicity (s = singlet, d = doublet, t = triplet, q = quartet, and m = multiplet), coupling constant (Hz), integration, and interpretation. Infrared spectra (IR) were obtained on a JASCO FT/IR-420 spectrometer. Mass spectra were obtained on a JEOL JMS-700. X-ray crystallography was performed on Rigaku R-AXIS RAPID/S imaging plate diffractometer. Column chromatography was performed using a SiO_2 (MERCK Silica gel 60).

2.4.2 Materials

$[RhCl(cod)]_2$ was prepared using the reported method.[20] 2,2'-Bis(diphenylphosphino) biphenyl (BIPHEP) was purchased by STREM CHEMICALS, INC. and used directly without further purification. 1,2-Diphenylethyne (**1a**) was purchased by Tokyo Chemical Industry Co,. Ltd. and used directly without further purification. Oct-4-yne (**1d**), prop-1-yn-1-ylbenzene (**1e**) and arylboronic acids (**2**) were purchased by Wako Pure Chemical Industries, Ltd. and used directly without further purification. Paraformaldehyde was purchased by Wako Pure Chemical Industries, Ltd. and dried with P_2O_5 under vacumn prior to use. 1, 4-Dioxane dehydrated was purchased by Wako Pure Chemical Industries, Ltd. and dried with 4A molecular sieve, which was degassed using freeze-pump-thaw method for 3 times and stored in glove box.

Synthesis of starting materials: (1b) and (1c)

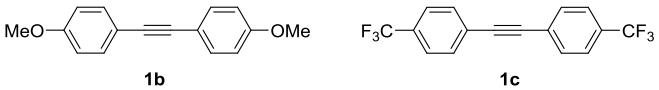

1b **1c**

1,2-Bis(4-methoxyphenyl)ethyne (**1b**), 1,2-bis(4-(trifluoromethyl)phenyl)ethyne (**1c**) were synthesized from the commercially available starting materials according to a general procedure:[21]

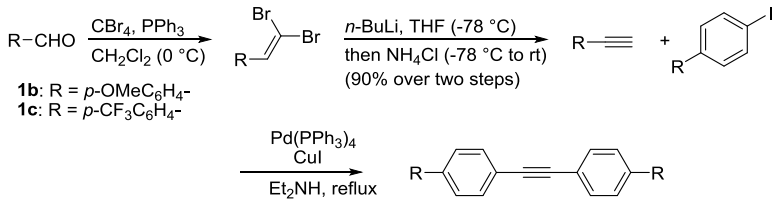

PPh_3 (3.0 equiv.) was added to a solution of CBr_4 (1.5 equiv.) in CH_2Cl_2 at 0 °C, and subsequently stirred for 15 min. A solution of the aldehyde (0.1 mol) in CH_2Cl_2 was added dropwise over 3 min and the mixture was stirred for an additional 30 min. The solvent was then removed under reduced pressure and a mixture of hexane/AcOEt (1:1) was added. The resulting mixture was filtered through a plug of silica. After the filtration, the silica plug was washed several times with hexane/AcOEt (1:1). The solvent of the combined filtrated was evaporated. A mixture of hexane/AcOEt (5:1) was added to the solid residue. The resulting solution was filtered again through a plug of silica to remove triphenylphosphine oxide and the solvent was removed under reduced pressure to yield dibromo-olefins.

Dibromo-olefin (0.1 mol) was then dissolved in dry THF and cooled to -78 °C under N_2. *n*-BuLi (4.0 equiv.) was added dropwise over 30 min and the solution was stirred at -78 °C for 2h, followed by the addition of 100 mL saturated NH_4Cl solution, and warmed to room temperature. The two layers were separated and the aqueous phase was extracted with ether. The combined organic phase was washed with brine, dried over $MgSO_4$, filtered and concentrated. The residue was purified by flash chromatography

(hexane/AcOEt).

Sonogashira coupling reaction: desired terminal alkyne and 1-iodo-4-methoxybenzene or 1-iodo-4-(trifluoromethyl)benzene (mole ratio: 1.2:1) were dissolved in pre-dried Et_2NH at r.t. under N_2. Subsequently, $Pd(PPh_3)_4$ (5 mol%) and CuI (10 mol%) were then added in the mixture under N_2 which was stirred under reflux. The resulting precipitate was filtered over silica. The solvent was removed and the residue was purified by column chromatography on silica to give relevant internal alkyne in 85% yield as white solid (hexane/AcOEt as the eluent).

Synthesis of starting material: hex-1-yn-1-ylbenzene (1f)

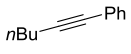

1f

Sonogashira coupling reaction: hex-1-yne and iodobenzene (mole ratio: 1.2:1) were dissolved in pre-dried Et_2NH at r.t. under N_2. Subsequently, $Pd(PPh_3)_4$ (5 mol%) and CuI (10 mol%) were then added in the mixture under N_2 which was stirred under reflux. The resulting reaction mixture was filtered over silica. The solvent was removed and the residue was purified by column chromatography on silica to give relevant internal alkyne in 92% yield as colorless liquid (hexane as the eluent).

1,2-Bis(4-methoxyphenyl)ethyne (1b)

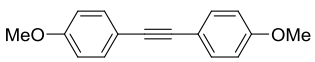

1b

Colorless solid; mp 140.8-142.2 °C; R_f 0.15; (hexane/AcOEt = 10/1); ^{1}H NMR (500 MHz, $CDCl_3$) δ: 3.83 (s, 6H), 6.86-6.89 (m, 4H), 7.44-7.47 (m, 4H); ^{13}C NMR (125 MHz, $CDCl_3$) δ: 55.3, 87.9, 113.9, 115.6, 1328, 159.3; IR (neat, cm^{-1}) 2965, 2837, 1606, 1566, 1518, 1457, 1440, 1302, 1285, 1171, 1024, 834; MS (EI): *m/z* (%) = 238 (99) [M^+], 223 (65), 195 (25), 180 (8), 152 (15), 119 (5), 83 (5); HRMS: *m/z* calcd [M^+]: 238.0994, found 238.0994.

1,2-Bis(4-(trifluoromethyl)phenyl)ethyne (1c)

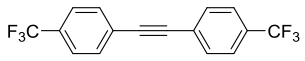

1c

Colorless solid; mp 106.2-107.0 °C; R_f 0.44; (hexane); ^{1}H NMR (500 MHz, $CDCl_3$) δ: 7.63-7.67 (m, 8H); ^{13}C NMR (125 MHz, $CDCl_3$) δ: 90.1, 123.8 (q, $^1J_{C\text{-}F}$ = 270.6 Hz), 125.4 (q, $^3J_{C\text{-}F}$ = 3.6 Hz), 126.3, 130.4 (q, $^2J_{C\text{-}F}$ = 32.3 Hz), 132.0; IR (neat, cm^{-1}) 2918, 2850, 1614, 1406, 1332, 1173, 1135, 1067, 1018, 840; MS (EI): *m/z* (%) = 314 (99) [M^+], 295 (25), 264 (15), 245 (6), 225 (8), 194 (5), 176 (5), 107 (5), 75 (2); HRMS: *m/z* calcd [M^+]: 314.0530, found 314.0529.

Hex-1-yn-1-ylbenzene (1f)

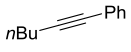

1f

Colorless liquid; R_f 0.38 (hexane); ^{1}H NMR (500 MHz, $CDCl_3$) δ: 0.95 (t, *J* = 7.5 Hz 3H), 1.44-1.52 (m, 2H), 1.55-1.62 (m, 2H), 2.41 (t, *J* = 7.0 Hz 2H), 7.25-7.29 (m, 3H), 7.38-7.40 (m.2H); ^{13}C NMR (125 MHz, $CDCl_3$) δ: 13.6, 19.1, 22.0, 30.8, 80.5, 90.3, 124.0, 127.4, 128.1, 131.5; IR (neat, cm^{-1}) 2957, 2932, 2871, 2231, 1598, 1489, 1441, 1069, 912, 754, 691; MS (EI): *m/z* (%) = 159 ($M+1^+$, 12), 158 (M^+, 99), 143 (92), 115 (63), 102 (10), 89 (9), 63 (7), 51 (3); HRMS: *m/z* calcd [M^+]: 158.1096, found 158.1095.

2.4.3 Typical procedure for the Rh(I)-catalyzed carbonylative arylation of alkyne with arylboronic acid in the presence of formaldehyde

In a 10mL screw-capped vial were placed $[RhCl(cod)]_2$ (24.6 mg, 0.05 mmol), BIPHEP (5.3 mg, 0.01 mmol), alkyne **1** (1 mmol), arylboronic acid **2** (2 mmol),

paraformaldehyde (150.2 mg, 5 mmol), and 1,4-dioxane (1 mL). The mixture was degassed by three freeze-pump-thaw cycles and then sealed under N_2. The mixture was stirred at 80 °C for 20 h, cooled to room temperature and then concentrated *in vacuo*. The residue was purified by flash chromatography on silica gel.

(*Z*)-1,2,3-Triphenyl-2-propen-1-one ((*Z*)-3aa)

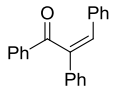

(*Z*)-**3aa**

Colorless solid; mp 85.0-86.7 °C; R_f 0.20 (hexane/AcOEt = 30/1); ^{1}H NMR (500 MHz, $CDCl_3$) δ: 7.14-7.21 (m, 4H), 7.29-7.32 (m, 3H), 7.34-7.38 (m, 4H), 7.46-7.50 (m, 3H), 7.99 (d, J = 7.5 Hz, 2H); ^{13}C NMR (125 MHz, $CDCl_3$) δ: 126.3, 128.0, 128.1, 128.4, 128.7, 128.7, 128.8, 129.6, 130.0, 133.6, 135.3, 136.2, 137.9, 140.7, 199.3; IR (neat, cm^{-1}) 3057, 3025, 2924, 2359, 1666 (C=O), 1596, 1579, 1448, 1224; MS (EI): *m/z* (%) = 284 (100) [M^+], 283 (21), 206 (12), 179 (35), 178 (53), 167 (18), 105 (82), 77 (42), 60 (11), 57 (15), 55 (11); HRMS: *m/z* calcd [M^+]: 284.1201, found 284.1201.

Crystallographic data for (*Z*)-**3aa** is as follows: $C_{21}H_{16}O$, *M*r = 284.36, colorless, block, 0.180 × 0.090 × 0.080 mm, monoclinic, Primitive, a = 9.4396(2) Å, b = 11.0396(2) Å, c = 14.6225(3) Å, β = 91.1326(7) °, V = 1523.50(5) Å^3, Z = 4, ρ_c = 1.240 g/cm^3, μ = 0.745 cm^{-1}, T = 123 K, λ = 0.71075 Å, 25829 reflections, 3490 unique [*R*(int) = 0.0271), Final *GoF* = 1.084, R_1 = 0.0725 ([$I > 2.00\sigma(I)$]), *w*R_2 = 0.1876 (all data). CCDC No.: 982719.

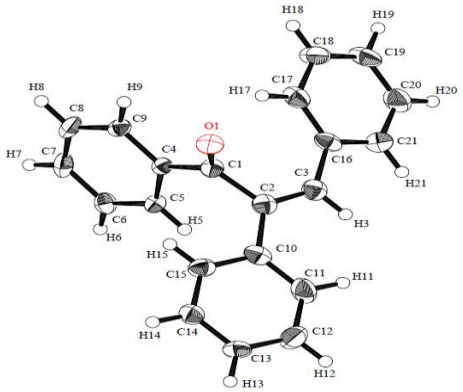

Figure 1 ORTEP representation of (*Z*)-**3aa** (50% thermal ellipsolids)

(*E*)-1,2,3-Triphenyl-2-propen-1-one ((*E*)-3aa)

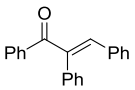

(*E*)-**3aa**

Colorless solid; mp 100.1–101.2 °C; R_f 0.14 (hexane/AcOEt = 30/1); ^{1}H NMR (500 MHz, $CDCl_3$) δ: 7.09 (d, *J* = 7.5 Hz, 2H), 7.16–7.23 (m, 4H), 7.27-7.29 (m, 2H), 7.33-7.36 (m, 3H) 7.45 (t, *J* = 8.0 Hz, 2H), 7.54 (t, *J* = 7.0, 1H), 7.86 (d, *J* = 7.0 Hz, 2H); ^{13}C NMR (125 MHz, $CDCl_3$) δ: 127.9, 128.2, 128.3, 128.8, 128.9, 129.6, 129.8, 130.3, 132.1, 134.7, 136.5, 138.1, 140.2, 140.7, 197.6; IR (neat, cm^{-1}) 3047, 3021, 1644 (C=O), 1595, 1576, 1444, 1250; MS (EI): *m/z* (%) = 284 (87) [M^+], 283 (33), 207 (13), 206 (20), 180 (10), 179 (60), 178 (82), 167 (32), 152 (15), 105 (100), 77 (60), 51 (14); HRMS: *m/z* calcd [M^+]: 284.1201, found 284.1200.

Crystallographic data for (*E*)-**3aa** is as follows: $C_{21}H_{16}O$, *M*r = 284.36, colorless, block, 0.210 × 0.110 × 0.100 mm, monoclinic, Primitive, *a* = 13.5721(3) Å, *b* = 5.7294(1) Å, *c* = 18.9083(4) Å, *β* = 93.4163(7) º, *V* = 1467.68(5) Å^3, *Z* = 4, ρ_c = 1.287 g/cm^3, μ = 0.773 cm^{-1}, *T* = 123 K, λ = 0.71075 Å, 13939 reflections, 3367 unique [*R*(int) = 0.0187), Final *GoF* = 1.134, R_1 = 0.0449 ([$I > 2.00\sigma(I)$]), wR_2 = 0.1174 (all data). CCDC No.: 982715.

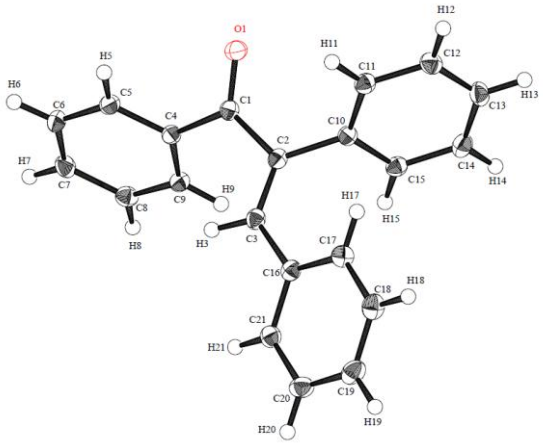

Figure 2 ORTEP representation of (*E*)-**3aa** (50% thermal ellipsolids)

Triphenylethylene ((*E*)-4aa)

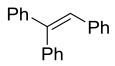

(*E*)-**4aa**

Colorless oil; R_f 0.31 (hexane); ^{1}H NMR (500 MHz, $CDCl_3$) δ: 6.99 (s, 2H), 7.04–7.07 (m, 2H), 7.11–7.17 (m, 3H), 7.20–7.25 (m, 2H), 7.26–7.38 (m, 8H); ^{13}C NMR (125 MHz, $CDCl_3$) δ: 126.7, 127.4, 127.5, 127.6, 127.9, 128.1, 128.2, 128.6, 129.5, 130.4, 137.4, 140.3, 142.6, 143.4; IR (neat, cm^{-1}) 3021, 1716, 1540, 1507, 1489, 1445, 1075, 1029, 760, 694, 588; MS (EI): *m/z* (%) = 257 (23) [M+1$^+$], 256 (100) [M$^+$], 255 (25), 241(11), 215 (5), 178 (26), 165 (9), 135 (12), 83(4), 69 (7), 57(10); HRMS: *m/z* calcd [M$^+$]: 256.1252, found 256.1252.

Products of Deuterium-Labelling Experiments

(*Z*)-1,2,3-Triphenyl-2-propen-1-one ((*Z*)-3aa)

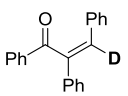

3aa
Z: 87% of D

Colorless solid; mp 85.3-86.7 °C; ^{1}H NMR (500 MHz, $CDCl_3$) δ: 7.14-7.21 (m, 3H), 7.29-7.32 (m, 3H), 7.34-7.38 (m, 4H), 7.46-7.50 (m, 3H), 7.99 (d, *J* = 7.5 Hz, 2H).

(*E*)-1,2,3-Triphenyl-2-propen-1-one ((*E*)-3aa)

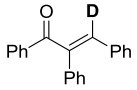

3aa
E: 76% of D

Colorless solid; mp 100.1–101.6 °C; ^{1}H NMR (500 MHz, $CDCl_3$) δ: 7.09 (d, *J* = 7.5 Hz, 2H), 7.16–7.23 (m, 3H), 7.27-7.29 (m, 2H), 7.33-7.36 (m, 3H) 7.45 (t, *J* = 8.0 Hz, 2H), 7.54 (t, *J* = 7.0, 1H), 7.86 (d, *J* = 7.0 Hz, 2H).

(*Z*)-1,2,3-Triphenyl-2-propen-1-one ((*Z*)-3aa)

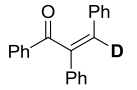

3aa
Z: <2% of D

Colorless solid; mp 85.3-86.7 °C; ^{1}H NMR (500 MHz, $CDCl_3$) δ: 7.14-7.21 (m, 4H), 7.29-7.32 (m, 3H), 7.34-7.38 (m, 4H), 7.46-7.50 (m, 3H), 7.99 (d, *J* = 7.5 Hz, 2H).

(*E*)-1,2,3-Triphenyl-2-propen-1-one ((*E*)-3aa)

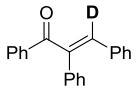

3aa
E: <2% of D

Colorless solid; mp 100.1–101.6 °C; ^{1}H NMR (500 MHz, $CDCl_3$) δ: 7.09 (d, *J* = 7.5 Hz, 2H), 7.16–7.23 (m, 4H), 7.27-7.29 (m, 2H), 7.33-7.36 (m, 3H) 7.45 (t, *J* = 8.0 Hz, 2H), 7.54 (t, *J* = 7.0, 1H), 7.86 (d, *J* = 7.0 Hz, 2H).

(*Z*)-1-(*p*-Methoxyphenyl)-2,3-diphenyl-2-propen-1-one ((*Z*)-3ab)

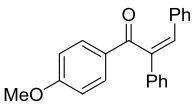

(*Z*)-**3ab**

Colorless solid; mp 88.5-89.9 °C; R_f 0.18 (hexane/AcOEt = 20/1). ^{1}H NMR (500 MHz, $CDCl_3$) δ: 3.80 (s, 3H), 6.83 (d, *J* = 8.5, 2H), 7.13–7.22 (m, 4H),7.27–7.36 (m, 5H), 7.47 (d, *J* = 8.0, 2H), 7.97 (d, *J* = 8.5, 2H); ^{13}C NMR (125 MHz, $CDCl_3$) δ: 55.3, 114.0, 126.2, 127.9, 128.1, 128.4, 128.8, 129.4, 129.5, 132.0, 135.4, 138.1, 140.9, 163.9, 197.8; IR (neat, cm^{-1}) 3056, 3026, 2932, 2839, 1658 (C=O), 1652, 1595, 1575, 1508, 1258, 1235, 1164; MS (EI): *m/z* (%) = 316 (27) [M+2$^+$], 315 (68) [M+1$^+$], 314 (100) [M$^+$,], 286 (38), 236 (21), 198 (21), 197 (62), 179 (55), 178 (68), 177 (47), 176 (52), 152 (41), 136 (56), 135 (100), 107 (52), 92 (57), 85 (31), 83 (47), 77 (60), 64 (26), 51 (23); HRMS: *m/z* calcd [M$^+$]: 314.1307, found 314.1308.

Crystallographic data for (*Z*)-**3ab** is as follows: $C_{22}H_{18}O_2$, *M*r = 314.38, colorless, block, 0.150 x 0.110 × 0.080 mm, monoclinic, Primitive, *a* = 5.9337(3) Å, *b* = 16.7259(8) Å, *c* = 16.9156(7) Å, *β* = 101.092(1) º, *V* = 1647.5(2) Å^3, *Z* = 4, ρ_c = 1.267 g/cm^3, *μ* = 0.798 cm^{-1}, *T* = 123 K, *λ* = 0.71075 Å, 16055 reflections, 3768 unique [*R*(int) = 0.0298), Final *GoF* = 1.055, R_1 = 0.0584 ([*I* > 2.00σ(*I*)]), *w*R_2 = 0.1392 (all data). CCDC No.: 982709.

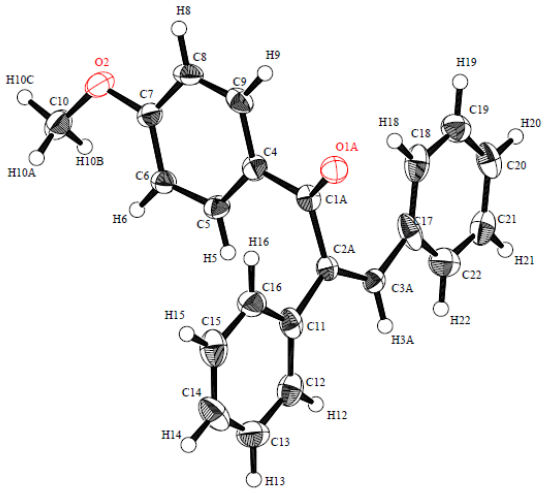

Figure 3 ORTEP representation of (*Z*)-**3ab** (50% thermal ellipsolids)

(*E*)-1-(*p*-Methoxyphenyl)-2,3-diphenyl-2-propen-1-one ((*E*)-3ab)

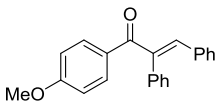

(*E*)-**3ab**

Colorless oil; R_f 0.18 (hexane/AcOEt = 20/1); ^{1}H NMR (500 MHz, $CDCl_3$) δ: 3.87 (s, 3H), 6.92 (d, *J* = 8.5, 2H), 7.11 (d, *J* = 7.5 Hz, 2H), 7.14 (s, 1H), 7.15–7.24 (m, 3H), 7.27–7.37 (m, 5H), 7.90 (d, *J* = 8.5, 2H); ^{13}C NMR (125 MHz, $CDCl_3$) δ: 55.5, 113.6, 127.9, 128.2, 128.6, 128.8, 129.5, 130.2, 130.4, 132.3, 135.0, 136.8, 137.8, 141.0, 163.1, 196.3; IR (neat, cm^{-1}) 3056, 2931, 2838, 1646 (C=O), 1599, 1574, 1312, 1508, 1253, 1166, 1027; MS (EI): *m/z* (%) = 316 (21) [M+2$^+$], 315 (70) [M+1$^+$], 314 (96) [M$^+$], 286 (25), 236 (22), 221 (17), 198 (18), 197 (63), 179 (57), 178 (76), 177 (37), 176 (48), 152 (33), 151 (22), 149 (34), 136 (56), 135 (100), 107 (50), 92 (53), 86 (60), 84 (71), 77 (65), 57 (52); HRMS: *m/z* calcd [M$^+$]: 314.1307, found 314.1305.

(*Z*)-1-(*p*-Methylphenyl)-2,3-diphenyl-2-propen-1-one ((*Z*)-3ac)

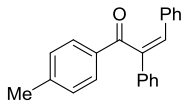

(*Z*)-**3ac**

Colorless oil; R_f 0.18 (hexane/AcOEt = 30/1); ^{1}H NMR (500 MHz, $CDCl_3$) δ: 2.33 (s, 3H), 7.12–7.21 (m, 6H), 7.26–7.36 (m, 5H), 7.46 (d, *J* = 7.5, 2H), 7.89 (d, *J* = 8.5, 2H); ^{13}C NMR (125 MHz, $CDCl_3$) δ: 21.7, 126.3, 127.9, 128.1, 128.4, 128.8, 129.5, 129.7, 129.9, 133.9, 135.4, 138.1, 140.9, 144.6, 199.0; IR (neat, cm^{-1}) 3056, 3025, 1663 (C=O), 1605, 1492, 1448, 1227, 1174; MS (EI): *m/z* (%) = 299 (12) [M+1$^+$], 298 (52) [M$^+$], 179 (12), 178 (28), 119 (100), 91 (39), 65 (13); HRMS: *m/z* calcd [M$^+$]: 298.1358, found 298.1357.

(*E*)-1-(*p*-Methylphenyl)-2,3-diphenyl-2-propen-1-one ((*E*)-3ac)

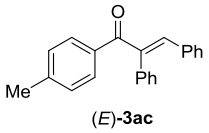

(*E*)-**3ac**

Colorless solid; mp 88.1-89.3 °C; R_f 0.14 (hexane/AcOEt = 30/1); ^{1}H NMR (500 MHz, $CDCl_3$) δ: 2.41 (s, 3H), 7.09 (d, *J* = 6.5, 2H), 7.15–7.37 (m, 11H), 7.79 (d, *J* = 8.5, 2H); ^{13}C NMR (125 MHz, $CDCl_3$) δ: 21.6, 127.8 128.2, 128.7, 128.7, 129.0, 129.6, 130.0, 130.2, 134.9, 135.3, 136.6, 139.1, 140.9, 143.0, 197.3; IR (neat, cm^{-1}) 3044, 1644 (C=O), 1605, 1494, 1448, 1381, 1318, 1264, 1181, 1064; MS (EI): *m/z* (%) = 299 (53) [M+1$^+$], 298 (71) [M$^+$], 297 (25), 236 (35), 221 (43), 220 (40), 182 (27), 181 (61), 180 (26), 179 (63), 178 (87), 177 (52), 176 (51), 152 (62), 151 (53), 119 (100); HRMS: *m/z* calcd [M$^+$]: 298.1358, found 298.1357.

Crystallographic data for (*E*)-**3ac** is as follows: $C_{22}H_{18}O$, *M*r = 298.38, colorless, block, 0.180 × 0.140 × 0.120 mm, orthorhombic, Primitive, *a* = 5.5301(2) Å, *b* = 8.0317(2) Å, *c* = 37.0417(7) Å, *V* = 1645.25(7) Å^3, *Z* = 4, ρ_c = 1.205 g/cm^3, μ = 0.721 cm^{-1}, *T* = 123 K, λ = 0.71075 Å, 28474 reflections, 3773 unique [*R*(int) = 0.0286), Final *GoF* = 1.112, R_1 = 0.0609 ([$I > 2.00\sigma(I)$]), *w*R_2 = 0.1478 (all data). CCDC No.: 982708.

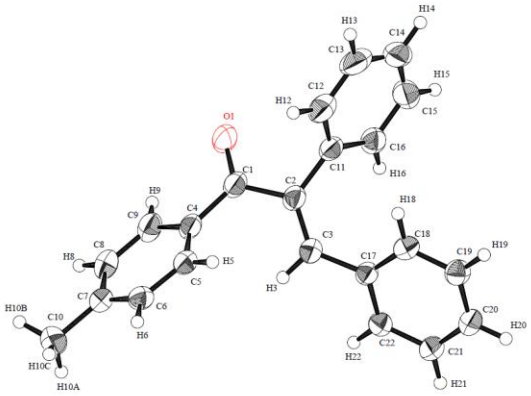

Figure 4 ORTEP representation of (*E*)-**3ac** (50% thermal ellipsolids)

(1-(*p*-Tolyl)-ethene-1,2-diyl)dibenzene ((*E*)-4ac)

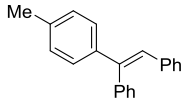

(*E*)-**4ac**

Colorless oil; *Rf:* 0.32 *(*Hexane); ^{1}H NMR (500 MHz, $CDCl_3$) δ: 2.35 (s, 3H), 6.94 (s, 1H), 7.01 (d, *J* = 8 Hz, 2H), 7.10-7.12 (m, 5H), 7.19-7.22 (m, 4H), 7.31-7.33 (m, 3H); ^{13}C NMR (125 MHz, $CDCl_3$) δ: 21.12, 126.6, 127.5, 127.9, 128.9, 129.5, 130.3, 137.4, 137.5, 140.5, 142.4; IR (neat, cm^{-1}) 3020, 1707, 1596, 1509, 1444, 1217, 1028, 862, 811, 755, 695, 632, 586, 511; MS (EI): *m/z* (%) = 271 (22) [M+1$^+$], 270 (100) [M$^+$], 269 (12), 255 (25), 178 (40), 126 (16), 83 (20), 51 (13); HRMS: *m/z* calcd [M$^+$]: 270.1409, found 270.1407.

(*Z*)-1-(*p*-Chlorophenyl)-2,3-diphenyl-2-propen-1-one ((*Z*)-3ad)

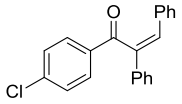

(*Z*)-**3ad**

Colorless solid; mp 104.3-105.6 °C; R_f 0.31 (hexane/AcOEt = 20/1); ^{1}H NMR (500 MHz, $CDCl_3$) δ: 7.14–7.21 (m, 4H), 7.24–7.37 (m, 7H), 7.44 (d, *J* = 8.0 Hz, 2H), 7.91 (d, *J* = 7.5 Hz, 2H); ^{13}C NMR (125 MHz, $CDCl_3$) δ: 126.3, 128.2, 128.3, 128.5, 128.8, 128.9, 129.1, 130.4, 131.0, 134.7, 135.2, 137.7, 140.1, 140.3, 198.1; IR (neat, cm^{-1}) 3082, 3057, 3023, 1663 (C=O), 1596, 1584, 1494, 1450, 1401, 1223, 1176, 1090, 1011; MS (EI): *m/z* (%) = 321 (10) [M+3$^+$], 320 (44) [M+2$^+$], 319 (42) [M+1$^+$], 318 (100) [M$^+$], 317 (32), 283 (47), 206 (12), 179 (38), 178 (48), 139 (50), 111 (16). HRMS: *m/z* calcd [M$^+$]: 318.0811, found 318.0810.

Crystallographic data for (*Z*)-**3ad** is as follows: $C_{21}H_{15}ClO$, *M*r = 318.80, colorless, block, 0.180 × 0.080 × 0.070 mm, monoclinic, Primitive, *a* = 5.8633(2) Å, *b* = 16.0703(4) Å, *c* = 17.1381(4) Å, *β*= 101.1664(7) °, *V* = 1584.27(6) Å^3, *Z* = 4, ρ_c = 1.336 g/cm^3, μ = 2.424 cm^{-1}, *T* = 123 K, λ = 0.71075 Å, 15557 reflections, 3631 unique [*R*(int) = 0.0244), Final *GoF* = 1.137, R_1 = 0.0524 ([$I > 2.00\sigma(I)$]), *w*R_2 = 0.1284 (all

data). CCDC No.: 982713.

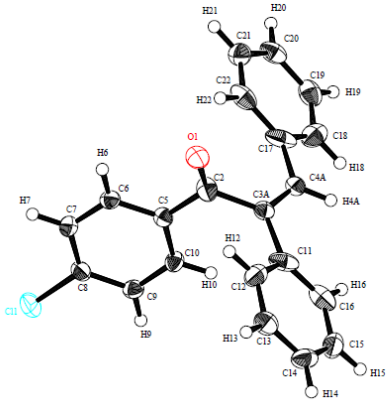

Figure 5 ORTEP representation of (*Z*)-**3ad** (50% thermal ellipsolids)

(*E*)-1-(*p*-Chlorophenyl)-2,3-diphenyl-2-propen-1-one ((*E*)-3ad)

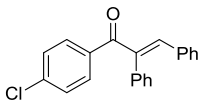

(*E*)-**3ad**

Colorless solid; mp 89.3-90.1 °C; R_f 0.26 (hexane/AcOEt = 20/1); ^{1}H NMR (500 MHz, $CDCl_3$) δ: 7.09 (d, *J* = 7.0 Hz, 2H), 7.19 (t, J = 7.5 Hz, 2H), 7.20–7.27 (m, 4H), 7.31–7.37 (m, 3H), 7.40 (d, *J* = 7.5 Hz, 2H), 7.78 (d, *J* = 8.0 Hz, 2H); ^{13}C NMR (125 MHz, $CDCl_3$) δ: 128.0, 128.3, 128.6, 128.8, 129.1, 129.6, 130.4, 131.1, 134.6, 136.2, 136.4, 138.5, 140.2, 140.4, 196.3; IR (neat, cm^{-1}) 3054, 3025, 1647 (C=O), 1592, 1443, 1257, 1087, 1013; MS (EI): *m/z* (%) = 321 (10) [M+3$^+$], 320 (48) [M+2$^+$], 319 (44) [M+1$^+$], 318 (M$^+$, 100), 317 (37), 283 (57), 201 (12), 180 (12), 179 (72), 178 (79), 177 (13), 176 (16), 152 (14), 141 (24), 139 (77), 111 (19). HRMS: *m/z* calcd [M$^+$]: 318.0811, found 318.0810.

Crystallographic data for (*E*)-**3ad** is as follows: $C_{21}H_{15}ClO$, *M*r = 318.80, colorless, block, 0.160 × 0.100 × 0.040 mm, monoclinic, Primitive, *a* = 13.9308(7) Å, *b* = 5.7298(3) Å, *c* = 20.307(1) Å, β = 102.919(1) °, *V* = 1579.9(2) Å^3, *Z* = 4, ρ_c = 1.340 g/cm^3, μ = 2.430 cm^{-1}, *T* = 123 K, λ = 0.71075 Å, 14900 reflections, 3633 unique

[*R*(int) = 0.0315), Final *GoF* = 1.139, R_1 = 0.0527 ([$I > 2.00\sigma(I)$]), wR_2 = 0.1562 (all data). CCDC No.: 982711.

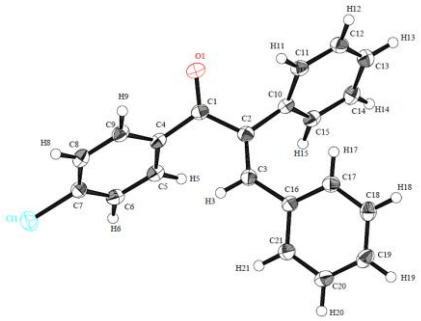

Figure 6 ORTEP representation of (*E*)-**3ad** (50% thermal ellipsolids)

(1-(4-Chlorophenyl)ethene-1,2-diyl)dibenzene ((*E*)-4ad)

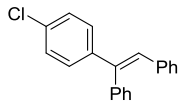

(*E*)-**4ad**

Colorless oil; R_f 0.36 (Hexane); ^{1}H NMR (500 MHz, $CDCl_3$) δ: 6.94 (s, 1H), 7.01-7.02 (m, 2H), 7.11-7.12 (m, 3H), 7.17-7.18 (m, 2H), 7.25-7.28 (m, 4H), 7.32-7.34 (m, 3H); ^{13}C NMR (125 MHz, $CDCl_3$) δ: 126.5, 126.9, 127.6, 128.0, 128.3, 130.0, 130.3, 133.3, 137.0, 139.9, 141.4, 141.9; IR (neat, cm^{-1}) 3021, 1490, 1444, 1420, 1091, 1012, 818, 775, 757, 695, 515; MS (EI): *m/z* (%) = 292 (32) [M+2$^+$], 291 (25) [M+1$^+$], 290 (99) [M$^+$], 253 (21), 178 (29), 126 (11), 77 (6), 51 (8); HRMS: *m/z* calcd [M$^+$]: 290.0862, found 290.0860.

(*Z*)-2,3-Diphenyl-1-(*p*-trifuluorophenylphenyl)-2-propen-1-one ((*Z*)-3ae)

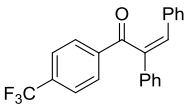

(*Z*)-**3ae**

Colorless solid; mp 105.3-107.2 ℃; R_f 0.26 (hexane/AcOEt = 30/1); ^{1}H NMR (500

MHz, $CDCl_3$) δ: 7.14–7.22 (m, 3H), 7.24–7.28 (m, 3H), 7.29–7.39 (m, 3H), 7.44 (d, *J* = 7.5, 2H), 7.61 (d, J = 8.5 Hz, 2H), 8.07 (d, *J* = 8.0, 2H); ^{13}C NMR (125 MHz, $CDCl_3$) δ: 123.5 (q, $^1J_{C\text{-}F}$= 273 Hz), 125.8 (q, $^3J_{C\text{-}F}$= 3.8 Hz), 126.4, 128.4, 128.5, 128.6, 128.8, 129.0, 129.9, 131.0, 134.6 (q, $^2J_{C\text{-}F}$ = 32.6 Hz), 135.1, 137.5, 138.9, 140.2, 198.3; IR (neat, cm^{-1}) 3069, 1672 (C=O), 1580, 1497, 1450, 1412, 1325, 1228, 1170, 1124, 1067, 1015; MS (EI): *m/z* (%) = 353 (15) [M+1$^+$], 352 (57) [M$^+$], 351 (21), 219 (10), 207 (12), 181 (12), 180 (16), 179 (95), 178 (100), 177 (43), 176 (35), 175 (11), 174 (11), 173 (63), 152 (26), 151 (19), 146 (11), 145 (67), 133 (40), 131 (21) 126 (15), 125 (16), 121 (11), 119 (21), 103 (28), 102 (22), 101 (24), 95 (20), 89 (45), 88 (42), 87 (43), 77 (25), 75 (35) 73 (41), 72 (20), 69 (41), 59 (41), 58 (36), 57 (29); HRMS: *m/z* calcd [M$^+$]: 352.1075, found 352.1076.

Crystallographic data for (*Z*)-**3ae** is as follows: $C_{22}H_{15}F_3O$, *M*r = 352.36, colorless, block, 0.190 × 0.180 × 0.170 mm, monoclinic, C-centered, *a* = 26.3108(9) Å, *b* = 8.0797(3) Å, *c* = 17.2065(5) Å, *β* = 110.2319(9) º, *V* = 3432.1(2) Å^3, *Z* = 8, ρ_c = 1.364 g/cm^3, *μ* = 1.046 cm^{-1}, *T* = 123 K, *λ* = 0.71075 Å, 16564 reflections, 3934 unique [*R*(int) = 0.0230), Final *GoF* = 1.104, R_1 = 0.0610 ([*I* > 2.00σ(*I*)]), *w*R_2 = 0.1563 (all data). CCDC No.: 982710.

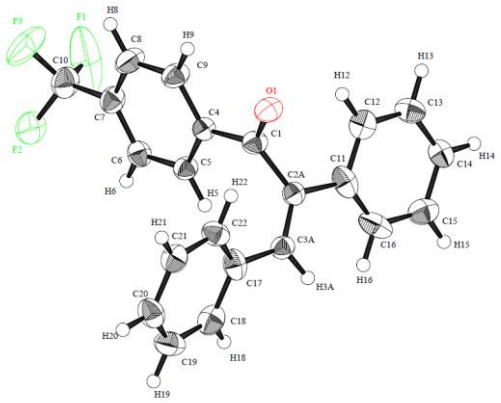

Figure 7 ORTEP representation of (*Z*)-**3ae** (50% thermal ellipsolids)

(*E*)-2,3-Diphenyl-1-(*p*-trifuluorophenylphenyl)-2-propen-1-one ((*E*)-3ae)

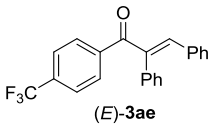

(*E*)-**3ae**

Colorless solid; mp 116.1-117.2 °C; R_f 0.17 (hexane/AcOEt = 30/1); ^{1}H NMR (500 MHz, $CDCl_3$) δ: 7.09 (d, *J* = 8.0, 2H), 7.16–7.21 (m, 2H), 7.22–7.28 (m, 4H), 7.33–7.40 (m, 3H), 7.70 (d, *J* = 8.0, 2H), 7.91 (d, *J* = 8.0, 2H); ^{13}C NMR (125 MHz, $CDCl_3$,.) δ: 123.7 (q, $^1J_{C\text{-}F}$ = 273 Hz), 125.3 (q, $^3J_{C\text{-}F}$ = 1.5 Hz), 128.2, 128.3, 128.8, 128.9, 129.4, 129.6, 129.8, 130.5, 133.3 (q, $^2J_{C\text{-}F}$ = 32.6 Hz), 134.4, 135.9, 140.3, 141.5, 141.9, 196.4; IR (neat, cm^{-1}) 3052, 1650 (C=O), 1493, 1443, 1405, 1332, 1255, 1167, 1142, 1108, 1069, 1016; MS (EI): *m/z* (*%*) = 353 (11) [M+1$^+$], 352 (36) [M$^+$], 351 (11), 341 (11), 295 (12), 257 (13), 256 (16), 255 (12), 237 (15), 236 (32), 221 (26), 180 (19), 179 (71), 178 (86), 177 (22), 176 (21), 173 (45), 152 (38), 149 (31), 145 (51), 137 (71), 136 (49), 127 (53), 123 (50), 121 (52), 109 (53), 95 (100), 82 (85), 57 (80); HRMS: *m/z* calcd [M$^+$]: 352.1075, found 352.1072.

Crystallographic data for (*E*)-**3ae** is as follows: $C_{22}H_{15}F_3O$, *M*r = 352.36, colorless, platelet, 0.140 × 0.050 × 0.010 mm, monoclinic, Primitive, *a* = 5.7547(4) Å, *b* = 8.6681(6) Å, *c* = 34.026(3) Å, □ = 91.207(2) °, *V* = 1696.9(2) Å^3, *Z* = 4, ρ_c = 1.379 g/cm^3, μ = 1.058 cm^{-1}, *T* = 123 K, λ = 0.71075 Å, 23005 reflections, 3097 unique [*R*(int) = 0.1235), Final *GoF* = 1.064, R_1 = 0.0752 ([$I > 2.00\sigma(I)$]), *w*R_2 = 0.1983 (all data). CCDC No.: 982712.

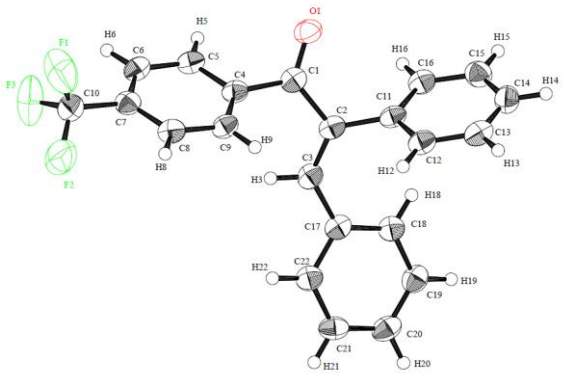

Figure 8. ORTEP representation of (*E*)-**3ae** (50% thermal ellipsolids)

(1-(4-(Trifluoromethyl)phenyl)ethene-1,2-diyl)dibenzene ((*E*)-4ae)

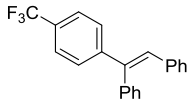

(*E*)-**4ae**

Colorless oil; R_f 0.36 (Hexane); ^{1}H NMR (500 MHz, $CDCl_3$) δ: 7.01-7.05 (m, 2H), 7.14-7.15 (m, 3H), 7.18-7.19 (m, 2H), 7.25-7.27 (m, 4H), 7.34-7.35 (m, 2H), 7.41-7.56 (m, 2H); ^{13}C NMR (125 MHz, $CDCl_3$) δ: 124.2 (q, $^1J_{C\text{-}F}$ = 272 Hz), 125.1 (q, $^3J_{C\text{-}F}$ = 3.9 Hz), 125.5 (q, $^2J_{C\text{-}F}$ = 3.9 Hz) 127.3, 127.9, 127.8, 128.1, 128.9, 129.7, 130.0, 131.0, 136.8, 139.6, 141.3, 146.9; IR (neat, cm^{-1}) 3022, 2927, 1614, 1489, 1445, 1410, 1323, 1166, 1124, 1067, 1015, 845, 757, 721, 694; MS (EI): *m/z* (%) = 325 (21) [M+1$^+$], 324 (100) [M$^+$], 253 (26), 179 (26), 126 (11), 77 (3), 51 (3); HRMS: *m/z* calcd [M$^+$]: 324.1126, found 324.1129.

(*Z*)-1-(*m*-Methoxyphenyl)-2,3-diphenyl-2-propen-1-one ((*Z*)-3af)

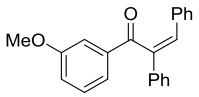

(*Z*)-**3af**

Colorless solid; mp 71.2-72.8 °C; R_f 0.29; (hexane/AcOEt = 10/1); ^{1}H NMR (500 MHz, $CDCl_3$) δ: 3.80 (s, 3H), 7.01–7.05 (m, 1H), 7.14–7.25 (m, 5H), 7.27–7.37 (m, 5H), 7.46 (d, *J* = 7.5, 2H), 7.53–7.57 (m, 2H); ^{13}C NMR (125 MHz, $CDCl_3$) δ: 55.3, 113.0, 120.4, 122.8, 126.3, 128.0, 128.1, 128.4, 128.8, 129.7, 130.0, 135.3, 137.6, 137.9, 140.8, 159.8, 199.1; IR (neat, cm^{-1}) 3056, 3024, 2938, 2835, 1666 (C=O), 1594, 1580, 1484, 1429, 1261, 1037; MS (EI): *m/z* (%) = 315 (40) [M+1$^+$], 314 (100) [M$^+$], 286 (18), 236 (14), 198 (15), 197 (95), 180 (13), 179 (94), 178 (96), 177 (40), 176 (47), 166 (10), 152 (47), 151 (25), 150 (10), 136 (37), 135 (98), 126 (14), 108 (25), 107 (95), 102 (20), 92 (94), 77 (95), 69 (73); HRMS: *m/z* calcd [M$^+$]: 314.1307, found 314.1310.

Crystallographic data for (*Z*)-**3af** is as follows: $C_{22}H_{18}O_2$, *M*r = 314.38, colorless, block, 0.180 × 0.170 × 0.170 mm^3, monoclinic, C-centered, *a* = 27.3859(6) Å, *b* = 8.0159(2) Å, *c* = 17.9647(4) Å, β = 121.0707(7) º, *V* = 3377.8(2) $Å^3$, Z = 8, ρ_c = 1.236 g cm^{-3}, μ = 0.779 cm^{-1}, *T* = 123(1) K, λ = 0.71075 Å, 28309 reflections, 3877 unique [*R*(int) = 0.0216), Final *GoF* = 1.083, R_1 = 0.0645 ([$I > 2\sigma(I)$]), *w*R_2 = 0.1630 (all data). CCDC No.: 982718.

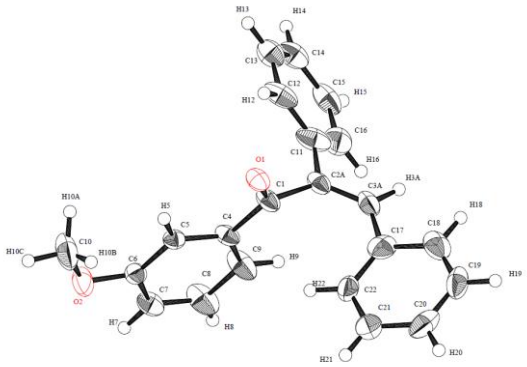

Figure 9 ORTEP representation of (*Z*)-**3af** (50% thermal ellipsolids)

(*E*)-1-(*m*-Methoxyphenyl)-2,3-diphenyl-2-propen-1-one ((*E*)-3af).

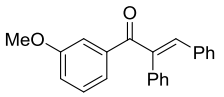

(*E*)-**3af**

Colorless solid; mp 88.4-89.5 °C; R_f 0.27; (hexane/AcOEt = 10/1); ^{1}H NMR (500 MHz, $CDCl_3$) δ: 3.82 (s, 3H), 7.06–7.10 (m, 3H), 7.16-7.23 (m, 3H), 7.25-7.29 (m, 3H), 7.32-7.38 (m, 5H), 7.44 (d, *J* = 7.0, 1H); ^{13}C NMR (125 MHz, $CDCl_3$) δ: 55.4, 114.1, 118.6, 122.5, 126.3, 127.9, 128.2, 128.8, 128.9, 129.2, 129.6, 130.3, 134.7, 136.4, 139.4, 140.1, 140.7, 159.5, 197.3; IR (neat, cm^{-1}) 3057, 2923, 2852, 2362, 1653 (C=O), 1597, 1495, 1443, 1269; MS (EI): *m/z* (%) = 315 (13) [$M+1^+$], 314 (59) [M^+], 197 (40), 179 (32), 178 (65), 177 (11), 176 (13), 152 (16), 136 (22), 135 (100), 108 (19), 107 (83), 92 (51), 86 (48), 84 (73), 77 (90), 69 (40); HRMS: *m/z* calcd [M^+]: 314.1307, found

314.1307.

Crystallographic data for (*E*)-**3af** is as follows: $C_{22}H_{18}O_2$, *M*r = 314.38, colorless, block, 0.140 × 0.130 × 0.100 mm, triclinic, Primitive, *a* = 9.3539(3) Å, *b* = 9.8134(3) Å, *c* = 10.3948(4) Å, α = 104.9234(8) °, *β* = 95.5597(8) °, γ = 111.7769(8) °, *V* = 836.28(5) Å^3, *Z* = 2, ρ_c = 1.248 g/cm^3, μ = 0.786 cm^{-1}, *T* = 123 K, λ = 0.71075 Å, 8402 reflections, 3820 unique [*R*(int) = 0.0146), Final *GoF* = 1.151, R_1 = 0.0492 ([*I* > 2.00σ(*I*)]), *w*R_2 = 0.1283 (all data). CCDC No.: 982714.

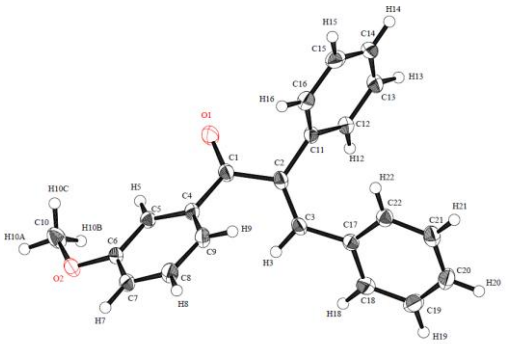

Figure 10 ORTEP representation of (*E*)-**3af** (50% thermal ellipsolids)

(1-(3-Methoxyphenyl)ethene-1,2-diyl)dibenzene ((*E*)-4af)

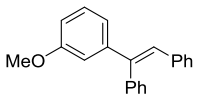

(*E*)-**4af**

Colorless oil; R_f 0.18 (Hexane/CH_2Cl_2 = 10/1); ^{1}H NMR (500 MHz, $CDCl_3$) δ: 3.78 (s, 3H), 6.84 (d, *J* = 8.0 Hz, 1H), 6.88 (s, 1H), 6.91 (d, *J* = 8.0 Hz, 1H), 6.97 (s, 1H), 7.02 (d, J = 7.0 Hz, 2H), 7.08-7.14 (m, 3H), 7.20-7.24 (m, 3H), 7.30-7.34 (m, 3H); ^{13}C NMR (125 MHz, $CDCl_3$) δ: 55.2, 112.8, 113.4, 120.3, 126.8, 127.9, 128.3, 128.6, 129.5, 130.3, 137.3, 140.2, 142.4, 144.9, 159.5; IR (neat, cm^{-1}) 3024, 2927, 1614, 1489, 1445, 1323, 1166, 1124, 1067, 1015, 845, 757, 694; MS (EI): *m/z* (%) = 287 (22) [M+1$^+$], 286 (80) [M$^+$], 253 (15), 178 (13), 126 (5), 83 (13), 73 (6), 57 (4); HRMS: *m/z* calcd [M$^+$]:

286.1358, found 286.1358.

(*Z*)-1-(*o*-Methoxyphenyl)-2,3-diphenyl-2-propen-1-one ((*Z*)-3ag)

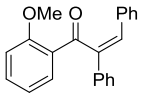

(*Z*)-**3ag**

Colorless solid; mp 91.4-92.5 °C; R_f 0.21; (hexane/AcOEt = 10/1); ^{1}H NMR (500 MHz, $CDCl_3$) δ: 3.75 (s, 3H), δ: 6.82 (d, *J* = 8.0 Hz, 1H), δ: 6.90 (t, *J* = 7.0 Hz, 1H), δ: 7.00 (s, 1H), δ: 6.82 (d, *J* = 8.0 Hz, 1H), δ: 6.90 (t, *J* = 7.0 Hz, 2H), δ: 7.14-7.33 (m, 5H), δ: 7.39 (t, *J* = 7.0 Hz, 1H), δ: 7.43-7.45 (m, 2H), δ: 7.85 (d, *J* = 9.0 Hz, 1H); ^{13}C NMR (125MHz, $CDCl_3$) δ: 55.5, 111.9, 120.3, 126.8, 127.6, 127.8, 128.2, 128.5, 128.8, 132.0, 134.5, 136.0, 138.2, 144.3, 159.4, 197.6; IR (neat, cm^{-1}) 3021, 1650 (C=O), 1595, 1483, 1285, 1248, 1213, 1162, 1021, 757, 727, 694, 673, 566, 523, 514; MS (EI): *m/z* (%) = 316 (3) [M+2$^+$], 315 (23) [M+1$^+$], 314 (94) [M$^+$], 178 (22), 135 (100), 92 (13), 77 (20), 51 (4); HRMS: *m/z* calcd [M$^+$]: 314.1307, found 314.1305.

Crystallographic data for (*Z*)-**3ag** is as follows: $C_{22}H_{18}O_2$, *M*r = 314.38, colorless, block, 0.120 × 0.100 × 0.090 mm, orthorhombic, Primitive, *a* = 8.0194(2) Å, *b* = 10.8524(3) Å, *c* = 19.1356(4) Å, *V* = 1665.37(7) Å^3, *Z* = 4, ρ_c = 1.254 g/cm^3, μ = 0.790 cm^{-1}, *T* = 123 K, λ = 0.71075 Å, 16656 reflections, 3814 unique [*R*(int) = 0.0236), Final *GoF* = 1.114, R_1 = 0.0376 ([$I > 2.00\sigma(I)$]), *w*R_2 = 0.0900 (all data). CCDC No.: 982716.

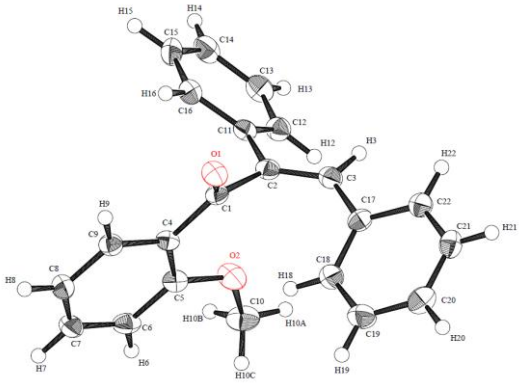

Figure 11 ORTEP representation of (*Z*)-**3ag** (50% thermal ellipsolids)

1-(*o*-Methoxyphenyl)-2,3-diphenyl-2-propen-1-one ((*Z*)- and (*E*)-3ag)

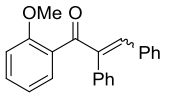

(*Z*)- and (*E*)-**3ag**

Colorless oil; R_f 0.21; (hexane/AcOEt = 10/1); ^{1}H NMR (500 MHz, $CDCl_3$) δ: 3.74 for *E* (s, 3H), 3.76 for *Z* (s, 3H); ^{13}C NMR (125MHz, $CDCl_3$) δ: 55.5, 55.6, 111.2, 111.9, 120.3, 120.5, 127.7, 128.1, 128.4, 128.5, 128.9, 129.3, 130.0, 130.6, 131.5, 132.0, 134.6, 150.0, 136.0, 136.1, 138.2, 141.7, 142.2, 144.3, 157.0, 159.4, 197.6, 198.0.

(1-(2-Methoxyphenyl)ethene-1,2-diyl)dibenzene ((*E*)-4ag)

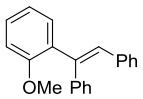

(*E*)-**4ag**

Colorless oil; R_f 0.18 (hexane/CH_2Cl_2 = 10/1); ^{1}H NMR (500 MHz, $CDCl_3$) δ: 3.53 (s, 3H), 6.72 (s, 1H), 6.81 (d, *J* = 8.0 Hz, 1H), 6.88 (t, *J* = 7.0 Hz, 1H), 7.00-7.01 (m, 2H), 7.05-7.07 (m, 3H), 7.12-7.21 (m, 7H); ^{13}C NMR (125 MHz, $CDCl_3$) δ: 55.6, 111.8, 120.5, 126.6, 126.7, 127.8, 128.0, 128.7, 129.4, 129.6, 130.2, 131.0, 133.7, 137.5, 140.3, 141.1, 157.3; IR (neat, cm^{-1}) 3053, 3020, 2957, 1595, 1575, 1487, 1456, 1433, 1253, 1110, 1026, 776, 753, 719, 696; MS (EI): *m/z* (%) = 287 (20) [$M+1^+$], 286 (99) [M^+], 165 (45), 126 (12), 83 (15), 77 (6), 51 (4); HRMS: *m/z* calcd [M^+]: 286.1358, found 286.1355.

(*Z*)-1,2,3-Tris(4-methoxyphenyl)prop-2-en-1-one ((*Z*)-3bb)

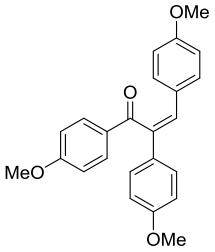

(*Z*)-**3bb**

Yellow oil; R_f 0.20; (hexane/AcOEt = 10/1); ^{1}H NMR (500 MHz, $CDCl_3$) δ: 3.73 (s, 3H), 3.79 (s, 3H), 3.81 (s, 3H), 6.85 (t, *J* = 8.5 Hz, 3H), 7.009 (s, 1H), 7.08 (d, *J* = 9.0 Hz, 2H), 7.21 (t, *J* = 9.0 Hz, 3H), 7.37 (d, *J* = 9.0 Hz, 2H), 7.97 (d, *J* = 8.5 Hz, 2H); ^{13}C NMR (125 MHz, $CDCl_3$) δ: 55.0, 55.1, 55.3, 113.9, 114.1, 127.2, 128.3, 129.5, 130.0, 130.1, 132.0, 138.3, 158.9, 159.2, 163.8, 198.5; FTIR (neat, cm^{-1}) 3024, 2958, 2928, 2836, 1656 (C=O), 1597, 1572, 1511, 1461, 1421, 1302, 1029, 904, 831; MS (EI): *m/z* (%) = 374 (88) [M^+], 355 (35), 295 (15), 281 (25), 266 (32), 239 (30), 227 (48), 221 (30), 169 (45), 149 (99), 135 (84), 113 (12), 83 (11), 71 (33), 57 (45); HRMS: *m/z* calcd [M^+]: 374.1518; found 374.1517.

(*E*)-1,2,3-Tris(4-methoxyphenyl)prop-2-en-1-one ((*E*)-3bb)

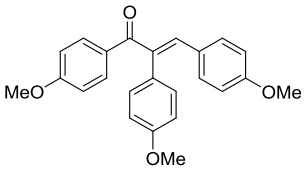

(*E*)-**3bb**

Yellow oil; R_f 0.20; (hexane/AcOEt = 10/1); ^{1}H NMR (500 MHz, $CDCl_3$) δ: 3.77 (s, 3H), 3.82 (s, 3H), 3.86 (s, 3H), 6.70-6.73 (m, 7H), 6.90 (t, *J* = 8.5 Hz, 3H), 7.11 (s, 1H), 7.85 (d, *J* = 9.0 Hz, 2H); ^{13}C NMR (125 MHz, $CDCl_3$) δ: 55.06, 55.09, 55.3, 113.3, 113.6, 114.2, 127.2, 127.6, 129.3, 130.1, 132.0, 138.2, 159.0, 159.8, 162.7, 196.6; IR neat, cm^{-1}) 3024, 2958, 2928, 2836, 1656 (C=O), 1597, 1572, 1511, 1461, 1421, 1302, 1029, 904, 831; MS (EI): *m/z* (%) = 374 (88) [M^+], 355 (35), 295 (15), 281 (25), 266 (32), 239 (30), 227 (48), 221 (30), 169 (45), 149 (99), 135 (84), 113 (12), 83 (11), 71

(33), 57 (45); HRMS: *m/z* calcd [M^+]: 374.1518; found 374.1517.

(*Z*)-2,3-bis(4-methoxyphenyl)-1-phenylprop-2-en-1-one ((*Z*)-3ba)

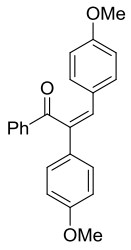

(*Z*)-**3ba**

Yellow oil; R_f 0.21; (hexane/AcOEt = 10/1); ^{1}H NMR (500 MHz, $CDCl_3$) δ: 3.72 (s, 3H), 3.79 (s, 3H), 6.71 (d, *J* = 8.5 Hz, 2H), 6.86 (d, *J* = 8.5 Hz, 2H), 7.06 (s, 1H), 7.21 (d, *J* = 8.5 Hz, 2H), 7.37 (m, 4H), 7.49 (t, *J* = 7.0 Hz, 1H), 8.00 (d, *J* = 7.0 Hz, 2H); ^{13}C NMR (125 MHz, $CDCl_3$) δ: 55.1, 55.3, 113.9, 114.2, 127.4, 128.0, 128.3,128.7, 129.7, 130.1, 130.8, 133.6, 136.4, 138.3, 159.1, 159.4, 200.0; IR (neat, cm^{-1}) 3020, 2955, 2835, 1651 (C=O), 1603, 1511, 1445, 1288, 1248, 879, 737; MS (EI): *m/z* (%) = 344 (22) [M^+], 278 (33), 262 (17), 239 (22), 195 (7), 169 (99), 141 (80), 128 (47), 115 (18), 81 (32), 69 (54), 57 (54); HRMS: *m/z* calcd [M^+]: 344.1412, found 344.1411.

(*E*)-2,3-bis(4-methoxyphenyl)-1-phenylprop-2-en-1-one ((*E*)-3ba)

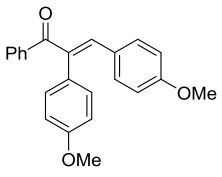

(*E*)-**3ba**

Yellow oil; R_f 0.21; (hexane/AcOEt = 10/1); ^{1}H NMR (500 MHz, $CDCl_3$) δ: 3.77 (s, 3H), 3.83 (s, 3H), 6.70-6.73 (m, 3H), 6.71 (d, *J* = 8.5 Hz, 2H), 7.05 (s, 1H), 7.19-7.21 (m, 4H), 7.43 (t, *J* = 8.0 Hz 2H), 7.81 (d, *J* = 8.5 Hz, 2H); ^{13}C NMR (125 MHz, $CDCl_3$)

δ: 55.2, 55.7, 113.7, 114.3, 128.0, 128.2, 129.0, 129.6, 130.1, 130.7, 131.7, 136.4, 138.2, 138.7, 159.4, 198.0; IR (neat, cm^{-1}) 3020, 2955, 2835, 1651 (C=O), 1603, 1511, 1445, 1288, 1248, 879, 737; MS (EI): *m/z* (%) = 344 (22) [M^+], 278 (33), 262 (17), 239 (22), 195 (7), 169 (99), 141 (80), 128 (47), 115 (18), 81 (32), 69 (54), 57 (54); HRMS: *m/z* calcd [M^+]: 344.1412, found 344.1411.

(*Z*)-2,3-bis(4-methoxyphenyl)-1-(4-(trifluoromethyl)phenyl)prop-2-en-1-one ((*Z*)-3be)

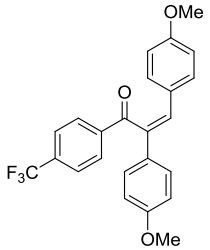

(*Z*)-**3be**

Yellow oil; R_f 0.30; (hexane/AcOEt = 10/1); ^{1}H NMR (500 MHz, $CDCl_3$) δ: 3.74 (s, 3H), 3.80 (s, 3H), 6.71-6.74 (m, 1H), 6.87 (d, *J* = 9.0 Hz, 2H), 7.12 (s, 1H), 7.17-7.19 (m, 3H), 7.33 (d, *J* = 8.5 Hz, 2H), 7.62 (d, *J* = 8.0 Hz, 2H), 8.08 (d, *J* = 8.0 Hz, 2H); ^{13}C NMR (125 MHz, $CDCl_3$) δ: 55.2, 55.3, 114.0, 114.5, 123.5 (q, $^1J_{C\text{-}F}$= 237.5 Hz), 125.8 (q, $^3J_{C\text{-}F}$ = 8.5 Hz), 127.5, 129.9, 130.1, 132.2, 134.5 (q, $^2J_{C\text{-}F}$ = 33.4 Hz) 142.5, 159.1, 159.6, 199.0; IR (neat, cm^{-1}) 3019, 2955, 2874, 1691 (C=O), 1604, 1563, 1511, 1441, 1250, 1107, 833, 638; MS (EI): *m/z* (%) = 412 (80) [M^+], 343 (8), 304 (58), 265 (16), 239 (99), 209 (51), 165 (53), 145 (77), 121 (55), 95 (15), 69 (54), 57 (35); HRMS: *m/z* calcd [M^+]: 412.1286, found 412.1285.

(*E*)-2,3-bis(4-methoxyphenyl)-1-(4-(trifluoromethyl)phenyl)prop-2-en-1-one ((*E*)-3be)

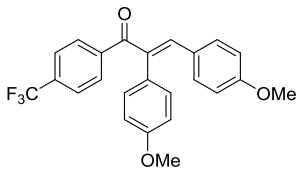

(*E*)-**3be**

Yellow oil; R_f 0.30; (hexane/AcOEt = 10/1); ^{1}H NMR (500 MHz, $CDCl_3$) δ: 3.78 (s, 3H), 3.85 (s, 3H), 6.71-6.74 (m, 4H), 6.92-6.94 (m, 2H), 7.06 (d, *J* = 9.0 Hz, 2H), 7.24 (s, 1H), 7.69 (d, *J* = 8.0 Hz, 2H), 7.85 (d, *J* = 8.0 Hz, 2H); ^{13}C NMR (125 MHz, $CDCl_3$) δ: 55.2, 55.4, 114.3, 123.6 (q, $^1J_{C\text{-}F}$ = 252.3 Hz), 125.2 (q, $^3J_{C\text{-}F}$ = 4.8 Hz), 129.6, 130.3, 132.9 (q, $^2J_{C\text{-}F}$ = 32.1 Hz), 137.6, 142.2, 159.3, 159.4, 196.8; IR (neat, cm^{-1}) 3019, 2955, 2874, 1691 (C=O), 1604, 1563, 1511, 1441, 1250, 1107, 833, 638; MS (EI): *m/z* (%) = 412 (80) [M^+], 343 (8), 304 (58), 265 (16), 239 (99), 209 (51), 165 (53), 145 (77), 121 (55), 95 (15), 69 (54), 57 (35); HRMS: *m/z* calcd [M^+]: 412.1286, found 412.1285.

(*Z*)-1-(4-Methoxyphenyl)-2,3-bis(4-(trifluoromethyl)phenyl)prop-2-en-1-one ((*Z*)-3cb)

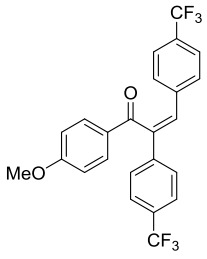

(*Z*)-**3cb**

Colorless solid; mp 103.9-105.2 °C; R_f 0.25; (hexane/AcOEt = 10/1); ^{1}H NMR (500 MHz, $CDCl_3$) δ: 3.83 (s, 3H), 6.87 (d, *J* = 8.5 Hz, 2H), 7.22 (s, 1H), 7.42-7.48 (m, 4H), 7.59-7.63 (m, 4H), 7.93 (d, *J* = 8.5 Hz, 2H); ^{13}C NMR (125 MHz, $CDCl_3$) δ: 55.3, 114.3, 123.8 (q, $^1J_{C\text{-}F}$ = 270.6 Hz), 123.9 (q, $^1J_{C\text{-}F}$ = 269.5 Hz), 125.4 (q, $^3J_{C\text{-}F}$ = 3.6 Hz), 125.8 (q, $^3J_{C\text{-}F}$ = 3.6 Hz) 126.6, 129.7, 129.9 (q, $^2J_{C\text{-}F}$ = 53.6 Hz), 130.2 (q, $^2J_{C\text{-}F}$ = 53.6 Hz), 132.0, 138.4, 140.9, 141.9, 164.5, 196.4; IR (neat, cm^{-1}) 2934, 2843, 1655 (C=O), 1614, 1596, 1573, 1462, 1322, 1237, 1164, 1015, 907, 781; MS (EI): *m/z* (%) = 450 (80) [M^+],

431 (20), 422 (9), 315 (8), 295 (20), 265 (23), 246 (22), 225 (11), 196 (8), 176 (9), 135 (99), 107 (38), 84 (72), 77 (69), 57 (18); HRMS: *m/z* calcd [M^+]: 450.1054, found 450.1055.

Crystallographic data for (*Z*)-**3cb** is as follows: $C_{24}H_{16}F_6O_2$, *M*r = 450.38, colorless, platelet, 0.100 × 0.060 × 0.010 mm, monoclinic, Primitive, a = 13.789(1) Å, b = 8.2551(6) Å, c = 17.588(2) Å, β = 96.860(2) °, V = 1987.6(3) Å^3, Z = 4, ρ_c = 1.505 g/cm^3, μ = 1.326 cm^{-1}, T = 123 K, λ = 0.71075 Å, 23005 reflections, 3630 unique [*R*(int) = 0.0586), Final *GoF* = 1.070, R_1 = 0.0592 ([$I > 2.00\sigma(I)$]), *w*R_2 = 0.1702 (all data). CCDC No.: 982720.

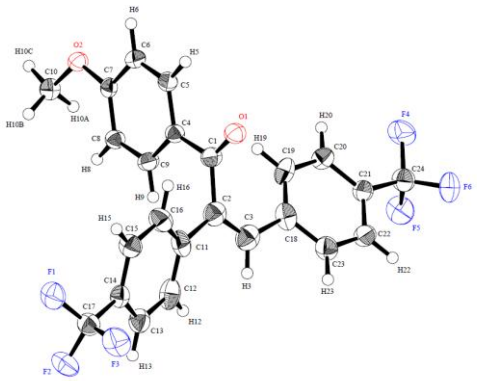

Figure 12 ORTEP representation of (*Z*)-**3cb** (50% thermal ellipsolids)

(*E*)-1-(4-Methoxyphenyl)-2,3-bis(4-(trifluoromethyl)phenyl)prop-2-en-1-one ((*E*)-3cb)

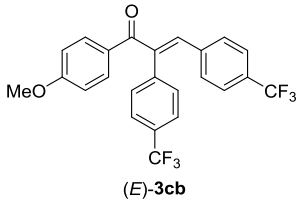

(*E*)-**3cb**

Colorless solid; mp 98.3-100.2 °C; R_f 0.16; (hexane/AcOEt = 10/1); ^{1}H NMR (500 MHz, $CDCl_3$) δ: 3.89 (s, 3H), 6.96 (d, *J* = 8.0 Hz, 2H), 7.18-7.20 (m, 3H), 7.41 (d, *J* = 8.0 Hz, 2H), 7.48 (d, *J* = 8.0 Hz, 2H), 7.61 (d, *J* = 8.0 Hz, 2H), 7.91 (d, *J* = 8.5 Hz, 2H);

^{13}C NMR (125 MHz, $CDCl_3$) δ: 55.5, 113.8, 123.9 (q, $^1J_{C\text{-}F}$ = 270.6 Hz), 125.4 (q, $^3J_{C\text{-}F}$ = 3.5 Hz), 125.8 (q, $^3J_{C\text{-}F}$ = 3.6 Hz) 129.5, 129.9, 130.1, 130.5 (q, $^2J_{C\text{-}F}$ = 26.3 Hz), 132.4, 136.5, 138.0, 139.8, 141.6, 163.6, 195.0; IR (neat, cm^{-1}) 2926, 1653 (C=O), 1597, 1573, 1419, 1322, 1256, 1164, 1016, 907, 839; MS (EI): *m/z* (%) = 450 (25) [M^+], 431 (5), 422 (4), 315 (10), 295 (30), 265 (12), 246 (26), 225 (11), 196 (8), 176 (6), 135 (99), 107 (28), 92 (42), 77 (48), 57 (14); HRMS: *m/z* calcd [M^+]: 450.1054, found 450.1060.

Crystallographic data for (*E*)-**3cb** is as follows: $C_{24}H_{16}F_6O_2$, *M*r = 450.38, colorless, block, 0.130 × 0.040 × 0.020 mm, monoclinic, Primitive, *a* = 9.234(1) Å, *b* = 5.6213(7) Å, *c* = 20.157(3) Å, *β* = 98.054(3) º, *V* = 1036.0(2) Å^3, *Z* = 2, ρ_c = 1.444 g/cm^3, μ = 1.272 cm^{-1}, *T* = 123 K, λ = 0.71075 Å, 14482 reflections, 3739 unique [*R*(int) = 0.0534), Final *GoF* = 1.023, R_1 = 0.0689 ([$I > 2.00\sigma(I)$]), wR_2 = 0.1750 (all data). CCDC No.: 982717.

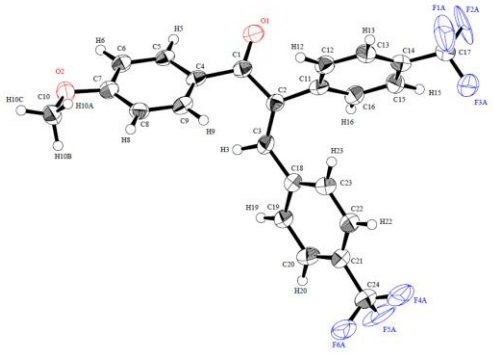

Figure 13 ORTEP representation of (*E*)-**3cb** (50% thermal ellipsoids)

(*Z*)-1-phenyl-2,3-bis(4-(trifluoromethyl)phenyl)prop-2-en-1-one ((*Z*)-3ca)

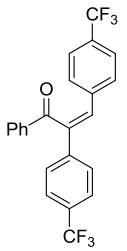

(*Z*)-**3ca**

Colorless liquid; R_f 0.26; (hexane/AcOEt = 10/1); ^{1}H NMR (500 MHz, $CDCl_3$) δ:

7.39-7.42 (m, 4H), 7.46-7.49 (m, 2H), 7.54 (t, J = 8.5 Hz, 1H), 7.61 (q, J = 8.5 Hz, 5H), 7.95 (d, J = 7.5 Hz, 2H); ^{13}C NMR (125 MHz, $CDCl_3$) δ: 123.8 (q, $^1J_{C\text{-}F}$ = 270.8 Hz), 123.9 (q, $^1J_{C\text{-}F}$ = 270.6 Hz), 125.4 (q, $^3J_{C\text{-}F}$ = 3.5 Hz), 125.9 (q, $^3J_{C\text{-}F}$ = 3.6 Hz), 126.7, 127.1, 128.2, 129.0, 129.6, 129.7 (q, $^2J_{C\text{-}F}$ = 45.4 Hz), 130.0, 130.2, 130.4 (q, $^2J_{C\text{-}F}$ = 32.3 Hz), 134.3, 135.6, 138.3, 140.7, 141.8, 198.1; IR (neat, cm^{-1}) 2932, 1665 (C=O), 1563, 1449, 1323, 1259, 1167, 1069, 1016, 907, 798; MS (EI): *m/z* (%) = 420 (73) [M^+], 401 (12), 392 (4), 355 (12), 351 (5), 315 (5), 295 (12), 246 (9), 167 (15), 149 (48), 105 (99), 77 (66), 73 (28), 57 (18); HRMS: *m/z* calcd [M^+]: 420.0949, found 420.0952.

(*E*)-1-phenyl-2,3-bis(4-(trifluoromethyl)phenyl)prop-2-en-1-one ((*E*)-3ca)

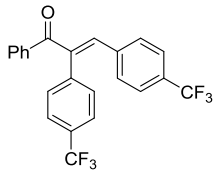

(*E*)-**3ca**

Colorless liquid; R_f 0.16; (hexane/AcOEt = 10/1); ^{1}H NMR (500 MHz, $CDCl_3$) δ: 7.18 (d, J = 8.5 Hz, 2H), 7.29 (s, 1H), 7.41 (d, J = 8.0 Hz, 2H), 7.47-7.51 (m, 4H), 7.59-7.64 (m, 3H), 7.88 (d, J = 7.5 Hz, 2H); ^{13}C NMR (125 MHz, $CDCl_3$) δ: 123.7 (q, $^1J_{C\text{-}F}$ = 270.8 Hz), 123.9 (q, $^1J_{C\text{-}F}$ = 270.8 Hz), 125.4 (q, $^3J_{C\text{-}F}$ = 3.5 Hz), 125.9 (q, $^3J_{C\text{-}F}$ = 4.8 Hz), 128.6, 129.8, 130.0, 130.2, 130.4 (q, $^2J_{C\text{-}F}$ = 32.0 Hz), 130.7 (q, $^2J_{C\text{-}F}$ = 32.1 Hz), 132.9, 137.2, 137.7, 138.9, 139.5, 141.3, 196.5; IR (neat, cm^{-1}) 2924, 2853, 1656 (C=O), 1614, 1448, 1323, 1256, 1166, 1124, 1068, 1016, 886, 724; MS (EI): *m/z* (%) = 420 (33) [M^+], 401 (4), 371 (2), 351 (3), 315 (5), 295 (3), 246 (3), 176 (2), 151 (2), 105 (99), 77 (26), 51(3); HRMS: *m/z* calcd [M^+]: 420.0949, found 420.0949.

(*Z*)-1,2,3-tris(4-(trifluoromethyl)phenyl)prop-2-en-1-one ((*Z*)-3ce)

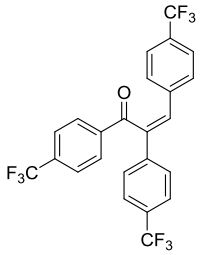

(*Z*)-**3ce**

Colorless solid; mp 128.4-129.6 ℃; R_f 0.28; (hexane/AcOEt = 10/1); ^{1}H NMR (500 MHz, $CDCl_3$) δ: 7.33 (s, 1H), 7.39 (d, *J* = 8.0 Hz, 2H), 7.49 (d, *J* = 8.5 Hz, 2H), 7.58 (d, *J* = 9.0 Hz, 2H), 7.65 (t, *J* = 8.0 Hz, 4H), 8.05 (d, *J* = 8.5 Hz, 2H); ^{13}C NMR (125 MHz, $CDCl_3$) δ: 123.3 (q, $^1J_{C\text{-}F}$ = 270.6 Hz), 123.7 (q, $^1J_{C\text{-}F}$ = 270.6 Hz), 123.8 (q, $^1J_{C\text{-}F}$ = 270.6 Hz), 125.7 (q, $^3J_{C\text{-}F}$ = 3.5 Hz), 126.1 (q, $^3J_{C\text{-}F}$ = 3.5 Hz), 129.0, 129.9, 130.0 (q, $^2J_{C\text{-}F}$ = 95.5 Hz), 130.6 (q, $^2J_{C\text{-}F}$ = 76.3 Hz), 131.1, 135.2, 135.4, 138.0, 138.2, 140.2, 141.1, 197.0; IR (neat, cm^{-1}) 2926, 1674 (C=O), 1615, 1409, 1323, 1223, 1165, 1068, 1015, 907, 752; MS (EI): *m/z* (%) = 488 (29) [M^+], 469 (5), 419 (4), 342 (2), 295 (7), 246 (5), 173 (99), 145 (26), 83 (6), 75 (2), 57 (1); HRMS: *m/z* calcd [M^+]: 488.0823, found 488.0826.

Crystallographic data for (*Z*)-**3ce** is as follows: $C_{24}H_{13}F_9O$, *M*r = 488.35, colorless, block, 0.140 × 0.100 × 0.030 mm, monoclinic, Primitive, *a* = 13.5689(4) Å, *b* = 9.0961(3) Å, *c* = 16.8281(5) Å, *β* = 101.1096(7) º, *V* = 2038.1(1) Å^3, *Z* = 4, ρ_c = 1.591 g/cm^3, μ = 1.529 cm^{-1}, *T* = 123 K, λ = 0.71075 Å, 34249 reflections, 4675 unique [*R*(int) = 0.0412), Final *GoF* = 1.115, R_1 = 0.0602 ([$I > 2.00\sigma(I)$]), *w*R_2 = 0.1701 (all data).

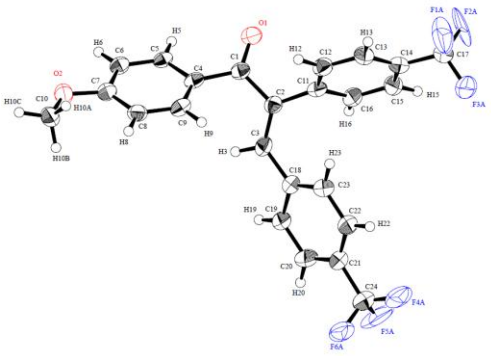

Figure 14 ORTEP representation of (*Z*)-**3ce** (50% thermal ellipsolids)

(*E*)-1,2,3-tris(4-(trifluoromethyl)phenyl)prop-2-en-1-one ((*E*)-3ce)

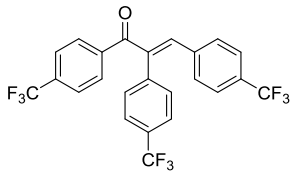

(*E*)-**3ce**

Colorless liquid; R_f 0.20; (hexane/AcOEt = 10/1); ^{1}H NMR (500 MHz, $CDCl_3$) δ: 7.18 (d, *J* = 8.0 Hz, 2H), 7.33 (s, 1H), 7.40 (d, *J* = 7.5 Hz, 2H), 7.49 (d, *J* = 8.0 Hz, 2H), 7.66 (d, *J* = 8.0 Hz, 2H), 7.76 (d, *J* = 8.0 Hz, 2H), 7.94 (d, *J* = 8.0 Hz, 2H); ^{13}C NMR (125 MHz, $CDCl_3$) δ: 123.5 (q, $^{1}J_{C\text{-}F}$ = 283.8 Hz), 123.6 (q, $^{1}J_{C\text{-}F}$ = 257.7 Hz), 123.9 (q, $^{1}J_{C\text{-}F}$ = 270.6 Hz) 125.5 (q, $^{3}J_{C\text{-}F}$ = 3.6 Hz), 125.7 (q, $^{3}J_{C\text{-}F}$ = 4.8 Hz), 126.1 (q, $^{3}J_{C\text{-}F}$ = 3.6 Hz) 129.9, 130.1, 130.5, 131.0 (q, $^{2}J_{C\text{-}F}$ = 32.1 Hz), 134.0 (q, $^{2}J_{C\text{-}F}$ = 33.4 Hz) 137.2, 138.9, 140.5, 140.6, 140.9, 195.4; IR (neat, cm^{-1}) 2925, 1662 (C=O), 1615, 1509, 1408, 1323, 1256, 1167, 1067, 1016, 899, 773; MS (EI): *m/z* (%) = 488 (44) [M^+], 469 (5), 419 (15), 343 (2), 295 (7), 246 (10), 173 (99), 145 (60), 83 (8), 75 (2), 55 (3); HRMS: *m/z* calcd [M^+]: 488.0823, found 488.0824.

(*Z*)-1-(4-Methoxyphenyl)-2-propylhex-2-en-1-one ((*Z*)-3db)

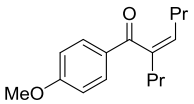

(*Z*)-**3db**

Colorless oil; R_f 0.33; (hexane/AcOEt = 15/1); ^{1}H NMR (500 MHz, $CDCl_3$) δ: 0.81 (t, *J* = 7.5 Hz, 3H), 0.91 (t, *J* = 7.5 Hz, 3H), 1.29–1.38 (m, 2H), 1.39–1.47 (m, 2H), 1.83 (q, *J* = 7.5 Hz, 2H), 2.27 (t, *J* = 7.5 Hz, 2H), 3.88 (s, 3H), 5.61 (t, *J* = 8.0 Hz, 1H), 6.94 (d, *J* = 9.5 Hz, 2H), 7.91 (d, *J* = 8.5 Hz, 2H); ^{13}C NMR (125 MHz, $CDCl_3$) δ: 13.7, 13.8, 21.5, 22.7, 31.7, 37.6, 55.5, 113.8, 130.1, 130.3, 131.7, 140.4, 163.7, 199.5; IR (neat, cm^{-1}) 3024, 2959, 2928, 2872, 1660 (C=O), 1600, 1574, 1508, 1463, 1258, 1160, 1030; MS (EI): *m/z* (%) = 246 (M^+, 22), 245 (13), 217 (34), 215 (54), 203 (70), 190 (15), 189 (20), 176 (15), 175 (23), 141 (25), 136 (10), 135 (100), 92 (18), 85 (31), 83 (50), 77 (18); HRMS: *m/z* calcd [M^+]: 246.1620, found 246.1622.

(*E*)-1-(4-Methoxyphenyl)-2-propylhex-2-en-1-one ((*E*)-3db)

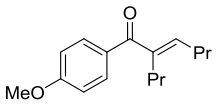

(*E*)-**3db**

Colorless oil; R_f 0.30; (hexane/AcOEt = 15/1); ^{1}H NMR (500 MHz, $CDCl_3$) δ: 0.95 (q, *J* = 7.0 Hz, 6H), 1.42–1.51 (m, 4H), 2.26 (q, *J* = 8.0 Hz, 2H), 2.46 (t, *J* = 8.0 Hz, 2H), 3.86 (s, 3H), 6.11 (t, *J* = 7.5 Hz, 1H), 6.92 (d, *J* = 8.5 Hz, 2H), 7.72 (d, *J* = 8.5 Hz, 2H); ^{13}C NMR (125 MHz, $CDCl_3$) δ: 14.0, 14.1, 22.1, 22.3, 29.1, 30.6, 55.4, 113.2, 131.3, 131.8, 141.0, 143.2, 162.5, 196.0; IR (neat, cm^{-1}) 3024, 2959, 2932, 2871, 1644 (C=O), 1601, 1575, 1508, 1463, 1255, 1162, 1031; MS (EI): *m/z* (%) = 246 (12) [M^+], 217 (16), 203 (11), 175 (10), 135 (100), 121 (11), 108 (15), 92 (67), 79 (15), 78 (12), 77 (67), 55 (33); HRMS: *m/z* calcd [M^+]: 246.1620, found 246.1618.

(*Z*)-1-(4-Methoxyphenyl)-2-methyl-3-phenylprop-2-en-1-one ((*Z*)-3eb)

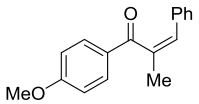

(*Z*)-**3eb**

Colorless oil; R_f 0.24 (hexane/AcOEt = 10/1); ^{1}H NMR (500 MHz, $CDCl_3$) δ: 2.16 (d, *J* = 1.5 Hz, 3H), 3.81 (s, 3H), 6.67 (d, *J* = 1.0 Hz, 1H), 6.82 (d, *J* = 9.5 Hz 2H), 7.05–7.35 (m, 5H), 7.88 (d, *J* = 8.5 Hz, 2H). ^{13}C NMR (125 MHz, $CDCl_3$) δ: 197.5, 163.8, 137.4, 135.8, 131.8, 129.2, 128.2, 128.0, 127.2, 126.1, 113.8, 55.4, 29.7; IR (neat, cm^{-1}) 3024, 2921, 1652 (C=O), 1558, 1507, 1465, 1396, 1260, 1027, 801; MS (EI): *m/z* (%) = 253 (7) [M+1$^+$], 252 (33) [M$^+$], 251 (16), 237 (14), 221 (16), 136 (7), 135 (80), 115 (28), 92 (26), 83 (100), 57 (55); HRMS: *m/z* calcd [M$^+$]: 252.1150, found 252.1151.

(*E*)-1-(4-Methoxyphenyl)-2-methyl-3-phenylprop-2-en-1-one ((*E*)-3eb)

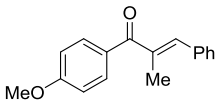

(*E*)-**3eb**

Colorless oil; R_f 0.21 (hexane/AcOEt = 10/1); ^{1}H NMR (500 MHz, $CDCl_3$) δ: 2.26 (d, *J* = 1.5 Hz, 3H), 3.88 (s, 3H), 6.96 (d, *J* = 9.0 Hz, 2H), 7.11 (d, *J* = 1.0 Hz 1H), 7.31–7.37 (m, 1H), 7.38–7.44 (m, 4H), 7.81 (d, *J* = 8.5 Hz, 2H); ^{13}C NMR (125 MHz, $CDCl_3$) δ: 14.9, 55.4, 113.5, 128.3, 128.4, 129.6, 130.6, 132.0, 135.9, 136.9, 140.0, 162.8, 198.3; IR (neat, cm^{-1}) 3022, 2958, 1641 (C=O), 1599, 1508, 1444, 1306, 1254, 1172, 1145, 1031, 1018; MS (EI): *m/z* (%) = 253 (28) [M+1$^+$], 252 (97) [M$^+$], 251 (52), 237 (34), 221 (36), 136 (12), 135 (100), 114 (30), 92 (32), 77 (57), 64 (18); HRMS: *m/z* calcd [M$^+$]: 252.1150, found 252.1147.

(*Z*)-1-(4-Methoxyphenyl)-2-phenylbut-2-en-1-one ((*Z*)-3eb')

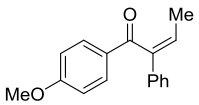

(*Z*)-**3'eb**

Colorless oil; R_f 0.24 (hexane/AcOEt = 10/1); ^{1}H NMR (500 MHz, $CDCl_3$) δ: 1.76 (d, *J* = 7.5 Hz, 3H), 3.85 (s, 3H), 6.31 (q, *J* = 7.5 Hz, 1H), 6.90 (d, *J* = 8.5 Hz 2H), 7.05–7.35 (m, 5H), 7.95 (d, *J* = 8.5 Hz, 2H). ^{13}C NMR (125 MHz, $CDCl_3$) δ: 199.7, 163.9, 141.9, 137.5, 132.1, 129.8, 128.7, 128.2, 127.5, 125.8, 113.9, 55.5, 23.0; IR (neat, cm^{-1}) 3024, 2921, 1653 (C=O), 1597, 1507, 1165, 1029, 800, 582, 520; MS (EI): *m/z* (%) = 253 (7) [M+1$^+$], 252 (33) [M$^+$], 251 (16), 237 (14), 221 (16), 136 (7), 135 (80), 115 (28), 92 (26), 83 (100), 57 (55); HRMS: *m/z* calcd [M$^+$]: 252.1150, found 252.1151.

(*E*)-1-(4-Methoxyphenyl)-2-phenylbut-2-en-1-one ((*E*)-3'eb)

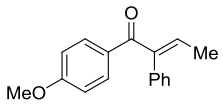

(*E*)-**3'eb**

Colorless oil; R_f 0.18 (hexane/AcOEt = 10/1); ^{1}H NMR (500 MHz, $CDCl_3$) δ: 1.89 (d, *J* = 7.0 Hz, 3H), 3.85 (s, 3H), 6.48 (q, *J* = 7.0 Hz, 1H), 6.88 (d, *J* = 9.0 Hz 2H), 7.25–7.40 (m, 5H), 7.80 (d, *J* = 8.5 Hz, 2H); ^{13}C NMR (125 MHz, $CDCl_3$) δ: 15.3, 55.4, 113.4, 127.4, 128.2, 129.4, 130.7, 132.1, 136.1, 136.7, 142.7, 162.9, 196.0; IR (neat, cm^{-1}) 3023, 2931, 1650 (C=O), 1599, 1509, 1441, 1311, 1256, 1169, 1028; MS (EI): *m/z* (%) = 253 (21) [M+1$^+$], 252 (100) [M$^+$], 251 (13), 237 (11), 235 (14), 221 (32), 178 (11), 165 (17), 136 (12), 135 (88), 115 (26), 92 (43), 91 (31), 77 (83), 64 (20); HRMS: *m/z* calcd [M$^+$]: 252.1150, found 252.1146.

(*Z*)-2-Benzylidene-1-(4-methoxyphenyl)hexan-1-one ((*Z*)-3fb)

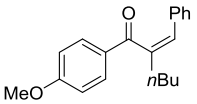

(*Z*)-**3fb**

Pale yellow oil; R_f 0.24 (hexane/AcOEt = 20/1); ^{1}H NMR (500 MHz, $CDCl_3$) δ: 0.90 (t, *J* = 7.0 Hz, 3H), 1.35-1.44 (m, 2H), 1.46-1.54 (m, 2H), 2.47 (td, *J* = 7.5, 1.5 Hz,

2H), 3.80 (s, 3H), 6.65 (s, 1H), 6.80 (d, *J* = 8.5 Hz, 2H), 7.03–7.35 (m, 5H), 7.87 (d, *J* = 9.0 Hz, 2H). ^{13}C NMR (125 MHz, $CDCl_3$) δ: 13.8, 22.4, 29.6, 31.5, 55.3, 113.7, 125.8, 127.1, 128.0, 128.3, 128.6, 129.9, 131.7, 132.0, 137.4, 141.9, 163.6, 199.6. IR (neat) 2956, 2929, 2857, 1654 (C=O), 1597, 1507, 1258, 1165, 1028, 842, 696; MS (EI): *m/z* (%) = 295 ($M+1^+$, 8), 294 (M^+, 30), 263 (7), 251 (11), 237 (3), 203 (3), 135 (100), 115 (50), 92 (32), 77 (35), 64 (10); Exact mass EI calcd for $C_{20}H_{22}O_2$ 294.1620, found 294.1613.

(*E*)-2-Benzylidene-1-(4-methoxyphenyl)hexan-1-one ((*E*)-3fb)

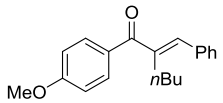

(*E*)-**3fb**

Pale yellow oil; R_f 0.22 (hexane/AcOEt = 20/1). ^{1}H NMR (500 MHz, $CDCl_3$) δ: 0.90 (t, *J* = 7.0 Hz, 3H), 1.35-1.44 (m, 2H), 1.48-1.55 (m, 2H), 2.73 (t, *J* = 8.0 Hz, 2H), 3.88 (s, 3H), 6.95 (d, *J* = 9.0 Hz, 2H), 6.97 (s, 1H), 7.30-7.42 (m, 5H), 7.85 (d, *J* = 8.5 Hz, 2H); ^{13}C NMR (125 MHz, $CDCl_3$) δ: 13.8, 22.9, 27.9, 30.8, 55.4, 113.4, 128.1, 128.4, 128.5, 129.0, 130.9, 132.0, 135.8, 138.3, 142.4, 162.9, 198.2; IR (neat) 2958, 2918, 2858, 1645 (C=O), 1600, 1507, 1457, 1170, 1028, 767, 700; MS (EI): *m/z* (%) = 295 ($M+1^+$, 13), 294 (M^+, 50), 263 (13), 251 (11), 237 (8), 203 (6), 135 (100), 115 (57), 92 (28), 77 (33), 64 (10); Exact mass EI calcd for $C_{20}H_{22}O_2$ 294.1620, found 294.1615.

(*Z*)-1-(4-Methoxyphenyl)-2-phenylhept-2-en-1-one ((*Z*)-3'fb)

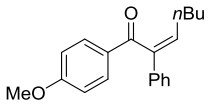

(*Z*)-**3'fb**

Pale yellow oil; R_f 0.24 (hexane/AcOEt = 20/1); ^{1}H NMR (500 MHz, $CDCl_3$) δ: 0.83 (t, *J* = 7.5 Hz, 3H), 1.24-1.32 (m, 2H), 1.35-1.44 (m, 2H), 2.09 (q, *J* = 7.0 Hz, 2H),

3.85 (s, 3H), 6.23 (t, J = 8.0 Hz, 1H), 6.90 (d, J = 9.5 Hz, 2H), 7.03-7.35 (m, 5H), 7.95 (d, J = 9.0 Hz, 2H). ^{13}C NMR (125 MHz, $CDCl_3$) δ: 13.8, 22.2, 30.2, 36.7, 55.4, 113.8, 127.4, 128.1, 128.5, 128.8, 129.3, 131.7, 135.9, 140.7, 163.6, 197.3. IR (neat) 2956, 2929, 2857, 1654 (C=O), 1597, 1507, 1258, 1165, 1028, 842, 696; MS (EI): *m/z* (%) = 295 ($M+1^+$, 8), 294 (M^+, 30), 263 (7), 251 (11), 237 (3), 203 (3), 135 (100), 115 (50), 92 (32), 77 (35), 64 (10); Exact mass EI calcd for $C_{20}H_{22}O_2$ 294.1620, found 294.1613.

(*E*)-1-(4-Methoxyphenyl)-2-phenylhept-2-en-1-one ((*E*)-3'fb)

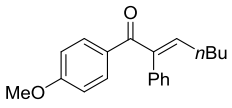

(*E*)-**3'fb**

Pale yellow oil; R_f = 0.16 (hexane/AcOEt = 20/1); ^{1}H NMR (500 MHz, $CDCl_3$) δ: 0.86 (t, J = 7.0 Hz, 3H), 1.28-1.37 (m, 2H), 1.41-1.48 (m, 2H), 2.26 (q, J = 7.5 Hz, 2H), 3.85 (s, 3H), 6.36 (t, J = 7.5 Hz, 1H), 6.90 (d, J = 8.5 Hz, 2H), 7.26-7.31 (m, 5H), 7.81 (d, J = 9.0 Hz, 2H); ^{13}C NMR (125 MHz, $CDCl_3$) δ: 13.8, 22.4, 29.1, 31.4, 55.4, 113.4, 113.9, 127.3, 128.2, 128.6, 129.4, 130.8, 132.1, 136.5, 141.4, 142.5, 162.8, 196.1; IR (neat) 2957, 2918, 2849, 1652 (C=O), 1699, 1541, 1507, 1310, 1257, 1167, 1026, 702; MS (EI): *m/z* (%) = 295 ($M+1^+$, 6), 294 (M^+, 30), 251 (10), 237 (2), 157 (2), 135 (100), 115 (15), 92 (15), 77 (18), 64 (5); Exact mass EI calcd for $C_{20}H_{22}O_2$ 294.1620, found 294.1617.

References

(1) Beller, M. Catalytic Carbonylation Reaction; Springer: Berlin, **2006**.

(2) Morimoto, T.; Kakiuchi, K. *Angew. Chem. Int. Ed.* **2004**, *43*, 5580.

(3) Brancour, C.; Fukuyama, T.; Mukai, Y.; Skrydstrup, T.; Ryu, I. *Org. Lett.* **2013**, *15*, 2794.

(4) Ueda, T.; Konishi, H.; Manabe, K. *Org. Lett.* **2012**, *14*, 3100.

(5) Ju, J.; Jeong, M.; Moon, J.; Jung, H. M.; Lee, S. *Org. Lett.* **2007**, *9*, 4615.

(6) Grushin, V. V.; Alper, H. *Organometallics* **1993**, *12*, 3846.

(7) Park, J. H.; Cho, Y.; Chung, Y. K. *Angew. Chem. Int. Ed.* **2010**, *49*, 5138.

(8) Korsager, S.; Taaning, R. H.; Lindhardt, A. T.; Skrydstrup, T. *J. Org. Chem.* **2013**, *78*, 6112.

(9) Nordeman, P.; Odell, L. R.; Larhed, M. *J. Org. Chem.* **2012**, *77*, 11393.

(10) (a) Lee, H. W.; Lee, L. N.; Chan, A. S. C.; Kwong, F. Y. *Eur. J. Org. Chem.* **2008**, *2008*, 3403. (b) Shibata, T.; Toshida, N.; Yamasaki, M.; Maekawa, S.; Takagi, K. *Tetrahedron* **2005**, *61*, 9974. (c) Jeong, N.; Kim, D. H.; Choi, J. H. *Chem. Commun.* **2004**, 1134. (d) Ikeda, K.; Morimoto, T.; Tsumagari, T.; Tanimoto, H.; Nishiyama, Y.; Kakiuchi, K. *Synlett* **2012**, *2012*, 393. (e) Fujioka, M.; Morimoto, T.; Tsumagari, T.; Tanimoto, H.; Nishiyama, Y.; Kakiuchi, K. *J. Org. Chem.* **2012**, *77*, 2911. (f) Makado, G.; Morimoto, T.; Sugimoto, Y.; Tsutsumi, K.; Kagawa, N.; Kakiuchi, K. *Adv. Synth. Catal.* **2010**, *352*, 299. (g) Morimoto, T.; Yamasaki, K.; Hirano, A.; Tsutsumi, K.; Kagawa, N.; Kakiuchi, K.; Harada, Y.; Fukumoto, Y.; Chatani, N.; Nishioka, T. *Org. Lett.* **2009**, *11*, 1777. (h) Fuji, K.; Morimoto, T.; Tsutsumi, K.; Kakiuchi, K. *Chem. Commun.* **2005**, 3295. (i) Fuji, K.; Morimoto, T.; Tsutsumi, K.; Kakiuchi, K. *Angew. Chem. Int. Ed.* **2003**, *42*, 2409. (j) Morimoto, T.; Fuji, K.; Tsutsumi, K.; Kakiuchi, K. *J. Am. Chem. Soc.* **2002**, *124*, 3806.

(11) Harada, Y.; Nakanishi, J.; Fujihara, H.; Tobisu, M.; Fukumoto, Y.; Chatani, N. *J. Am. Chem. Soc.* **2007**, *129*, 5766.

(12) (a) Artok, L.; Kuş, M.; Aksın-Artok, Ö.; Dege, F. N.; Özkılınç, F. Y. *Tetrahedron* **2009**, *65*, 9125. (b) Kuş, M.; Artok, Ö. A.; Ziyanak, F.; Artok, L. *Synlett* **2008**, *17*, 2587. (c) Aksn, O.; Dege, N.; Artok, L.; Turkmen, H.; Cetinkaya, B. *Chem. Commun.* **2006**, 3187.

(13) Dierkes, P.; W. N. M. van Leeuwen, P. *Journal of the Chemical Society, Dalton Transactions* **1999**, *0*, 1519.

(14) (a) van Leeuwen, P. W. N. M.; Kamer, P. C. J.; Reek, J. N. H.; Dierkes, P. *Chem. Rev.* **2000**, *100*, 2741. (b) Freixa, Z.; van Leeuwen, P. W. N. M. *Dalton Transactions* **2003**, 1890.

(15) (a) Fristrup, P.; Kreis, M.; Palmelund, A.; Norrby, P.-O.; Madsen, R. *J. Am. Chem. Soc.* **2008**, *130*, 5206. (b) Calderazzo, F. *Angew. Chem. Int. Ed. Engl.* **1977**, *16*, 299.

(16) (a) Sasaki, K.; Nishimura, T.; Shintani, R.; Kantchev, E. A. B.; Hayashi, T. *Chem. Sci.* **2012**, *3*, 1278. (b) Hayashi, T.; Inoue, K.; Taniguchi, N.; Ogasawara, M. *J. Am. Chem. Soc.* **2001**, *123*, 9918.

(17) Hayashi, T.; Takahashi, M.; Takaya, Y.; Ogasawara, M. *J. Am. Chem. Soc.* **2002**, *124*, 5052.

(18) (a) Nishimura, T.; Takiguchi, Y.; Hayashi, T. *J. Am. Chem. Soc.* **2012**, *134*, 9086. (b) Nishimura, T.; Noishiki, A.; Ebe, Y.; Hayashi, T. *Angew. Chem. Int. Ed.* **2013**, *52*, 1777.

(19) (a) Pucheault, M.; Darses, S.; Genet, J.-P. *J. Am. Chem. Soc.* **2004**, *126*, 15356. (b) Sakai, M.; Ueda, M.; Miyaura, N. *Angew. Chem. Int. Ed.* **1998**, *37*, 3279.

(20) Giordano, G.; Crabtree, R. H. *Inorg. Synth.* **1979**, *19*, 218.

(21) Mahoney, S. J.; Moon, D. T.; Hollinger, J.; Fillion, E. *Tetrahedron Lett.* **2009**, *50*, 4706.

CHAPTER 3 Rh(I)-Catalyzed Arylative Double-Carbonylation of Alkynes with Arylboronic Acids Using Formaldehyde to Butenolides

3.1 Introduction

In 2006, the group of Artok reported a rhodium-catalyzed carbonylative arylation of internal alkynes with arylboronic acids under 20 atm CO yielding 5-aryl-2(5*H*)-furanones in moderate to good yields (Scheme 3-1a).[1] The authors envisioned that prompt protonation of the alkenylrhodium intermediate, before insertion of CO, which leads to the formation of the enone product. Hence, they considered that the presence of acidic additive would promote the protodemetalation step, provided that the catalyst retains the activity. Addition of TFA changed the structure of main product from the furanone compounds to *α*,*β*-unsaturated ketones under 5 atm CO (Scheme 3-1b).[2]

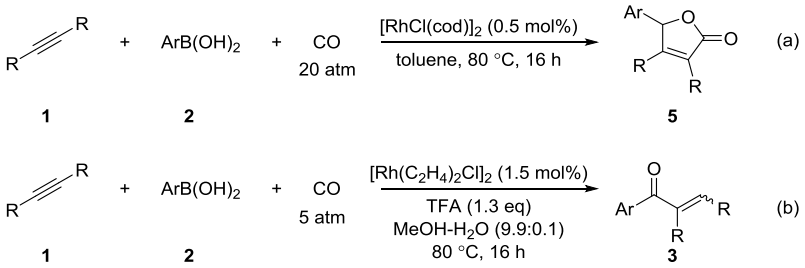

Scheme 3-1 Rh-catalyzed arylative carbonylation of alkynes with arylboronic acids under CO

In the chapter 2, I have described novel CO gas-free arylative mono-carbonylation of alkynes with arylboronic acids in the presence of formaldehyde as a carbonyl source for the selective synthesis of enone derivatives (Scheme 3-2a).[3] The above reaction proceeds *via* the vinylrhodium intermediate (**E**), which includes one carbonyl moiety abstracted from formaldehyde. If the generated carbonyl moiety is increased, that is, a catalyst working in the decarbonylation of formaldehyde increased, the second incorporation of the abstracted carbonyl moiety can take place to give the diketonerhodium intermediate (**F**). Next, I planned to increase amount of an added

phosphine in the similar catalytic conditions with the above reaction. This chapter focuses on the selective synthesis of another valuable product, butenolide derivatives, *via* the arylative double-carbonylation of alkynes with arylboronic acids in the presence of formaldehyde by a suitable modification of the reaction conditions without the direct use of CO gas (Scheme 3-2b).

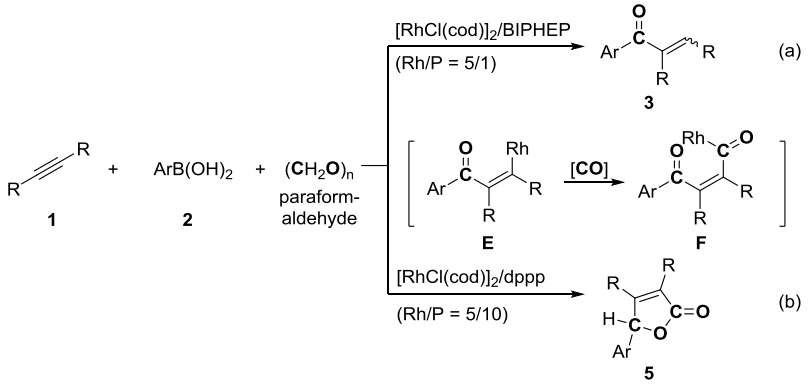

Scheme 3-2 Phosphine-free and ligated dual-Rh-catalyzed arylative carbonylation reactions using formaldehyde as the CO source

3.2 Results and Discussion

3.2.1 Preliminary Investigation for Arylative Double-Carbonylation

Based on the results for the varying amount of BIPHEP ligand to 5 mol% $[RhCl(cod)]_2$, I have isolated 16% yield of butenolide derivatives **5aa** and **6aa** under the catalytic conditions consisting of 5 mol% $[RhCl(cod)]_2$ and 10 mol% BIPHEP (Scheme 3-3, the result sees Chapter 2, Table 2-3, enrty 5). Actually I observed 3 kinds of lactone products **5aa**-**7aa** after the catalytic reaction. These lactone products can be partially separated *via* silica gel column chromatography because unstable compound **7aa** was gradually transformed to the more stable butenolides **5aa** and **6aa** during the purification. Lactone frameworks of **5aa**-7**aa** are constructed from a diphenylacetylene and two carbonyl units abstracted from formaldehyde.

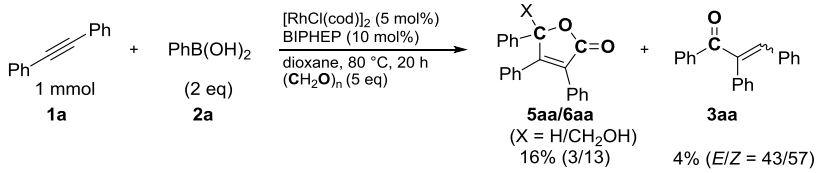

Scheme 3-3 The reaction under 5 mol% of $[RhCl(cod)]_2$ and 10 mol% BIPHEP

Each product can be recrystallized from corresponding hexane-CH_2Cl_2 solvent. The X-ray crystallographic analysis was shown in Figure 3-1.

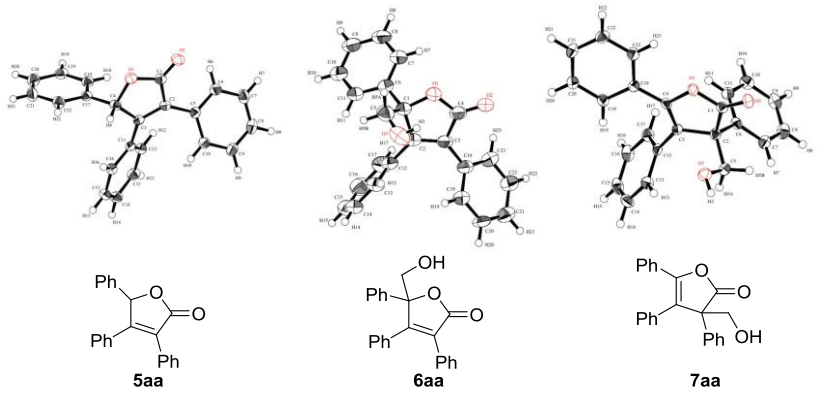

Figure 3-1 ORTEP representation of double-carbonylated products **5aa**-**7aa** (50% thermal ellipsolids)

In order to make unstable product **7aa** into **5aa** and **6aa** totally, I found that **7aa** was transformed into **5aa** and **6aa** completely by treating with activated alumina (pH: 9-11) in ethyl acetate at room temperature for 1h *via* retro-aldol reaction and enol-ketone tautomerism (Scheme 3-4).

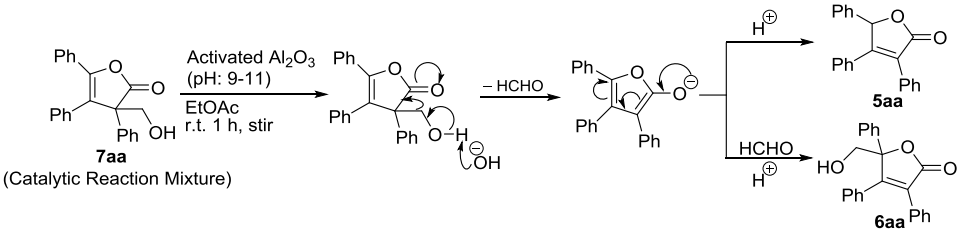

Scheme 3-4 Transformation of unstable lactone **7aa**

In order to confirm this transformation, lactone **7aa** isolated in pure form was stirred with activated alumina (pH: 9-11) in ethyl acetate at room temperature for 1h. The

unstable compound **7aa** was totally transformed to more stable butenolides derivatives **5aa** and **6aa** (Scheme 3-5).

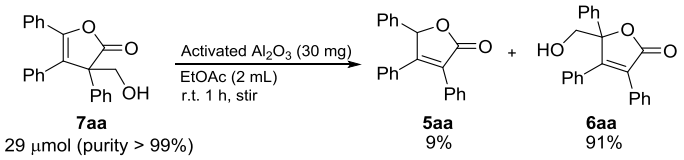

Scheme 3-5 Transformation of unstable lactone **7aa** isolated in pure form

3.2.2 Phosphine Ligand Screening

With above-mentioned observation in hand employing 10 mol% BIPHEP, I next examined multifarious phosphines ligand to the rhodium catalyst in the arylative double-carbonylation of **1a** with **2a** in order to improve chemical yield of butenolides. The results are summarized in Table 3-1. Among other bidentate phosphine ligands used (Table 3-1, entries 1–6), dppp gave the best result (Table 3-1, entry 6).

Previous work shows that dppp is the best diphosphine ligand for the decarbonylation of aldehyde due to the suitable bite angle (approximately 90°) and flexibility.[4] Probably, dppp-ligated Rh catalyst could easily decarbonylate formaldehyde to generate much Rh-CO species and enhance the rate of CO insertion transfer with dppp-free Rh catalyst to give me double-carbonylated product.

Table 3-1 Screening of Phosphine Ligand in Synthesis of **5aa** and **6aa**[a]

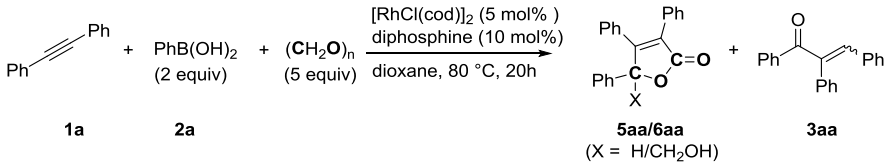

Entry	Phosphine	Yield (%)[b]		
		5aa + 6aa	(**5aa** / **6aa**)	**3aa**
1	BIPHEP	16	(3 / 13)	4
2	BINAP	9	(1 / 08)	5
3	Xantphos	8	(2 / 06)	trace
4	dppf	8	(1 / 07)	3
5	dppb	7	(1 / 06)	5
6	dppp	64	(8 / 56)	5

[a] Reaction conditions: **1a** (1 mmol), **2a** (2 mmol), paraformaldehyde (5 mmol), $[RhCl(cod)]_2$ (5 mol%), phosphine as ligand (10 mol%) in dioxane (1 mL) at 80 °C for 20 h.

[b] Isolated yield.

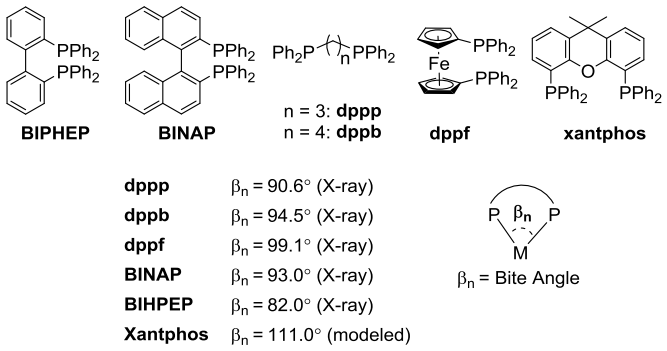

Scheme 3-6 The structure and bite angle of diphosphine ligands

3.2.3 Effect of dppp

I subsequently examined varying amounts of added dppp from 0 mol% to 20 mol% with keeping 5 mol% of $[RhCl(cod)]_2$ (Table 3-2, entries 1 – 7). The use of 10 mol% of dppp gave rise to the best results, 64% total yield of **5aa** and **6aa**. The hydroarylated product **4aa** was mainly obtained without dppp (Table 3-2, entry 1). Diphenylacetylene (**1a**) was recovered in 90% yield when 20 mol% of dppp was injected (Table 3-2, entry 7). The optimized catalytic conditions for the arylative double-carbonylation reaction

were determined to be 5 mol% of $[RhCl(cod)]_2$ and 10 mol% of dppp.

Table 3-2 Effect of dppp in Rhodium(I)-Catalyzed Reaction of **1a** with **2a** Using Paraformaldehyde as a CO Source[a]

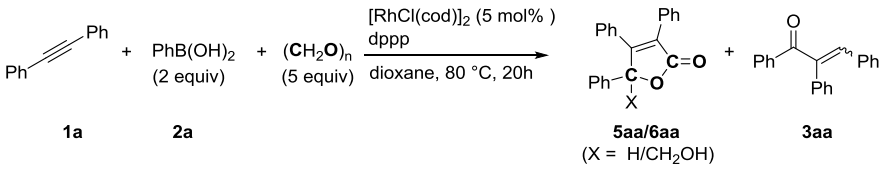

1a **2a** **5aa/6aa** (X = H/CH_2OH) **3aa**

Entry	dppp (mol%)	Yield (%)[b]	
		5aa + 6aa (**5aa** / **6aa**)	**3aa**
1	-	0 (0 / 00)	32
2	2	6 (1 / 05)	45
3	5	29 (4 / 25)	13
4	8	49 (7 / 42)	21
5	10	64 (8 / 56)	5
6	12	17 (3 / 14)	3
7	20	0 (0 / 00)	0

[a] Reaction conditions: **1a** (1 mmol), **2a** (2 mmol), paraformaldehyde (5 mmol), $[RhCl(cod)]_2$ (5 mol%), in dioxane (1 mL) at 80 °C for 20 h.

[b] Isolated yield.

In the case of less than 8 mol% dppp, the yield of butenolide was so low. Probably, the *in-situ* generated $RhCl(dppp)_2$ *vide infra* is not enough to decarbonylate formaldehyde to afford much more carbonyl species. However, more than 12 mol% dppp was not effective for affording a high yield of butenolide, probably because dppp can cover almost the phosphine-free rhodium, $[RhCl(cod)]_2$, which is the main actual catalyst for the arylative double-carbonylation of alkynes with arylboronic acids, and therefore, catalytic arylative double-carbonylation is not likely to proceed. On account of the experimental results, I believed that 10 mol% of dppp must partially cover phosphine-free rhodium complex, resulting in the formation of dppp-ligated complex along with intact $[RhCl(cod)]_2$. This is mainly responsible for the decarbonylation of formaldehyde and the subsequent arylative double-carbonylation, respectively.

3.2.4 Diverse Arylboronic Acids on Arylative Double-Carbonylation

With the above-mentioned optimum conditions in hand, the effect of the electronic nature of the substituent on the aromatic ring of arylboronic acids (**2**) on the arylative double-carbonylation of diphenylacetylene (**1a**) was next investigated. Employing arylboronic acids with electron-rich group at the *para*-position of the aromatic ring, such as *p*-methoxyphenylboronic acid (**2b**) and *p*-methylphenylboronic acid (**2c**), afforded the corresponding double-carbonylative products **5ab**/**6ab** and **5ac**/**6ac** in 77% and 71% total yields, along with a 4% and a 5% yield of the enone derivatives **3ab** and **3ac**, respectively (Table 3-3, entries 1 and 2). On the other hand, the introduction of an electron-withdrawing group into an arylboronic acid substrate (*p*-Cl: **2d**; *p*-CF_3: **2e**) decreased the yields of the double-carbonylated products **5ad/6ad** (58%) and **5ae/6ae** (48%), while the yields of mono-carbonylated products **3ad** and **3ae** were slightly increased (Table 3-3, entries 4 and 5).

These observations can be rationalized that an electron donating group at *para*-position of the aromatic ring makes carbonyl oxygen of aroyl group more electron-rich to proceed ring closure smoothly (Scheme 3-7).

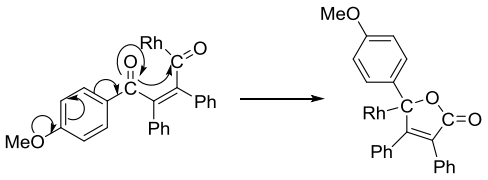

Scheme 3-7 Electron-rich arylboronic acid makes the ring closure smoothly

Table 3-3 Reaction of **1a** with Various **2** Using Paraformaldehyde as a CO Source[a]

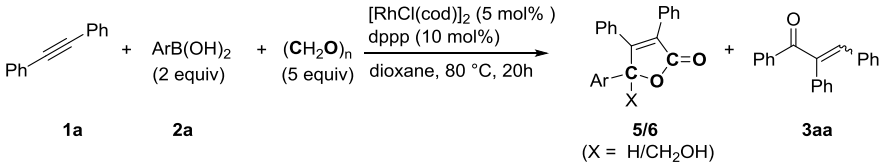

Entry	Ar **2**	Yield (%)[b]	
		5 + **6** (**5** / **6**)	**3**
1	4-$MeOC_6H_4$ (**2b**)	77 (**5ab**: 10 / **6ab**: 67)	**3ab**: 4
2	4-MeC_6H_4 (**2c**)	71 (**5ac**: 11 / **6ac**: 60)	**3ac**: 5
3	C_6H_5 (**2a**)	64 (**5aa**: 08 / **6aa**: 56)	**3aa**: 5
4	4-ClC_6H_4 (**2d**)	58 (**5ad**: 09 / **6ad**: 49)	**3ad**: 8
5	4-$CF_3C_6H_4$ (**2e**)	48 (**5ae**: 07 / **6ae**: 41)	**3ae**: 9
6	3-$MeOC_6H_4$ (**2f**)	63 (**5af**: 10 / **6af**: 53)	**3af**: 5
7	2-$MeOC_6H_4$ (**2g**)	16 (**5ag**: 12 / **6ag**: 4)	**3ag**: 1

[a] Reaction conditions: **1a** (1 mmol), **2a** (2 mmol), paraformaldehyde (5 mmol), $[RhCl(cod)]_2$ (5 mol%), dppp (10 mol%) in dioxane (1 mL) at 80 °C for 20 h.

[b] Isolated yield.

As the position of the substituent on the aromatic ring of arylboronic acids was changed from *para* to *meta* (**2f**) and *ortho* (**2g**), the yield of the arylative double-carbonylated products (**5ab/6ab**, **5af/6af**, and **5ag/6ag**) decreased, and that of the arylative mono-carbonylated products (**3ab**, **3af**, and **3ag**) increased (Table 3-3, entries 1, 6 and 7). The lower yield for desired product probably seems from the fact that the *o*-substituted acyl-rhodium(I) intermediate **I** is not reactive enough for the 1,2-addition to the carbon–carbon triple bond due to the highly steric hindrance between Rh and OMe. 80% yield of **1a** was recovered (Scheme 3-8).

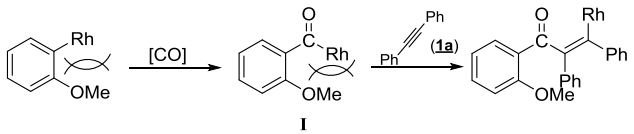

Scheme 3-8 Steric hindrance between Rh and OMe

3.2.5 Various Alkynes with Arylboronic Acids on Arylative Double-Carbonylation

The feasibility of other internal alkynes under the present arylative double-carbonylated conditions was inspected (Table 3-4). Reactions of diphenylacetylene derivatives **1b** and **1c** with *p*-$MeOC_6H_4B(OH)_2$ (**2b**) gave the corresponding butenolides **5bb/6bb** and **5cb/6cb** in 68% and 63% total yields, respectively (Table 3-4, entries 1 and 4). The same tendency which is no less than that for the reactions of diphenylacetylene (**1a**) with varying electronic nature of *para*-substituted arylboronic acids **2** (Chapter 3, Table 3-3, entries 1–5) has been observed. With increasing in electron-withdrawing effect of the substituent on the aromatic ring of $ArB(OH)_2$, the yield of butenolides **5/6** decreased. For unsymmetrical alkynes having phenyl and alkyl groups (**1e** and **1f**), the reactions proceeded with moderate regioselectivity to give predominantly the butenolides **5eb/6eb** and **6fb/7fb**, respectively (Table 3-4, entries 7 and 8), in both of which phenyl group is located at the α-position of the carbonyl group due to the steric hindrance between Ar and R_L group (Scheme 3-9).

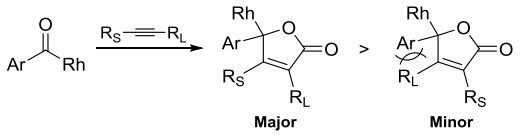

Scheme 3-9 Regioselectivity due to steric hindrance

A third isomer (**7fb**) in 11% yield was also detected by NMR analyses after treating with activated aluminium oxide (Table 3-4, entry 8). Its structure was assigned to be 4-alkyl-5-aryl-2-(3CH_2OH)-furanone by NMR nOe analysis. It can't be totally transformed *via* retro-aldol reaction and subsequent enol-ketone tautomerism under stirring with activated aluminium oxide due to the relative stable structure.

Table 3-4 Reaction of Various Alkynes **1** with Various **2** Using Paraformaldehyde as a CO Source[a]

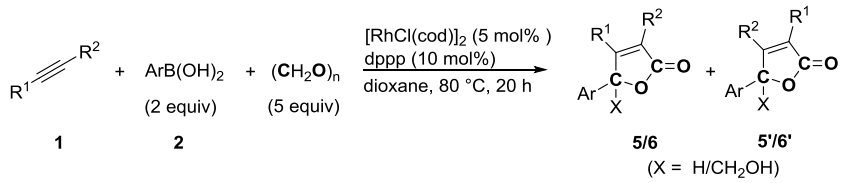

1 **2** **5/6** **5'/6'** (X = H/CH_2OH)

Entry	**1**	R^1	R^2	**2**	Yield (%)[b] **5** + **6** (**5** / **6**)	
1	**1b**	4-$MeOC_6H_4$		4-$MeOC_6H_4$ (**2b**)	68	(**5bb**: 13 / **6bb**: 55)
2				C_6H_5 (**2a**)	60	(**5ba**: 11 / **6ba**: 49)
3				4-$CF_3C_6H_4$ (**2e**)	46	(**5be**: 11 / **6be**: 35)
4	**1c**	4-$CF_3C_6H_4$		4-$MeOC_6H_4$ (**2b**)	63	(**5cb**: 06 / **6cb**: 57)
5				C_6H_5 (**2a**)	47	(**5ca**: 05 / **6ca**: 42)
6				4-$CF_3C_6H_4$ (**2e**)	26	(**5ce**: 00 / **6ce**: 26)
7	**1e**	Me	Ph	4-$MeOC_6H_4$ (**2b**)	32	(**5eb**: 15 / **6eb**: 17)
					20	(**5'eb**: 15 / **6'eb**: 5)
8[c]	**1f**	*n*-Bu	Ph	4-$MeOC_6H_4$ (**2b**)	28	(**5fb**: 00 / **6fb**: 28)
					25	(**5'fb**: 00 / **6'fb**: 25)

[a] Reaction conditions: **1a** (1 mmol), **2a** (2 mmol), paraformaldehyde (5 mmol), $[RhCl(cod)]_2$ (5 mol%), dppp (10 mol%) in dioxane (1 mL) at 80 °C for 20 h.

[b] Isolated yield.

[c] 7fb was obtained in 11% yield.

3.2.5 Utilization of $[RhCl(C_2H_4)_2]_2$ as catalyst

In order to examine the catalytic system catalyzed by phosphine-free Rh(I) complex, the same category one $[RhCl(C_2H_4)_2]_2$ instead of $[RhCl(cod)]_2$ was introduced in the reaction of diphenylacetylene (**1a**) and phenylboronic acid (**2a**) in the presence of formaldehyde under the catalytic condition consisting 5 mol% $[RhCl(C_2H_4)_2]_2$ and 10 mol% dppp (Scheme 3-10), which resulted in the similar yield of butenolide (Table 3-1, entry 6).

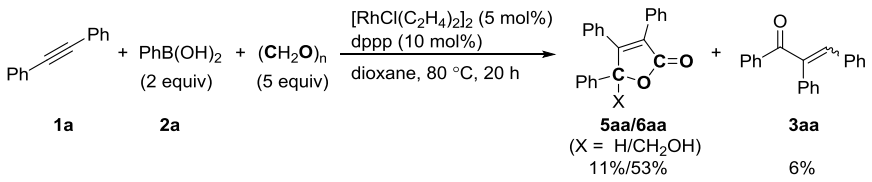

Scheme 3-10 Utilization of $[RhCl(C_2H_4)_2]_2$ as catalyst

Since C_2H_4 (ethylene) is more easily substituted by phosphine ligand than cod, ^{31}P NMR experiment shows mainly the existence of two kinds of phosphine-ligated rhodium species, which can be assigned to $RhCl(dppp)_2$ and $[RhCl(dppp)]_2$. Moreover, there is no free dppp (Figure 3-2). Based on this spectra, *in-situ* generated phosphine-ligated rhodium and intact $[RhCl(C_2H_4)_2]_2$ are mainly involved in the decarbonylation and arylative double-carbonylation processes, respectively (Scheme 3-11).

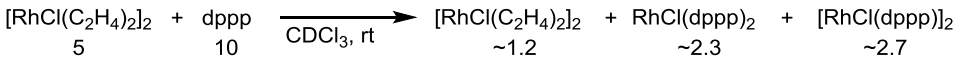

Scheme 3-11 The mixture of 5 mol% of $[RhCl(C_2H_4)_2]_2$ with 10 mol% of dppp

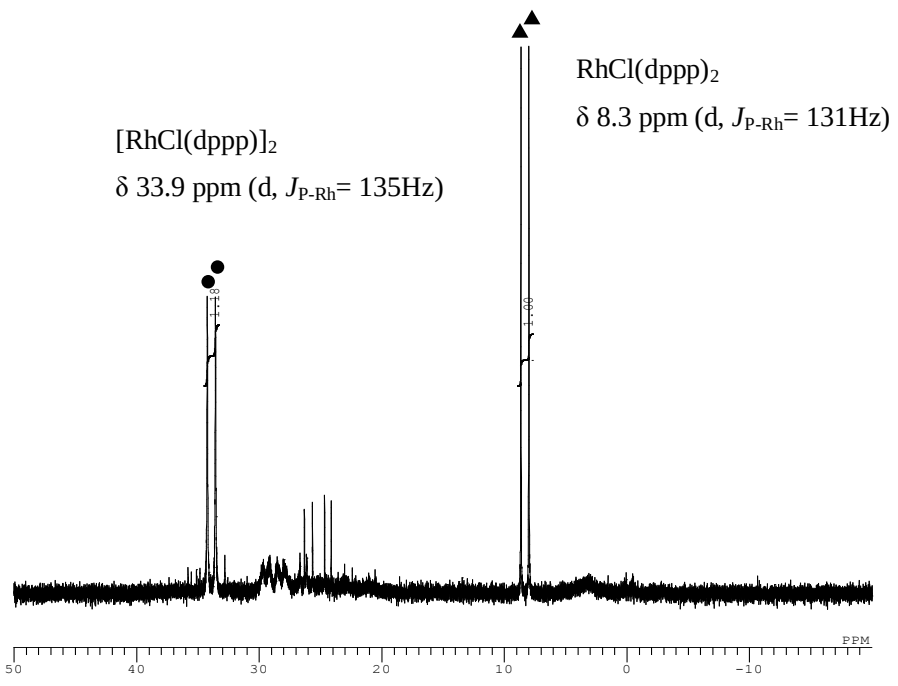

Figure 3-2 ^{31}P NMR for the mixture of 5 mol% of $[RhCl(C_2H_4)_2]_2$ with 10 mol% of dppp

3.2.6 Proposed Reaction Pathway

A plausible reaction pathway for the present reactions is shown in Scheme 3-12. As shown in chapter 2.2.8, the addition of diphosphines, the amount of which can't cover all of the loaded rhodium metal, leads to the partial formation of a Rh-phosphine species, along with the intact $[RhCl(cod)]_2$. The former phosphine-ligated Rh(I) species mainly decarbonylates formaldehyde to generate the carbonyl unit and hydrogen, while the latter predominantly catalyzes the actual arylative double-carbonylation process. Thus, RhOH (**A**) generated *in situ* from RhCl and H_2O is transmetalated with $PhB(OH)_2$ to generate RhPh (**B**). The carbonyl moiety derives from the decarbonylation process catalyzed by dppp-ligated Rh catalyst is transferred to **B**, followed by the migratory insertion of CO in formed ArRhCO intermediate (**C**) to the Aryl-Rh bond, yielding ArCORh intermediate (**D**). The subsequent aroylrhodation to an alkyne **1** in a *syn*-manner, followed by the protonation of the formed vinylrhodium **E**, producing the primary enone product, as shown in Scheme 2-13 in Chapter 2.2.8. Another carbonyl moiety from the decarbonylation process is transferred to **E** to generate diketonerhodium complex **F**, followed by a ring closure, forms an σ-furanoyl complex (**G**). Displacement of Rh from the cyclic complex by protonation or reacting with formaldehyde leads to a butenolides derivatives.

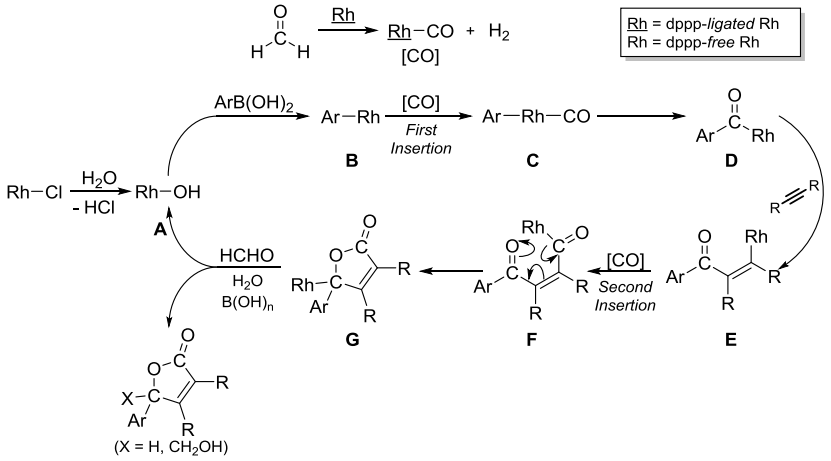

Scheme 3-12 Possible reaction pathway of Rh-catalyzed arylative double-carbonylation

σ-Furanoyl rhodium complex (G) can take place 1,3-rhodium shift reaction to generate the intermediate (**H**), followed by reacting with formaldehyde and protonation, yielding the unstable lactone (**7**) that was treated with activated alumina to give more stable butenolides **5** and **6** (Scheme 3-13).

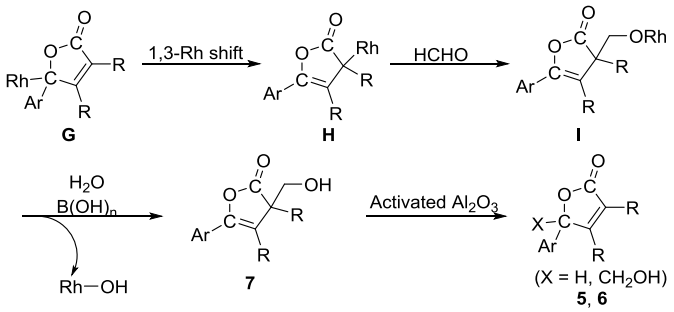

Scheme 3-13 Possible reaction pathway for product formation

3.3 Conclusion

In this chapter, I found the Rh(I)-catalysed CO gas-free arylative double-carbonylation reactions of internal alkynes with various arylboronic acids in the presence of formaldehyde as a carbonyl source to yield butenolides derivatives. The injection of dppp, the amount of which must not overlay all the total phosphine-free rhodium complex $[RhCl(cod)]_2$, results in the partial formation of dppp-ligated complex along with intact $[RhCl(cod)]_2$, which are mainly responsible for the decarbonylation of formaldehyde to generate a carbonyl moiety and the subsequent arylative double-carbonylation of alkynes with arylboronic acids using the resulting carbonyl moiety, respectively, leading to an efficient arylative double-carbonylation to produce butenolides derivatives (Scheme 3-14).

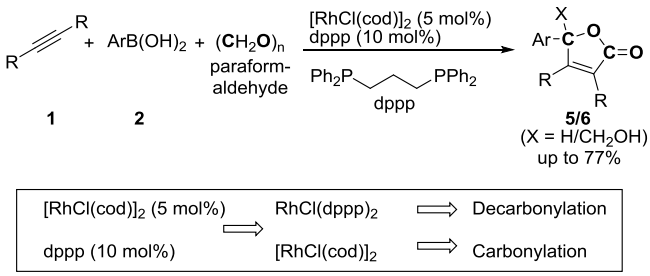

Scheme 3-14 Rh(I)-catalyzed arylative double-carbonylation of alkynes with arylboronic acids in the presence of formaldehyde

3.4 Experiment Section

3.4.1 General measurement

^{1}H NMR and ^{13}C NMR were recorded on a JEOL JNM-ECP500 spectrometer in $CDCl_3$ using tetramethylsilane (0 ppm) as an internal standard and ^{31}P NMR was also recorded on a JEOL JNM-ECP500 spectrometer in $CDCl_3$ employing phosphoric acid (0 ppm) as an external standard. Data are reported as follows: chemical shift in ppm (δ), multiplicity (s = singlet, d = doublet, t = triplet, q = quartet, and m = multiplet), coupling constant (Hz), integration, and interpretation. Infrared spectra (IR) were obtained on a JASCO FT/IR-420 spectrometer; Mass spectra were obtained on a JEOL JMS-700. X-ray crystallography was performed on Rigaku R-AXIS RAPID/S imaging plate diffractometer. Column chromatography was performed using a SiO_2 (MERCK Silica gel 60).

3.4.2 Materials

[RhCl(cod)]$_2$ was prepared using the reported method.[5] 2,2'-Bis(diphenylphosphino) biphenyl (BIPHEP) was purchased by STREM CHEMICALS, INC. and used directly without further purification. 1,2-Diphenylethyne (**1a**) and phosphine ligands were purchased by Tokyo Chemical Industry Co,. Ltd. and used directly without further purification. prop-1-yn-1-ylbenzene (**1e**) and arylboronic acids (**2**) were purchased by

Wako Pure Chemical Industries, Ltd. and used directly without further purification. Paraformaldehyde was purchased by Wako Pure Chemical Industries, Ltd. and dried with P_2O_5 under vacumn prior to use. 1, 4-Dioxane dehydrated was purchased by Wako Pure Chemical Industries, Ltd. and dried with 4Å molecular sieve, which was degassed using freeze-pump-thaw method for 3 times and stored in glove box and used directly without further purification.

3.4.3 Typical procedure for the Rh(I)-catalyzed arylative double-carbonylation of alkynes with arylboronic acids in the presence of formaldehyde

In a 10 mL screw-capped vial were placed $[RhCl(cod)]_2$ (24.6 mg, 0.05 mmol), dppp (41.4 mg, 0.1 mmol), alkyne **1** (1 mmol), arylboronic acid **2** (2 mmol), paraformaldehyde (150.2 mg, 5 mmol), and 1,4-dioxane (1 mL). The mixture was degassed by three freeze-pump-thaw cycles and then sealed under N_2. The mixture was stirred at 80 °C for 20 h, cooled to room temperature and then transferred in 50 mL flask using 10 mL ethyl acetate and treated with 8 g activated aluminium oxide (Al_2O_3) to stir for 1 h. The reaction mixture was filtered through a short path of celite and the filtrate was concentrated *in vacuo*. The residue was purified by flash chromatography on silica gel.

3,4,5-triphenylfuran-2(5*H*)-one (5aa)

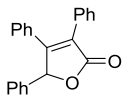

5aa

Colorless solid; mp 124.0-125.2 °C; R_f 0.47 (hexane/AcOEt = 2/1); ^{1}H NMR (500 MHz, $CDCl_3$) δ: 6.27 (s, 1H), 7.11 (d, J = 8.5 Hz, 2H), 7.21 (t, J = 7.5 Hz, 2H), 7.31-7.37 (m, 9H), 7.47-7.48 (m, 2H); ^{13}C NMR (125 MHz, $CDCl_3$) δ: 83.7, 126.8,

127.4, 127.6, 128.1, 128.3, 128.5, 128.7, 128.9, 129.1, 129.2, 129.4, 129.7, 129.9, 131.0, 134.7, 159.3, 172.5; IR (neat, cm^{-1}) 2923, 2853, 1752 (C=O), 1012, 963, 745, 695; MS (EI): *m/z* (%) = 312 (21) [M^+], 284 (3), 265 (7), 252 (6), 239 (5), 207 (12), 178 (100), 152 (20), 105 (42), 77 (51), 51 (26); HRMS: *m/z* calcd [M^+]: 312.1150, found 312.1152.

Crystallographic data for **5aa** is as follows: $C_{22}H_{16}O_2$, *M*r = 312.37, colorless, block, 0.120 × 0.070 × 0.030 mm, monoclinic, Primitive, a = 10.6542(9) Å, b = 8.8328(7) Å, c = 17.640(2) Å, β = 96.005(3) °, V = 1650.9(2) $Å^3$, Z = 4, ρ_c = 1.257 g/cm^3, μ = 0.794 cm^{-1}, T = 123 K, λ = 0.71075 Å, 15833 reflections, 3373 unique [R(int) = 0.0429), Final *GoF* = 1.077, R_1 = 0.0471 ([$I > 2.00\sigma(I)$]), wR_2 = 0.1080 (all data). CCDC No.: 1002969.

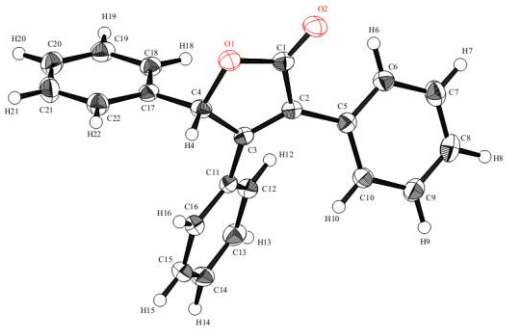

Figure 1 ORTEP representation of **5aa** (50% thermal ellipsolids)

5-(hydroxymethyl)-3,4,5-triphenylfuran-2(5*H*)-one (6aa)

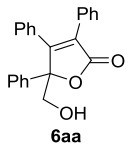

6aa

Colorless solid; mp 143.1-144.6 °C; R_f 0.28 (hexane/AcOEt = 2/1); ^{1}H NMR (500 MHz, $CDCl_3$) δ: 2.36 (s, 1H), 4.27 (s, 2H), 6.92 (d, J = 7.0 Hz, 2H), 7.19-7.39 (m, 13H); ^{13}C NMR (125 MHz, $CDCl_3$) δ: 64.0, 90.9, 125.7, 128.1, 128.3, 128.5, 128.6, 129.2, 131.7, 135.0, 162.6, 172.5; IR (neat, cm^{-1}) 3449, 3058, 2925, 1752 (C=O), 1409,

1445, 1178, 1005, 749, 696; MS (EI): *m/z* (%) = 342 (5) [M^+], 312 (63), 311 (60), 284 (3), 265 (7), 252 (6), 207 (40), 179 (50), 178 (49), 152 (6), 105 (100), 77 (35), 51 (4); HRMS: *m/z* calcd [M^+]: 342.1256, found 342.1254.

Crystallographic data for **6aa** is as follows: $C_{23}H_{18}O_2$, *M*r = 342.39, colorless, block, 0.170 × 0.110 × 0.030 mm, orthorhombic, Primitive, a = 24.4574(5) Å, b = 15.1514(3) Å, c = 10.3240(2) Å, V = 3825.7(2) Å^3, Z = 8, ρ_c = 1.189 g/cm^3, μ = 0.779 cm^{-1}, T = 123 K, λ = 0.71075 Å, 52627 reflections, 6977 unique [R(int) = 0.0823), Final *GoF* = 1.077, R_1 = 0.0542 ([$I > 2.00\sigma(I)$]), wR_2 = 0.1427 (all data). CCDC No.: 1002983.

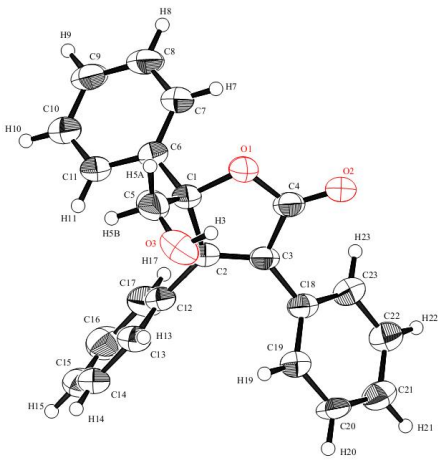

Figure 2 ORTEP representation of **6aa** (50% thermal ellipsolids)

5-(4-methoxyphenyl)-3,4-diphenylfuran-2(5*H*)-one (5ab)

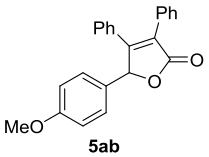

5ab

Colorless solid; mp 112.0-113.1 °C; R_f 0.39 (hexane/AcOEt = 2/1); ^{1}H NMR (500 MHz, $CDCl_3$) δ: 3.78 (s, 3H), 6.23 (s, 1H), 6.85 (d, J = 9.0 Hz, 2H), 7.11 (d, J = 7.0 Hz, 2H), 7.21-7.27 (m, 5H), 7.34-7.37 (m, 3H), 7.46-7.48 (m, 2H); ^{13}C NMR (125 MHz, $CDCl_3$) δ: 55.1, 83.3, 114.2, 126.5, 126.7, 128.3, 128.5, 128.6, 128.7, 129.0, 129.3,

129.7, 129.8, 131.1, 159.2, 160.2, 172.5; IR (neat, cm^{-1}) 2921, 2851, 1750 (C=O), 1608, 1514, 1457, 1158; MS (EI): *m/z* (%) = 342 (55) [M^+], 314 (3), 285 (7), 252 (11), 237 (11), 207 (15), 178 (80), 135 (100), 126 (6), 77 (13), 57 (8); HRMS: *m/z* calcd [M^+]: 342.1256, found 342.1255.

5-(hydroxymethyl)-5-(4-methoxyphenyl)-3,4-diphenylfuran-2(5*H*)-one (6ab)

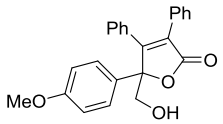

6ab

Colorless solid; mp 164.6-165.8 °C; R_f 0.20 (hexane/AcOEt = 2/1); ^{1}H NMR (500 MHz, $CDCl_3$) δ: 2.47-2.49 (m, 1H), 3.81 (s, 3H), 4.20-4.24 (m, 2H), 6.86 (d, *J* = 6.0 Hz, 2H), 6.92 (d, *J* = 6.5 Hz, 2H), 7.13 (d, *J* = 6.5 Hz, 2H), 7.23-7.40 (m, 8H); ^{13}C NMR (125 MHz, $CDCl_3$) δ: 55.1, 63.8, 90.8, 113.9, 126.8, 127.1, 127.6, 128.0, 128.3, 128.5, 129.0, 129.1, 129.4, 131.7, 159.6, 162.7, 172.6; IR (neat, cm^{-1}) 3449, 3057, 3020, 2933, 2837, 1752 (C=O), 1609, 1513, 1255, 833, 760, 698; MS (EI): *m/z* (%) = 342 (8) [M^+], 312 (3), 311 (2), 281 (1), 237 (2), 207 (4), 178 (5), 135 (12), 83 (100), 69 (6), 59 (7); HRMS: *m/z* calcd [M^+]: 372.1362, found 372.1363.

3,4-diphenyl-5-(*p*-tolyl)furan-2(5*H*)-one (5ac)

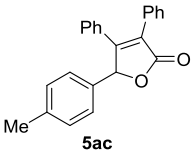

5ac

Colorless solid; mp 119.0-120.2 °C; R_f 0.47 (hexane/AcOEt = 2/1); ^{1}H NMR (500 MHz, $CDCl_3$) δ: 2.31 (s, 3H), 6.23 (s, 1H), 7.10-7.48 (m, 14H); ^{13}C NMR (125 MHz, $CDCl_3$) δ: 21.2, 83.6, 127.6, 128.3, 128.5, 128.6, 128.8, 129.4, 129.6, 129.8, 131.1, 131.6, 139.3, 159.3, 172.6; IR (neat, cm^{-1}) 3055, 2923, 2853, 1752 (C=O), 1598, 1445,

963, 695; MS (EI): *m/z* (%) = 326 (35) [M^+], 298 (3), 269 (5), 252 (7), 221 (11), 207 (32), 178 (100), 176 (30), 152 (20), 119 (65), 91 (35), 57 (10); HRMS: *m/z* calcd [M^+]: 326.1307, found 326.1306.

5-(hydroxymethyl)-3,4-diphenyl-5-(*p*-tolyl)furan-2(5*H*)-one (6ac)

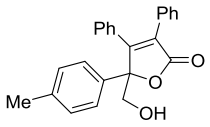

6ac

Colorless solid; mp 158.8-160.0 °C; R_f 0.28 (hexane/AcOEt = 2/1); ^{1}H NMR (500 MHz, $CDCl_3$) δ: 2.35 (s, 3H), 2.54-2.56 (m, 1H), 4.20-4.25 (m, 2H), 6.93 (d, *J* = 7.0 Hz, 2H), 7.11 (dd, *J* = 30.5, 8.5 Hz, 4H), 7.22-7.39 (m, 8H); ^{13}C NMR (125 MHz, $CDCl_3$) δ: 20.8, 63.7, 90.7, 125.4, 127.4, 127.8, 128.1, 128.3, 128.9, 129.0, 129.2, 131.5, 131.7, 138.3, 162.4, 172.3; IR (neat, cm^{-1}) 3435, 3057, 3024, 2923, 2876, 1752 (C=O), 1513, 1444, 1180, 1007, 819, 758; MS (EI): *m/z* (%) = 356 (8) [M^+], 325 (95), 323 (8), 298 (11), 265 (12), 252 (11), 221 (21), 207 (55), 179 (70), 178 (69), 152 (13), 119 (100), 91 (60), 65 (14), 57 (12); HRMS: *m/z* calcd [M^+]: 356.1412, found 356.1412.

5-(4-chlorophenyl)-3,4-diphenylfuran-2(5*H*)-one (5ad)

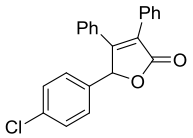

5ad

Colorless solid; mp 132.0-133.2 °C; R_f 0.47 (hexane/AcOEt = 2/1); ^{1}H NMR (500 MHz, $CDCl_3$) δ: 6.25 (s, 1H), 7.09-7.48 (m, 14H); ^{13}C NMR (125 MHz, $CDCl_3$) δ: 82.8, 128.2, 128.6, 128.8, 128.9, 129.2, 129.3, 129.5, 130.1, 130.8, 133.2, 135.2, 159.0, 172.3; IR (neat, cm^{-1}) 2923, 2853, 1752 (C=O), 1598, 1445, 1156, 963, 852; MS (EI): *m/z* (%) = 346 (35) [M^+], 318 (3), 265 (11), 241 (7), 208 (4), 207 (32), 178 (100), 176

(32), 139 (42), 111 (22), 77 (15), 75 (14), 51 (12); HRMS: *m/z* calcd [M^+]: 346.0761, found 346.0761.

5-(4-chlorophenyl)-5-(hydroxymethyl)-3,4-diphenylfuran-2(5*H*)-one (6ad)

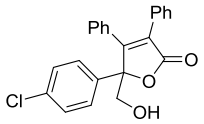

6ad

Colorless solid; mp 155.1-157.0 °C; R_f 0.28 (hexane/AcOEt = 2/1); ^{1}H NMR (500 MHz, $CDCl_3$) δ: 2.38 (t, *J* = 7.0 Hz, 1H), 4.20-4.22 (m, 2H), 6.93 (d, *J* = 7.0 Hz, 2H), 7.11 (d, *J* = 8.5 Hz, 2H), 7.22-7.38 (m, 10H); ^{13}C NMR (125 MHz, $CDCl_3$) δ: 63.8, 90.6, 127.1, 127.9, 128.0, 128.2, 128.6, 128.7, 129.1, 131.4, 133.6, 134.6, 162.3, 172.3; IR (neat, cm^{-1}) 3434, 3056, 3024, 2925, 2876, 1755 (C=O), 1492, 1176, 1005, 696; MS (EI): *m/z* (%) = 376 (3) [M^+], 346 (65), 345 (35), 312 (25), 283 (6), 265 (8), 241 (6), 207 (50), 179 (70), 179 (69), 178 (50), 139 (43), 105 (23), 83 (100), 69 (20), 57 (13); HRMS: *m/z* calcd [M^+]: 376.0866, found 376.0871.

3,4-diphenyl-5-(4-(trifluoromethyl)phenyl)furan-2(5*H*)-one (5ae)

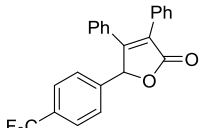

5ae

Colorless solid; mp 132.6-133.7 °C; R_f 0.47 (hexane/AcOEt = 2/1); ^{1}H NMR (500 MHz, $CDCl_3$) δ: 6.33 (s, 1H), 7.12 (d, *J* = 7.5 Hz, 2H), 7.23-7.48 (m, 10H), 7.58 (d, *J* = 7.0 Hz, 2H); ^{13}C NMR (125 MHz, $CDCl_3$) δ: 82.6, 122.6, 125.8, 125.9 (*tet*), 127.0, 127.8, 128.2, 128.6, 128.9, 129.1, 129.3, 129.4, 130.2, 130.7, 131.5, 138.8, 158.9, 172.1; IR (neat, cm^{-1}) 3059, 2924, 2853, 1758 (C=O), 1446, 1325, 1068, 850; MS (EI): *m/z* (%) = 380 (30) [M^+], 361 (3), 352 (2), 275 (5), 208 (8), 207 (60), 179 (100), 178

(53), 145 (7), 126 (4), 105 (5), 77 (4), 51 (3); HRMS: *m/z* calcd [M^+]: 380.1024, found 380.1024.

5-(hydroxymethyl)-3,4-diphenyl-5-(4-(trifluoromethyl)phenyl)furan-2(5*H*)-one (6ae)

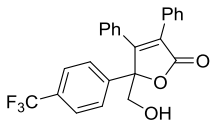

6ae

Colorless solid; mp 143.7-145.2 °C; R_f 0.28 (hexane/AcOEt = 2/1); ^{1}H NMR (500 MHz, $CDCl_3$) δ: 2.57 (dd, *J* = 9.0, 6.0 Hz, 1H), 4.20-4.30 (m, 2H), 6.95 (d, *J* = 7.5 Hz, 2H), 7.22-7.40 (m, 10H), 7.58 (d, *J* = 8.5 Hz, 2H); ^{13}C NMR (125 MHz, $CDCl_3$) δ: 64.0, 90.8, 123.7 (q, $^1J_{C\text{-}F}$ = 270.6 Hz), 125.4 (q, $^3J_{C\text{-}F}$ = 3.6 Hz), 126.1, 126.9, 128.1, 128.2, 128.3, 128.6, 128.9, 129.1, 129.4, 130.7 (q, $^2J_{C\text{-}F}$ = 32.1 Hz), 131.3, 139.2, 162.0, 172.3; IR (neat, cm^{-1}) 3434, 3056, 3024, 2925, 2876, 1758 (C=O), 1326, 1170, 1005, 843; MS (EI): *m/z* (%) = 410 (3) [M^+], 380 (35), 379 (20), 352 (4), 281 (2), 265 (4), 235 (15), 207 (12), 173 (62), 145 (27), 126 (5), 105 (6), 83 (100), 69 (15), 60 (10); HRMS: *m/z* calcd [M^+]: 410.1130, found 410.1130.

5-(3-methoxyphenyl)-3,4-diphenylfuran-2(5*H*)-one (5af)

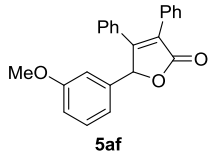

5af

Colorless liquid; R_f 0.42 (hexane/AcOEt = 2/1); ^{1}H NMR (500 MHz, $CDCl_3$) δ: 3.68 (s, 3H), 6.15 (s, 1H), 6.73-7.39 (m, 14H); ^{13}C NMR (125 MHz, $CDCl_3$) δ: 55.3, 70.6, 83.5, 113.2, 114.6, 120.0, 127.5, 128.3, 128.5, 128.7, 129.0, 129.4, 129.8, 136.2, 159.2, 159.8, 172.4; IR (neat, cm^{-1}) 2921, 2851, 1755 (C=O), 1599, 1450, 1165; MS (EI): *m/z*

(%) = 342 (25) [M^+], 314 (3), 285 (4), 252 (11), 237 (7), 207 (18), 178 (100), 152 (25), 135 (28), 107 (26), 77 (33), 57 (43); HRMS: *m/z* calcd [M^+]: 342.1256, found 342.1256.

5-(hydroxymethyl)-5-(3-methoxyphenyl)-3,4-diphenylfuran-2(5*H*)-one (6af)

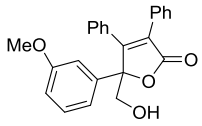

6af

Colorless liquid; R_f 0.26 (hexane/AcOEt = 2/1); ^{1}H NMR (500 MHz, $CDCl_3$) δ: 2.49 (t, *J* = 7.0 Hz, 1H), 3.71 (s, 3H), 4.24 (d, *J* = 6.0 Hz, 2H), 6.72-6.76 (m, 2H), 6.88 (dd, *J* = 8.0, 2.0 Hz, 1H), 6.97 (d, *J* = 7.0 Hz, 2H), 7.22-7.39 (m, 9H); ^{13}C NMR (125 MHz, $CDCl_3$) δ: 64.1, 90.9, 111.4, 114.2, 118.0, 127.9, 128.1, 128.4, 128.5, 128.7, 129.1, 129.2, 129.3, 131.8, 136.6, 159.5, 162.4, 172.4; IR (neat, cm^{-1}) 3433, 3056, 3022, 2933, 2837, 1752 (C=O), 1600, 1490, 1264, 1007, 786; MS (EI): *m/z* (%) = 372 (3) [M^+], 342 (50), 341 (38), 314 (5), 252 (8), 207 (22), 178 (100), 135 (88), 107 (30), 77 (38), 57 (18); HRMS: *m/z* calcd [M^+]: 372.1362, found 372.1366.

5-(2-methoxyphenyl)-3,4-diphenylfuran-2(5*H*)-one (5ag)

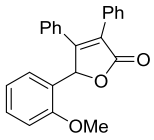

5ag

Colorless liquid; R_f 0.43 (hexane/AcOEt = 2/1); ^{1}H NMR (500 MHz, $CDCl_3$) δ: 3.75 (s, 3H), 6.73 (s, 1H), 6.80-7.40 (m, 14H); ^{13}C NMR (125 MHz, $CDCl_3$) δ: 55.6, 70.6, 111.2, 120.9, 122.9, 126.1, 127.5, 128.5, 128.7, 129.0, 129.3, 129.4, 156.1, 159.6, 173.0; IR (neat, cm^{-1}) 2921, 2851, 1752 (C=O), 1690, 1657, 1158; MS (EI): *m/z* (%) = 342 (13) [M^+], 314 (3), 281 (2), 252 (4), 236 (20), 207 (8), 178 (80), 152 (22), 135 (23), 105 (13), 83 (100), 77 (33), 51 (31); HRMS: *m/z* calcd [M^+]: 342.1256, found 342.1254.

5-(hydroxymethyl)-5-(2-methoxyphenyl)-3,4-diphenylfuran-2(5*H*)-one (6ag)

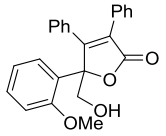

6ag

Colorless solid; mp 62.5-63.9 °C; R_f 0.20 (hexane/AcOEt = 2/1); ^{1}H NMR (500 MHz, $CDCl_3$) δ: 2.19 (t, *J* = 7.5 Hz, 1H), 3.51 (s, 3H), 4.19-4.35 (m, 2H), 6.78 (d, *J* = 5.0 Hz, 2H), 6.84 (d, *J* = 10.0 Hz, 1H), 6.91 (m, 1H), 7.12-7.33 (m, 10H); ^{13}C NMR (125 MHz, $CDCl_3$) δ: 55.4, 64.3, 89.6, 112.0, 120.8, 122.4, 128.0, 128.2, 128.3, 128.6, 128.7, 129.0, 129.2, 129.4, 130.6, 132.2, 158.3, 160.6, 172.7; IR (neat, cm^{-1}) 3409, 2917, 2849, 1744 (C=O), 1598, 1180, 1076, 751; MS (EI): *m/z* (%) = 372 (1) [M^+], 342 (21), 341 (28), 314 (4), 252 (8), 207 (8), 178 (80), 135 (56), 107 (13), 83 (100), 57 (45); HRMS: *m/z* calcd [M^+]: 372.1362, found 372.1371.

3,4,5-tris(4-methoxyphenyl)furan-2(5*H*)-one (5bb)

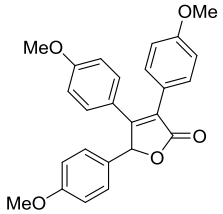

5bb

Colorless liquid; R_f 0.19 (hexane/AcOEt = 2/1); ^{1}H NMR (500 MHz, $CDCl_3$) δ: 3.74 (s, 3H), 3.77 (s, 3H), 3.83 (s, 3H), 6.18 (s, 1H), 6.71 (d, *J* = 9.0 Hz, 2H), 6.84 (d, *J* = 9.0 Hz, 2H), 6.91 (d, *J* = 9.0 Hz, 2H), 7.10 (d, *J* = 9.0 Hz, 2H), 7.22 (d, *J* = 9.0 Hz, 2H), 7.44 (d, *J* = 8.5 Hz, 2H); ^{13}C NMR (125 MHz, $CDCl_3$) δ: 55.1, 55.2, 55.2, 83.1, 114.0, 114.1, 114.2, 122.5, 122.7, 124.0, 127.2, 127.5, 128.7, 129.1, 129.7, 130.0, 130.2, 130.7, 131.1, 149.9, 157.6, 160.1, 160.5, 172.4; IR (neat, cm^{-1}) 3003, 2933, 2837, 1747 (C=O), 1606, 1513, 1457, 1252, 1177, 1029, 833; HRMS (ESI): *m/z* calcd for $C_{25}H_{22}NaO_5$:

425.1365, found 425.1365.

5-(hydroxymethyl)-3,4,5-tris(4-methoxyphenyl)furan-2(5*H*)-one (6bb)

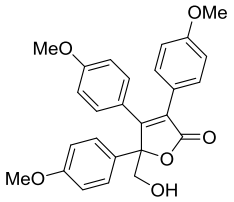

6bb

Colorless liquid; R_f 0.11 (hexane/AcOEt = 2/1); ^{1}H NMR (500 MHz, $CDCl_3$) δ: 2.35-2.37 (m, 1H), 3.77 (s, 3H), 3.79 (s, 3H), 3.82 (s, 3H), 4.14-4.27 (m, 2H), 6.78 (d, *J* = 9.0 Hz, 4H), 6.86-6.88 (m, 4H), 7.18 (d, *J* = 9.0 Hz, 2H), 7.37 (d, *J* = 8.5 Hz, 2H); ^{13}C NMR (125 MHz, $CDCl_3$) δ: 55.0, 55.1, 55.1, 64.0, 90.4, 113.5, 113.9, 114.0, 122.1, 123.2, 123.9, 126.4, 127.2, 127.3, 129.9, 130.5, 159.4, 159.6, 160.0, 160.5, 172.8; IR (neat, cm^{-1}) 3451, 2958, 2934, 2837, 1747 (C=O), 1607, 1513, 1253, 1175, 1031, 833; HRMS (ESI): *m/z* calcd for $C_{26}H_{24}NaO_5$: 455.1471, found 455.1471.

3,4-bis(4-methoxyphenyl)-5-phenylfuran-2(5*H*)-one (5ba)

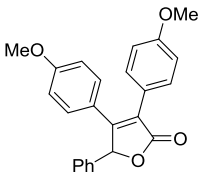

5ba

Colorless liquid; R_f 0.28 (hexane/AcOEt = 2/1); ^{1}H NMR (500 MHz, $CDCl_3$) δ: 3.74 (s, 3H), 3.84 (s, 3H), 6.21 (s, 1H), 6.72 (d, *J* = 9.5 Hz, 2H), 6.91 (d, *J* = 8.5 Hz, 2H), 7.11 (d, *J* = 9.0 Hz, 2H), 7.29-7.34 (m, 5H), 7.45 (d, *J* = 9.5 Hz, 2H); ^{13}C NMR (125 MHz, $CDCl_3$) δ: 55.2, 55.2, 83.4, 114.0, 122.4, 123.4, 124.9, 127.7, 128.9, 129.3, 129.9, 130.7, 135.3, 157.4, 159.8, 160.6, 173.0; IR (neat, cm^{-1}) 2933, 2837, 1750 (C=O), 1605, 1517, 1253, 1025, 835; HRMS (ESI): *m/z* calcd for $C_{24}H_{20}NaO_4$: 395.1259, found

395.1259.

5-(hydroxymethyl)-3,4-bis(4-methoxyphenyl)-5-phenylfuran-2(5*H*)-one (6ba)

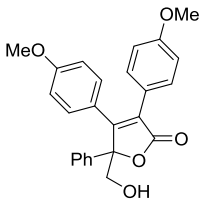

6ba

Colorless liquid; R_f 0.14 (hexane/AcOEt = 2/1); ^{1}H NMR (500 MHz, $CDCl_3$) δ: 2.52 (br, 1H), 3.77 (s, 3H), 3.79 (s, 3H), 4.19-4.29 (m, 2H), 6.76-7.34 (m, 13H); ^{13}C NMR (125 MHz, $CDCl_3$) δ: 29.2, 31.7, 55.1, 64.0, 69.7, 90.8, 113.6, 114.2, 122.1, 124.0, 125.9, 126.8, 128.6, 128.7, 129.9, 130.0, 130.6, 135.6, 159.6, 160.1, 160.7, 173.0; IR (neat, cm^{-1}) 3451, 2934, 2837, 1751 (C=O), 1606, 1516, 1251, 1175, 828; HRMS (ESI): *m/z* calcd for $C_{25}H_{22}NaO_5$: 425.1365, found 425.1365.

3,4-bis(4-methoxyphenyl)-5-(4-(trifluoromethyl)phenyl)furan-2(5*H*)-one (5be)

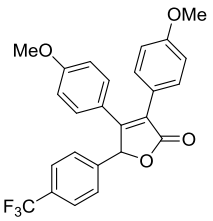

5be

Colorless liquid; R_f 0.28 (hexane/AcOEt = 2/1); ^{1}H NMR (500 MHz, $CDCl_3$) δ: 3.73 (s, 3H), 3.81 (s, 3H), 6.28 (s, 1H), 6.72 (d, *J* = 8.5 Hz, 2H), 6.89 (d, *J* = 9.0 Hz, 2H), 7.09 (d, *J* = 9.0 Hz, 2H), 7.40-7.43 (m, 4H), 7.56 (d, *J* = 8.0 Hz, 2H); ^{13}C NMR (125 MHz, $CDCl_3$) δ: 55.2, 55.3, 82.3, 114.1, 114.3, 122.0, 123.0, 125.1, 125.9 (*tet*), 128.0, 129.8, 130.7, 139.4, 157.0, 160.8, 172.7; IR (neat, cm^{-1}) 2916, 1752 (C=O), 1606, 1507, 1254, 1124, 834; HRMS (ESI): *m/z* calcd for $C_{25}H_{19}F_3NaO_4$: 463.1133, found 463.1133.

5-(hydroxymethyl)-3,4-bis(4-methoxyphenyl)-5-(4-(trifluoromethyl)phenyl)furan-2(5*H*)-one (6be)

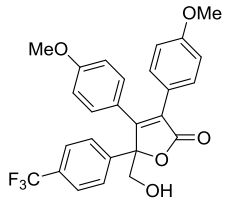

6be

Colorless liquid; R_f 0.14 (hexane/AcOEt = 2/1); ^{1}H NMR (500 MHz, $CDCl_3$) δ: 2.40 (t, *J* = 10.0 Hz, 1H), 3.77 (s, 3H), 3.82 (s, 3H), 4.24 (d, *J* = 6.5 Hz, 2H), 6.77 (d, *J* = 9.0 Hz, 2H), 6.84-6.89 (m, 4H), 7.33-7.36 (m, 4H), 7.59 (d, *J* = 8.5 Hz, 2H); ^{13}C NMR (125 MHz, $CDCl_3$) δ: 55.1, 55.2, 64.3, 90.4, 113.6, 114.4, 121.6, 123.7 (q, $^1J_{C\text{-}F}$ = 270.6 Hz), 124.8, 125.4 (q, $^3J_{C\text{-}F}$ = 3.6 Hz), 126.3, 127.1, 129.8, 130.5, 135.7 (q, $^2J_{C\text{-}F}$ = 32.6 Hz), 139.7, 159.6, 160.2, 172.5; IR (neat, cm^{-1}) 2916, 1752 (C=O), 1606, 1507, 1254, 1124, 834; HRMS (ESI): *m/z* calcd for $C_{26}H_{21}F_3NaO_5$: 493.1239, found 493.1239.

5-(4-methoxyphenyl)-3,4-bis(4-(trifluoromethyl)phenyl)furan-2(5*H*)-one (5cb)

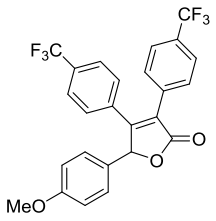

5cb

Colorless liquid; R_f 0.36 (hexane/AcOEt = 2/1); ^{1}H NMR (500 MHz, $CDCl_3$) δ: 3.80 (s, 3H), 6.25 (s, 1H), 6.88 (d, *J* = 9.0 Hz, 2H), 7.19 (t, *J* = 9.0 Hz, 4H), 7.51 (d, *J* = 5.0 Hz, 2H), 7.58 (d, *J* = 8.0 Hz, 2H), 7.64 (d, *J* = 10.0 Hz, 2H); ^{13}C NMR (125 MHz, $CDCl_3$) δ: 55.3, 83.6, 114.6, 125.3, 125.7, 126.0, 127.2, 128.6, 129.0, 129.8, 159.1, 160.6, 171.3; IR (neat, cm^{-1}) 3059, 2925, 2853, 1757 (C=O), 1612, 1548, 1324, 1168, 1068; MS (EI): *m/z* (%) = 478 (45) [M^+], 459 (8), 421 (6), 314 (35), 295 (8), 246 (4),

225 (3), 135 (100), 71(13); HRMS: *m/z* calcd [M^+]: 478.1004, found 478.1004.

5-(hydroxymethyl)-5-(4-methoxyphenyl)-3,4-bis(4-(trifluoromethyl)phenyl)furan-2(5*H*)-one (6cb)

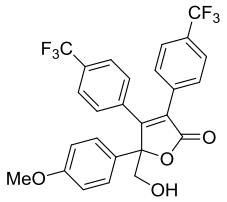

6cb

Colorless solid; mp 80.5-81.7 °C; R_f 0.22 (hexane/AcOEt = 2/1); ^{1}H NMR (500 MHz, $CDCl_3$) δ: 2.63 (br, 1H), 3.83 (s, 3H), 4.16-4.28 (m, 2H), 6.89 (d, *J* = 9.5 Hz, 2H), 7.05 (d, *J* = 8.0 Hz, 2H), 7.09 (d, *J* = 8.5 Hz, 2H), 7.49 (dd, *J* = 21.5, 8.5 Hz 4H), 7.58 (d, *J* = 8.5 Hz, 2H); ^{13}C NMR (125 MHz, $CDCl_3$) δ: 55.3, 63.6, 91.2, 114.3, 123.9 (q, $^1J_{C\text{-}F}$ = 272.5 Hz), 124.0 (q, $^1J_{C\text{-}F}$ = 271.3 Hz), 125.3 (q, $^3J_{C\text{-}F}$ = 3.8 Hz), 125.7, 125.8 (q, $^3J_{C\text{-}F}$ = 3.8 Hz), 127.0, 128.0, 128.8, 129.5, 131.0 (q, $^2J_{C\text{-}F}$ = 32.5 Hz), 131.6 (q, $^2J_{C\text{-}F}$ = 32.5 Hz), 131.7, 132.5, 135.0, 160.1, 162.9, 171.7; IR (neat, cm^{-1}) 3434, 2916, 1757 (C=O), 1613, 1514, 1325, 1257, 828; MS (EI): *m/z* (%) = 508 (1) [M^+], 478 (100), 477 (90), 421 (13), 320 (5), 314 (72), 246 (8), 225 (6), 176 (3), 135 (100), 57 (19); HRMS: *m/z* calcd [M^+]: 508.1109, found 508.1109.

5-phenyl-3,4-bis(4-(trifluoromethyl)phenyl)furan-2(5*H*)-one (5ca)

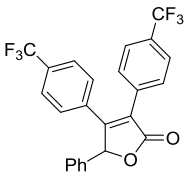

5ca

Colorless liquid; R_f 0.42 (hexane/AcOEt = 2/1); ^{1}H NMR (500 MHz, $CDCl_3$) δ: 6.28 (s, 1H), 7.18 (d, *J* = 8.0 Hz, 2H), 7.36-7.54 (m, 6H), 7.58 (d, *J* = 8.0 Hz, 3H), 7.64 (d, *J*

= 8.5 Hz, 2H); ^{13}C NMR (125 MHz, $CDCl_3$) δ: 69.6, 83.9, 125.7 (*tet*), 126.0 (*tet*), 127.5, 128.6, 128.9, 129.1, 129.2, 129.7, 129.8, 136.0, 158.8, 171.4; IR (neat, cm^{-1}) 2920, 1763 (C=O), 1324, 1168, 1128, 1018; MS (EI): *m/z* (%) = 448 (32) [M^+], 447 (8), 343 (6), 314 (35), 295 (9), 210 (18), 173 (100), 134 (79), 105 (97), 77 (30); HRMS: *m/z* calcd [M^+]: 448.0898, found 448.0897.

5-(hydroxymethyl)-5-phenyl-3,4-bis(4-(trifluoromethyl)phenyl)furan-2(5*H*)-one (6ca)

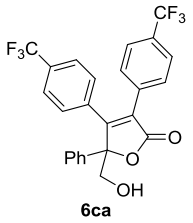

6ca

Colorless liquid; R_f 0.33 (hexane/AcOEt = 2/1); ^{1}H NMR (500 MHz, $CDCl_3$) δ: 2.54 (dd, *J* = 8.5, 5.0 Hz, 1H), 4.26 (qd, *J* = 21.0, 12.5, 9.0 Hz, 2H), 7.05 (d, *J* = 8.0 Hz, 2H), 7.15-7.17 (m, 2H), 7.36-7.40 (m, 3H), 7.49 (dd, *J* = 24.0, 8.0 Hz, 4H), 7.59 (d, *J* = 8.0 Hz, 2H); ^{13}C NMR (125 MHz, $CDCl_3$) δ: 63.6, 91.4, 123.6 (q, $^1J_{C\text{-}F}$ = 270.0 Hz), 123.7 (q, $^1J_{C\text{-}F}$ = 271.3 Hz), 125.3 (q, $^3J_{C\text{-}F}$ = 3.8 Hz), 125.5, 125.9 (q, $^3J_{C\text{-}F}$ = 3.6 Hz), 127.9, 128.8, 129.0, 129.3, 129.5, 130.7 (q, $^2J_{C\text{-}F}$ = 31.3 Hz), 131.6 (q, $^2J_{C\text{-}F}$ = 32.5 Hz), 132.4, 134.0, 134.9, 162.9, 171.7; IR (neat, cm^{-1}) 3403, 3081, 2920, 1753 (C=O), 1617, 1328, 1166, 1123, 826; HRMS (ESI): *m/z* calcd for $C_{25}H_{16}F_6NaO_3$: 501.0901, found 501.0901.

5-(hydroxymethyl)-3,4,5-tris(4-(trifluoromethyl)phenyl)furan-2(5*H*)-one (6ce)

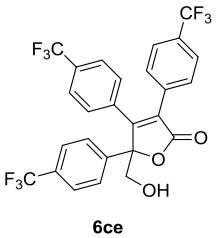

6ce

Colorless solid; mp 71.3-72.5 °C; R_f 0.33 (hexane/AcOEt = 2/1); ^{1}H NMR (500 MHz, $CDCl_3$) δ: 2.88 (br, 1H), 4.25 (qd, *J* = 17.5, 12.5, 5.0 Hz, 2H), 7.11 (d, *J* = 8.0 Hz, 2H), 7.26-7.27 (m, 2H), 7.47 (dd, *J* = 32.5, 8.5 Hz, 4H), 7.63 (dd, *J* = 14.5, 8.0 Hz, 4H); ^{13}C NMR (125 MHz, $CDCl_3$) δ: 63.8, 91.2, 123.4 (q, $^1J_{C\text{-}F}$ = 271.3 Hz), 123.5 (q, $^1J_{C\text{-}F}$ = 271.3 Hz), 123.5 (q, $^1J_{C\text{-}F}$ = 270.9 Hz), 125.2 (q, $^3J_{C\text{-}F}$ = 3.8 Hz), 125.8 (q, $^3J_{C\text{-}F}$ = 3.6 Hz), 125.8, 126.1 (q, $^3J_{C\text{-}F}$ = 3.5 Hz), 128.3, 128.7, 129.4, 129.3, 129.5, 130.6 (q, $^2J_{C\text{-}F}$ = 32.5 Hz), 131.1 (q, $^2J_{C\text{-}F}$ = 27.5 Hz), 131.6 (q, $^2J_{C\text{-}F}$ = 30.0 Hz), 131.9, 132.0, 134.4, 138.1, 162.2, 171.4; IR (neat, cm^{-1}) 3448, 2936, 1760 (C=O), 1617, 1327, 1123, 1069, 844; MS (EI): *m/z* (%) = 546 (4) [M^+], 516 (90), 497 (20), 315 (100), 314 (25), 246 (12), 173 (61), 145 (17), 115 (3), 91 (2); HRMS: *m/z* calcd [M^+]: 546.0877, found 546.0877.

5-(4-methoxyphenyl)-4-methyl-3-phenylfuran-2(5*H*)-one (5eb)

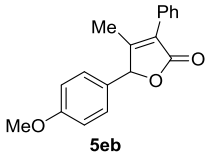

5eb

Colorless liquid; R_f 0.36 (hexane/AcOEt = 2/1); ^{1}H NMR (500 MHz, $CDCl_3$) δ: 2.00 (s, 3H), 3.83 (s, 3H), 5.72 (s, 1H), 6.93 (d, *J* = 8.5 Hz, 2H), 7.21 (d, *J* = 8.5 Hz, 2H), 7.33-7.41 (m, 1H), 7.46 (t, *J* = 8.0 Hz, 2H), 7.56 (d, *J* = 7.0 Hz, 2H); ^{13}C NMR (125 MHz, $CDCl_3$) δ: 13.4, 30.9, 55.3, 84.6, 114.4, 126.5, 128.5, 131.5, 158.1, 160.4, 172.8; IR (neat, cm^{-1}) 2917, 1752 (C=O), 1610, 1513, 1250, 1176, 834; HRMS (ESI): *m/z* calcd for $C_{18}H_{16}NaO_3$: 303.0997, found 303.0997.

5-(hydroxymethyl)-5-(4-methoxyphenyl)-4-methyl-3-phenylfuran-2(5*H*)-one (6eb)

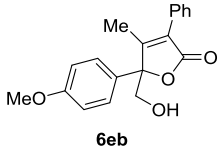

6eb

Colorless liquid; R_f 0.08 (hexane/AcOEt = 2/1); ^{1}H NMR (500 MHz, $CDCl_3$) δ: 2.07 (s, 3H), 2.30-2.32 (m, 1H), 3.82 (s, 3H), 4.20-4.33 (m, 2H), 6.93 (d, *J* = 8.5 Hz, 2H), 7.29-7.51 (m, 7H); ^{13}C NMR (125 MHz, $CDCl_3$) δ: 12.8, 55.3, 63.9, 90.6, 114.2, 126.8, 127.3, 127.4, 128.3, 128.4, 129.1, 129.8, 159.7, 162.2, 172.7; IR (neat, cm^{-1}) 3449, 2917, 1746 (C=O), 1513, 1255, 982, 834; MS (EI): *m/z* (%) = 310 (3) [M^+], 279 (100), 262 (8), 237 (3), 223 (5), 178 (4), 135 (93), 115 (15), 97 (6), 77 (9), 57 (10); HRMS: *m/z* calcd [M^+]: 310.1205, found 310.1202.

5-(4-methoxyphenyl)-3-methyl-4-phenylfuran-2(5*H*)-one (5eb')

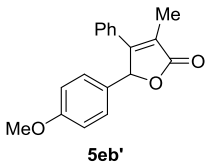

5eb'

Colorless liquid; R_f 0.36 (hexane/AcOEt = 2/1); ^{1}H NMR (500 MHz, $CDCl_3$) δ: 2.17 (s, 3H), 3.75 (s, 3H), 6.16 (s, 1H), 6.80 (d, *J* = 9.0 Hz, 2H), 7.14 (d, *J* = 8.5 Hz, 2H), 7.27-7.41 (m, 5H);^{13}C NMR (125 MHz, $CDCl_3$) δ: 10.4, 29.7, 31.7, 55.2, 114.2, 124.1, 126.9, 128.5, 128.8, 129.0, 160.1, 174.5; IR (neat, cm^{-1}) 2917, 1752 (C=O), 1610, 1513, 1250, 1176, 834; HRMS (ESI): *m/z* calcd for $C_{18}H_{16}NaO_3$: 303.0997, found 303.0997.

5-(hydroxymethyl)-5-(4-methoxyphenyl)-3-methyl-4-phenylfuran-2(5*H*)-one (6eb')

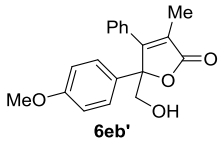

6eb'

Colorless liquid; R_f 0.19 (hexane/AcOEt = 2/1); ^{1}H NMR (500 MHz, $CDCl_3$) δ: 1.88 (s, 3H), 2.23 (br, 1H), 3.80 (s, 3H), 4.10-4.21 (m, 2H), 6.83 (d, *J* = 9.0 Hz, 2H), 6.96-6.99 (m, 2H), 7.07 (d, *J* = 9.0 Hz, 2H), 7.34-7.39 (m, 3H); ^{13}C NMR (125 MHz, $CDCl_3$) δ: 9.6, 55.3, 64.3, 91.1, 113.9, 127.0, 128.0, 128.7, 129.2, 159.7, 162.1, 174.0;

IR (neat, cm^{-1}) 3447, 2917, 1751 (C=O), 1513, 1254, 1032, 831; MS (EI): *m/z* (%) = 310 (3) [M^+], 279 (100), 265 (6), 251 (3), 221 (3), 178 (4), 135 (96), 115 (17), 92 (6), 77 (11), 57 (10); HRMS: *m/z* calcd [M^+]: 310.1205, found 310.1205.

4-butyl-5-(hydroxymethyl)-5-(4-methoxyphenyl)-3-phenylfuran-2(5*H*)-one (6fb)

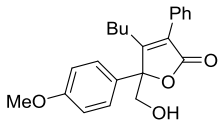

6fb

Colorless liquid; R_f 0.14 (hexane/AcOEt = 2/1); ^{1}H NMR (500 MHz, $CDCl_3$) δ: 0.72 (t, *J* = 7.0 Hz, 3H), 1.03-1.33 (m, 4H), 2.24 (t, *J* = 7.5 Hz, 1H), 2.34-2.37 (m, 2H), 3.83, (s, 3H), 4.23-4.40 (m, 2H), 6.93 (d, *J* = 9.0 Hz, 2H), 7.29 (d, *J* = 8.5 Hz, 2H), 7.36-7.49 (m, 5H); ^{13}C NMR (125 MHz, $CDCl_3$) δ: 13.3, 22.7, 26.5, 29.1, 55.2, 63.8, 90.7, 114.1, 126.9, 127.3, 127.6, 128.3, 128.8, 130.3, 159.7, 166.3, 173.2; IR (neat, cm^{-1}) 3447, 2917, 1751 (C=O), 1513, 1254, 1032, 831; HRMS (ESI): *m/z* calcd for $C_{22}H_{24}NaO_4$: 375.1572, found 375.1572.

3-butyl-5-(hydroxymethyl)-5-(4-methoxyphenyl)-4-phenylfuran-2(5*H*)-one (6fb')

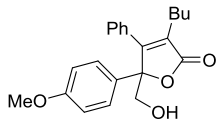

6fb'

Colorless liquid; R_f 0.28 (hexane/AcOEt = 2/1); ^{1}H NMR (500 MHz, $CDCl_3$) δ: 0.79 (t, *J* = 7.5 Hz, 3H), 1.20-1.27 (m, 2H), 1.42-1.52 (m, 2H), 2.22 (t, *J* = 8.0 Hz, 2H), 2.27 (br, 1H), 3.80, (s, 3H), 4.08-4.17 (m, 2H), 6.82 (d, *J* = 9.0 Hz, 2H), 6.93 (d, *J* = 6.5 Hz, 2H), 7.03 (d, *J* = 9.0 Hz, 2H), 7.33-7.39 (m, 3H); ^{13}C NMR (125 MHz, $CDCl_3$) δ: 13.7, 22.3, 23.8, 30.1, 55.2, 64.2, 90.9, 113.8, 126.9, 127.1, 128.0, 128.5, 128.9, 129.9, 131.6, 159.5, 162.6, 173.8; IR (neat, cm^{-1}) 3447, 2956, 2929, 2871, 1752 (C=O), 1513, 1254,

1034, 832; HRMS (ESI): *m/z* calcd for $C_{22}H_{24}NaO_4$: 375.1572, found 375.1572.

4-butyl-3-(hydroxymethyl)-5-(4-methoxyphenyl)-3-phenylfuran-2(3*H*)-one (7fb)

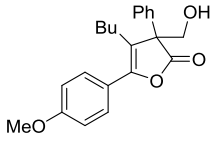

7fb

Colorless liquid; R_f 0.36 (hexane/AcOEt = 2/1); ^{1}H NMR (500 MHz, $CDCl_3$) δ: 0.88 (t, *J* = 7.5 Hz, 3H), 1.25-1.36 (m, 3H), 1.43-1.49 (m, 2H), 1.73 (td, *J* = 15.0, 5.0 Hz, 1H), 1.88 (br, 1H), 3.65 (*J* = 11.0 Hz, 1H), 3.78, (s, 3H), 3.85-3.89 (m, 1H), 6.76 (d, *J* = 9.5 Hz, 2H), 7.27-7.31 (m, 4H), 7.40-7.45 (m, 3H); ^{13}C NMR (125 MHz, $CDCl_3$) δ: 13.8, 22.6, 26.1, 31.0, 55.2, 60.3, 65.3, 113.6, 115.8, 120.8, 128.2, 128.4, 129.2, 129.6, 132.3, 147.7, 160.0, 179.8; IR (neat, cm^{-1}) 3498, 2933, 1793 (C=O), 1608, 1513, 1255, 1027, 836; HRMS (ESI): *m/z* calcd for $C_{22}H_{24}NaO_4$: 375.1572, found 375.1572.

References

(1) Aksn, O.; Dege, N.; Artok, L.; Turkmen, H.; Cetinkaya, B. *Chem. Commun.* **2006**, 3187.

(2) (a) Kuş, M.; Artok, Ö. A.; Ziyanak, F.; Artok, L. *Synlett* **2008**, *17*, 2587. (b) Artok, L.; Kuş, M.; Aksın-Artok, Ö.; Dege, F. N.; Özkılınç, F. Y. *Tetrahedron* **2009**, *65*, 9125.

(3) Wang, C.; Morimoto, T.; Kanashiro, H.; Tanimoto, H.; Nishiyama, Y.; Kakiuchi, K.; Artok, L. *Synlett* **2014**, *25*, 1155.

(4) Kreis, M.; Palmelund, A.; Bunch, L.; Madsen, R. *Adv. Synth. Catal.* **2006**, *348*, 2148.

(5) Giordano, G.; Crabtree, R. H. *Inorg. Synth*. **1979**, *19*, 218.

CHAPTER 4 Summary

In conclusion, a novel catalytic arylative carbonylation method using formaldehyde as a carbonyl source has been described in the thesis, which has demonstrated the combination of phosphine ligand with phosphine-free rhodium catalyst in the presence of formaldehyde give a new synthetic protocol for the CO gas-free carbonylation reactions. The observations involved two chapters of my thesis are summarized as follows:

In chapter 2, the Rh(I)-catalysed arylative mono-carbonylation of alkynes with various arylboronic acids in the presence of formaldehyde as a carbonyl source was studied, resulting in a CO gas-free reaction to afford *α,β*-enones derivatives. The addition of BIPHEP, the amount of which must not account for all the total phosphine-free rhodium complex $[RhCl(cod)]_2$ leads to the partial formation of phosphine-ligated complex $[RhCl(BIPHEP)]_2$ along with intact $[RhCl(cod)]_2$, which are mainly involved in the decarbonylation of formaldehyde to produce a carbonyl moiety and the subsequent carbonylative arylation of alkynes with arylboronic acids using the resulting carbonyl moiety, respectively (Scheme 4-1).

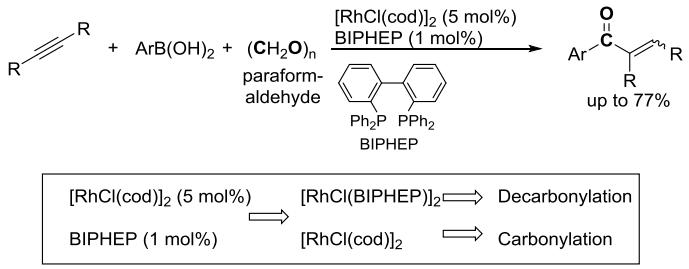

Scheme 4-1 Rh(I)-catalyzed arylative mono-carbonylation of alkynes with arylboronic acids in the presence of formaldehyde

The reaction proceeds generally in a stereoselective fashion favouring (*Z*)-isomer of the enones derivatives. The electron-rich *p*-substituted arylboronic acids on this Rh(I)-catalyzed arylative mono-carbonylation of alkynes with arylboronic acids produced high yields of enones. The reaction proceeds with moderate regioselectivity to

give predominantly the corresponding enones, in both of which lager group is located at the β-position of the enones.

In chapter 3, I studied on the Rh(I)-catalysed arylative double-carbonylation of alkynes with diverse arylboronic acids in the presence of formaldehyde as a carbonyl source, leading to a CO gas-free reaction to afford α,β-butenolides derivatives. In this reaction, the key to success is also to control the amount of added phosphine ligand so that rhodium complexes both with and without phosphine ligand are present, thus permitting both decarbonylation and carbonylation to proceed in a single catalyst system. Consequently, the phosphine-ligated rhodium species, $[RhCl(dppp)_2]$, which are generated *in situ* and the intact phosphine-free rhodium species, $[RhCl(cod)]_2$, would be involved in the decarbonylation and carbonylative arylation processes, respectively, to lead to the overall efficient CO gas-free arylative double-carbonylation (Scheme 4-2).

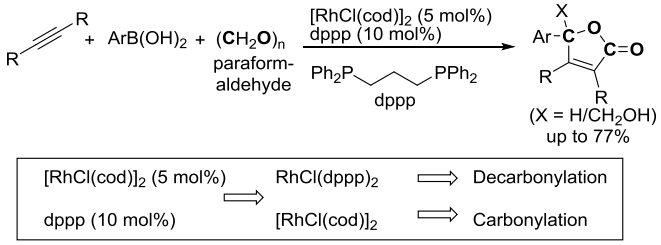

Scheme 4-2 Rh(I)-catalyzed arylative double-carbonylation of alkynes with arylboronic acids in the presence of formaldehyde

Employing *p*-substituted arylboronic acids with electronic rich group on the aylative double-carbonylation reaction afforded higher yields of butenolides derivatives than that using electron-poor ones. The reaction also proceeds with moderate regioselectivity to give predominantly the corresponding butenolides, in both of which more sterically hindered group located at the α-position of the carbonyl group.

The successful utilization of formaldehyde as a carbonyl source in two kinds of arylative carbonylation reactions of alkynes with arylboronic acids have been achieved, which are originally catalyzed by a phosphine-free rhodium(I) complex in the presence

of CO. The key to success is to control the amount of added phosphine ligand so that rhodium complexes both with and without phosphine ligand are present, thus permitting both decarbonylation and carbonylation to proceed in a single catalyst system.

Perspective: The CO gas-free protocol consisting of a rhodium catalyst and formaldehyde has the potential to be compatible with various carbonylation reactions that are catalyzed by ligand-free rhodium complexes. I will apply this CO gas-free protocol catalyzed phosphine-free and -ligated dual Rh catalysts using formaldehyde as a carbonyl source for some carbonylations catalyzed by ligand-free rhodium complex without direct use of toxic carbon monoxide. Such as Rhodium dual catalyzed 1,4-carbonylative addition of arylboronic acids to α,β-unsaturated ketones for the synthesis of 1,4-diketone.

By controlling the amount of added phosphine ligands, the *in-situ* generated phosphine-ligated rhodium species and intact phosphine-free rhodium species would be involved in the decarbonylation and carbonylation processes, respectively.

It can substitute for the conventional carbonylations catalyzed by ligand-free rhodium complexes and avoids directly employing carbon monoxide.

Acknowledgements

I would like to express my sincere and heartfelt gratefulness to my supervisor Professor Kiyomi Kakiuchi for his valuable suggestion and encouragement during my doctoral course. Under his guide, I have obtained a balanced training on how to accomplish research work, overcome the problems I met and become an independent researcher. I wish to afford my special appreciation to Associate Professor Tsumoru Morimoto for his helpful advice and constructive comments throughout my research.

I wish to offer my deepest gratitude to my co-supervisors, Professor Jun-ichi Kikuchi and Associate Professor Takashi Matsuo, for their useful suggestion and comment. I also would like to appreciate Assistant Professor, Dr. Hiroki Tanimoto and Dr. Yasuhiro Nishiyama for their meritorious opinions.

Furthermore, I would like to gratitude my friends and colleagues of my laboratory for their kind help and support.

I am obliged to all of the staffs especially the technical service team that belongs to Graduate School of Materials Science for their technical supports.

I would like to thank Grant-in-Aid research fellowship on Innovative Areas “Molecular Activation Directed toward Straightforward Synthesis” from the Ministry of Education, Culture, Sports, Science and Technology, Japan.

Finally, I greatly appreciate my parents and family for their forever support and encourage.

Nara, Japan.

September, 2014

Chuang Wang

List of Publications

Main Papers in the Ph.D. Thesis

(1) "Rhodium(I)-Catalyzed Carbonylative Arylation of Alkynes with Arylboronic Acids Using Formaldehyde as a Carbonyl Source"
Chuang Wang, Tsumoru Morimoto, Hiroyuki Kanashiro, Hiroki Tanimoto, Yasuhiro Nishiyama, Kiyomi Kakiuchi, and Levent Artok.
Synlett **2014**, *25*, 1155.

(2) "Rh(I)-Catalyzed Arylative Carbonylation of Alkynes with Arylboronic Acids Using Formaldehyde as a CO Source"
Chuang Wang, Tsumoru Morimoto, Hiroki Tanimoto, Yasuhiro Nishiyama, Kiyomi Kakiuchi, and Levent Artok.
(*Manuscript in Preparation*)

Referenced Papers

(1) "Synthesis and Micellization of a New Amphiphilic Star-Shape Poly(D,L-lactide) /Polyphosphoester Block Copolymer"
Qiuhua Wu, Chuang Wang, Dan Zhang, Ximing Song, Daliang Liu, Liping Wang, and Guolin Zhang.
Reactive and Functional Polymers **2012**, *72*, 372.

(2) "Synthesis and Micellization of Amphiphilic Biodegradable Methoxypolyethylene Glycol/Poly(D, L-lactide)/Polyphosphate Block Copolymer"
Qiuhua Wu, Chuang Wang, Dan Zhang, Ximing Song, Francis Verpoort, and Guolin Zhang.
Reactive and Functional Polymers **2011**, *71*, 980.

Academic Conferences

International Conferences

(1) "Rh(I)-Catalyzed Arylative Carbonylation Reactions of Alkynes with Arylboronic Acids in the Presence of Formaldehyde"
Tsumoru Morimoto, Chuang Wang, Kiyomi Kakiuchi, and Levent Artok
International Symposium of Catalysis and Fine Chemicals (*C&FC2013*), Beijing, China, Dec. 1-5, 2013 (Short Talk and Poster Presentation OPP-19).

(2) "Rh(I)-Catalyzed Carbonylative Arylation of Alkynes with Arylboronic Acids Using Formaldehyde as a Carbonyl Source"
Tsumoru Morimoto, Chuang Wang, Levent Artok, and Kiyomi Kakiuchi
The 12th International Kyoto Conference on New Aspects of Organic Chemistry (*IKCOC-12*), Kyoto, Japan, Nov.12-16, 2012 (Poster Presentation PB-062).

Domestic Conferences

(1) "Rh(I)-Catalyzed Arylative Double-Carbonylation of Alkynes with Arylboronic Acids Using Formaldehyde as a CO Source"
Tsumoru Morimoto, Chuang Wang, Kiyomi Kakiuchi, and Levent Artok
The 94th Annual Meeting of Chemical Society of Japan, Nagoya, Japan, Mar. 27-30, 2014 (Oral Presentation 3B3-30).

(2) "Rh(I)-Catalyzed Carbonylative Arylation of Alkynes with Arylboronic Acids Using Formaldehyde as a Carbonyl Source"
Tsumoru Morimoto, Chuang Wang, Kiyomi Kakiuchi, and Levent Artok
The 93th Annual Meeting of Chemical Society of Japan, Shiga, Japan, Mar. 22-25, 2013 (Oral Presentation 4F5-19).

(3) "Rh(I)-Catalyzed Carbonylative Arylation of Alkynes with Arylboronic Acids Using Formaldehyde as a Carbonyl Source"

Tsumoru Morimoto, Chuang Wang, Levent Artok, and Kiyomi Kakiuchi

The 59th Organometallic Chemistry Symposium, Osaka, Japan, Sept.13-15, 2012 (Short Talk and Poster Presentation P3B-11).